

AN ABSTRACT OF THE THESIS OF

Jeff L. Waldman for the degree of Master of Science in Geology
presented on March 12, 1990.

Title: Stratigraphy and Depositional Environments of the Upper Devonian
Fenstermaker Limestone, Eureka County, Nevada.

Abstract approved: _____

Redacted for Privacy

J. G. Johnson

The Upper Devonian Fenstermaker Limestone is a thickening-upward sequence of interbedded sandy intrapelsparite and subordinate calcareous siltstone and mudstone which averages 190 ft (58 m) thick in the northern Antelope Range. The Fenstermaker Limestone is revised and restricted herein to include only those rocks above a basinal shale sequence of the upper Denay Limestone and below the Mississippian Davis Spring Formation, and replaces the names "Devonian sandstone" of Trojan (1978) and the "Fenstermaker Wash Formation" of Hose and others (1982).

Sandy limestone of the Fenstermaker Limestone was deposited rapidly, above upper Denay basinal shales, as resedimented beds in Frasnian Montagne Noir conodont zone 13 and the Lower Famennian Middle *triangularis* Zone. Reworked conodonts are present at numerous stratigraphic levels in the Fenstermaker, indicating erosion on the inner or middle carbonate platform during two Upper Devonian eustatic regressions (in lower and upper T-R cycle IId; western U. S. events 7 and 8). Deposition of the Fenstermaker Limestone was by allodapic sediment gravity flows on an outer-shelf-basin ramp or at the toe of a low-angle ($<4^\circ$) carbonate slope during incipient outer-shelf-basin filling, i.e. as reciprocal sedimentation.

Detrital quartz sand averages 11% but ranges much higher in sand-rich laminae preserved in strata along the western range front. Sorting characteristics of the sand were attained in a siliciclastic beach environment prior to deposition in the carbonate lithotope. Pitting and frosting of grain surfaces are at least partially diagenetic in origin and not necessarily a product of eolian transport.

Two allochthonous limestone blocks in the southern Fish Creek Range, northern Nye County (blocks A and C of Sans, 1986), are assigned to the Fenstermaker Limestone and are considered to have been derived from the west.

Beds the age of the Fenstermaker Limestone are absent at an unconformity in the Cortez Mountains, west-central Eureka County.

Detrital quartz sand concentrated along stylolites in the Upper Devonian part of the Popovich Formation, southern Tuscarora Mountains, northern Eureka County, were point-counted as an aid in determining formational thickness loss due to pressure-solution. Thickness reductions are estimated at 12-13%.

Stratigraphy and Depositional Environments
of the
Upper Devonian Fenstermaker Limestone,
Eureka County, Nevada

by

Jeff L. Waldman

A THESIS

submitted to

Oregon State University

in partial fulfillment of
the requirements for the
degree of

Master of Science

Completed March 12, 1990

Commencement June 1990

APPROVED:

Redacted for Privacy

Professor of Geology, in charge of major

Redacted for Privacy

Chairman of the Department of Geosciences

Redacted for Privacy

Dean of the Graduate School

Date thesis is presented March 12, 1990

Typed by Jeff L. Waldman for Jeff L. Waldman

ACKNOWLEDGEMENTS

First and foremost, I would like to thank Dr. J. G. Johnson, who served as thesis advisor, department chairman, and friend throughout the production of the thesis. I am indebted to him for his scientific, financial, and moral support. Dr. A. R. Niem provided helpful insight and useful criticism; he and Dr. G. W. Moore served on the thesis committee. Claudia Regier cheerfully and meticulously segregated formic acid residues, picked conodonts, and was helpful in various ways during both the research and production stages.

Funding for the thesis was provided by Mobil Oil Corp., Chevron Scholarships, Dr. Johnson through his National Science Foundation grant, and my family, whom I thank and owe so much. Amoco Production Co. processed several of the conodont samples and provided several critical sand residues from their ANA collections. Atlas Precious Metals, Inc. provided employment during most of 1988 and provided access to critical comparative sections in Eureka County. Charles Zimmerman of Newmont Mining granted access to Newmont property in the Tuscarora Mountains. Dr. Gilbert Klapper, University of Iowa, identified all conodonts. Brachiopods were identified by Dr. Johnson, and Dr. A. R. Ormiston of Amoco Production Co. identified radiolarians recovered from one sample.

Drs. H. E. Cook and M. E. Taylor of the U. S. Geological Survey made an enlightening field visit in 1986. Dr. J. C. Wendte of Canadian Hunter Exploration provided useful consultation during a 1989 visit to O.S.U. Jeff Dawley and Dalillah El-Sabbagh volunteered their time as field assistants. Without Dawley's help when I broke my foot under a block of fallen limestone, I would probably still be there! T. Berkman, G. Huftile, M. Parker, I. Ryu, and N. Zhang, all of Oregon State University, provided help in various ways.

TABLE OF CONTENTS

INTRODUCTION	1
Purpose	1
Abbreviations	2
Location and Accessibility	3
Northern Antelope Range	3
Previous Work	3
Northern Antelope Range	3
Southern Fish Creek Range	12
Southern Cortez Mountains	12
Southern Tuscarora Mountains	13
Methods	13
Regional Geology	16
Upper Devonian Conodont Zonation	18
FENSTERMAKER LIMESTONE	21
Nomenclature	21
Thickness and Distribution	22
Measured Sections	24
Lithology and Contacts	28
Petrography	37
Diagenesis	42
BIOSTRATIGRAPHY	48
Conodont Biostratigraphy	48
Conodont Biofacies	54
Conodont Alteration Indices (C. A. I.)	55
Significance of Reworked Conodonts	56
Brachiopods	61
Other Fossils	61
Late Frasnian Mass-Extinction Event	64
TIME-CORRELATIVE UNITS	67
Southern Fish Creek Range	67
Southern Tuscarora Mountains	71
Southern Cortez Mountains	82
GRAIN-SIZE ANALYSIS	85
DEPOSITIONAL ENVIRONMENTS	101
Quartz Sand Provenance and Mixing	101
Depositional Models	106
Depositional Mechanisms	111

CONCLUSIONS	115
REFERENCES	117
APPENDICES	126
Appendix A: Faunal Collections	126
Appendix B: Statistical Parameters from Sieve Analysis of Quartz Sand Fractions	158

LIST OF FIGURES

<u>Figure</u>	<u>Page</u>
1. Location map of Antelope Valley showing access routes.	4
2. Index map of east-central Nevada with enlargement of Eureka County showing locations of main thesis study areas.	5
3. Stratigraphic sections and conodont zonation in the northern Antelope Range.	7
4. Geologic map of the northern Antelope Range showing the locations of measured sections.	8
5. Photograph of TA IV/ ANA II/ ANA III sections.	10
6. Comparison chart of Upper Devonian stratigraphic nomenclature in east-central Nevada.	11
7. Comparison chart of Upper Devonian (Frasnian) conodont zonation schemes.	20
8. Time-rock transect across the Siluro-Devonian outer continental shelf of central Nevada.	23
9. Photograph of dip slope above ANA III 96.	25
10. Photograph of traceable, wavy limestone bed which links ANA II 142 to ANA III 0.	27
11. Photograph of the upper half of section WNA II.	29
12. Photograph of rhythmic bedding in the vicinity of ANA I.	31
13. Photograph of WNA II 196 hand sample showing possible low-angle cross-bedding in quartz sand layers.	34
14. Photograph of ANA II 142 bed showing erosional downcutting of limestone bed into underlying shale/mudstone beds.	35
15. Photograph of chert nodules south of ANA I.	36
16. A. Photomicrograph of ANA I 0 showing typical mixture of peloids and intraclasts. B. Photomicrograph of ANA III 116 showing double-walled calcispheres within large peloids.	38
17. A. Photomicrograph of TA IV 185 showing high quartz sand percentage. B. Photomicrograph of ANA III 107 showing crinoidal fragment with syntaxial rim cement.	40

18. A. Photomicrograph of ANA I 280 showing tetracoral fragment.	
B. Photomicrograph of WNA I 2 showing incipient neomorphism.	41
19. A. Photomicrograph of TA IV 100 showing contact between chertified and unaltered limestone.	
B. Photomicrograph of TA IV 100 showing siderite rhombs.	43
20. A. Photomicrograph of WNA I 6 showing diagenetic etching of quartz sand grains by neomorphic microspar.	
B. Photomicrograph of ANA I 286 showing partial replacement of detrital quartz sand grain by neomorphic microspar.	45
21. A. Photomicrograph of ANA III 122 showing iron-oxide-rich stylolite truncating intraclast.	
B. Photomicrograph of WNA I 12 showing stylolite crossing sparry calcite vein.	46
22. Upper Devonian eustatic curve.	59
23. Time-rock chart for five regions of the Devonian Euramerican platforms showing principal deepening events.	60
24. Devonian eustatic curve with principal western U. S. Devonian stratigraphic units plotted.	62
25. Comparison chart between Upper Devonian conodont zones, depopphase T-R cycles of Johnson and others (1985), Devonian western U. S. events of Sandberg and others (1989), and Devonian Euramerican eustatic events of Johnson and others (1985).	63
26. Photograph of typical exposure of southern Fish Creek Range allochthonous block C.	68
27. Photomicrograph of WFC 3 from allochthonous block A displaying Fenstermaker Limestone microfacies.	69
28. Photomicrograph of WRC I 122 showing peloid amalgamation in Popovich Formation micrite intraclast.	73
29. Photomicrograph of WRC I 172 showing typical silty chert bed in the Popovich Formation.	75
30. Photomicrograph of WRC I 212 sandy intrapelmicrite.	76
31. Photomicrograph of WRC I 237 sample used to determine percent thickness reduction during quartz-rich stylolite formation.	78
32. Hand sample of WRC I 237 quartz-rich stylolites.	79
33. CW I stratigraphic section, southern Cortez Mountains.	84

34. Combined SBH and WBH stratigraphic section, south Burbank Hills, Utah.	86
35. ANA I and ANA II grain-size histograms.	89
36. ANA III, Oxyoke Canyon (Dno), and TA V grain-size histograms.	90
37. WNA I and WNA II grain-size histograms.	91
38. Southern Fish Creek Range (WFC) and southern Tuscarora Mountains (WRC I) grain-size histograms.	92
39. Cherry Creek Range (WIC) and south Burbank Hills, Utah (WBH), grain-size histograms.	93
40. Friedman bivariate graph of median diameter versus skewness.	95
41. Friedman bivariate graph of simple sorting measure versus simple skewness measure.	96
42. Friedman bivariate graph of inclusive graphic standard deviation versus inclusive graphic skewness.	97
43. Friedman bivariate graph of inclusive graphic standard deviation versus mean grain size.	98
44. Passega CM plot.	100
45. Paleobiogeographic lithofacies map of Lower <i>gigas</i> Zone.	103
46. Paleobiogeographic lithofacies map of Lower <i>triangularis</i> Zone.	104
47. Diagram of reciprocal sedimentation model.	107
48. Inferred position of Upper Devonian outer-shelf basin in central Nevada.	108
49. Depositional environment model for the Fenstermaker Limestone.	113

LIST OF TABLES

<u>Table</u>	<u>Page</u>
1. Selected quartz sand weight percentages.	33
2. ANA I conodont checklist.	49
3. WNA I conodont checklist.	50
4. WNA II conodont checklist	51
5. Reworked conodonts.	57

LIST OF PLATES

Plate

- | | |
|---|-----------|
| 1. Stratigraphic correlations. | in pocket |
| 2. Integrated ANA II/ ANA III/ TA IV collections. | in pocket |

STRATIGRAPHY AND DEPOSITIONAL ENVIRONMENTS
OF THE UPPER DEVONIAN FENSTERMAKER LIMESTONE,
EUREKA COUNTY, NEVADA

INTRODUCTION

PURPOSE

In the years following Trojan's (1978) study of the Devonian stratigraphy in the northern Antelope Range, uncertainty over the timing and depositional setting of his "Devonian sandstone" unit, above the Denay Limestone, was created when Hose and others (1982) included it in their "Fenstermaker Wash Formation". That unit, as defined by Hose and others (1982), had a lower boundary that is well down in the lower member of the Denay Limestone, leaving questions concerning rock nomenclature. Further questions were raised regarding the biostratigraphy and depositional environments of this unit when geologists of Amoco Production Company discovered additional sandy limestone beds in 1985 which contain the controversial Frasnian-Famennian boundary.

The primary purpose of this study was to interpret the depositional environment(s) of this unit and to discuss possible depositional models. The main goals of the study were to: (1) describe the stratigraphy of the Upper Devonian carbonate sequence above the Denay Limestone in the northern Antelope Range; (2) assign ages to these rocks for regional stratigraphic control through the aid of conodont and brachiopod biostratigraphy; (3) document faunal and lithologic changes that may have occurred across the Frasnian-Famennian boundary; (4) examine these rocks petrographically and interpret microfacies and diagenetic relationships; (5) examine and interpret the quartz sand fractions of these rocks; (6) interpret the depositional

environments of these rocks and discuss possible depositional models; and (7), make comparisons and correlations with coeval rocks of similar lithology in the southern Fish Creek Range, the southern Cortez Mountains, and in the southern Tuscarora Mountains.

ABBREVIATIONS

The following abbreviations are used throughout the text:

- ANA: "Amoco (1985) northern Antelope (Range)" biostratigraphic section(s).
 CW: "Cortez (Mountains) Waldman" biostratigraphic section.
 DVG: "Devils Gate" biostratigraphic section of Sandberg and Poole (1977).
 F-F: "Frasnian-Famennian" boundary or faunal diversity crisis.
 M. N.: "Montagne Noir" Frasnian conodont zone of Klapper (1989).
 TA: "Trojan (1978) (northern) Antelope (Range)" biostratigraphic section(s).
 WBH: "Waldman (southern) Burbank Hills" stratigraphic section.
 WIC: "Waldman Indian Creek" (Cherry Creek Range) locality.
 WFC: "Waldman (southern) Fish Creek (Range)" collection.
 WNA: "Waldman northern Antelope (Range)" biostratigraphic section(s).
 WRC: "Waldman Rodeo Creek" (southern Tuscarora Mountains) biostratigraphic section.

LOCATION AND ACCESSIBILITY

Northern Antelope Range

The northern Antelope Range study area is located in the northern half of the Summit Mountain, 1:100,000-scale quadrangle, southern Eureka County, Nevada, about 23 mi southwest of Eureka. Figure 1 shows the road network of southern Eureka County. From Eureka, access to the mountain range can be attained by following U.S. 50 about 20 miles west to Route 82 (sign marked "Antelope"). Take Route 82 south about 21 miles then branch to the east, crossing the Antelope Valley. Two main jeep trails provide access to the range from the gravel road that runs along the west flank.

PREVIOUS WORK

Northern Antelope Range

Geologic work conducted in the northern Antelope Range, southern Eureka County, Nevada (Fig. 2), has been focused primarily on Devonian biostratigraphy. Merriam (1963) indicated the approximate extent of Devonian outcrops on a reconnaissance map, but did not assign the units formation names. Trojan (1978) mapped the northern Antelope Range at a scale of 1:12,000, describing the geology, stratigraphy, and depositional environments. He did not concentrate on the Upper Devonian sandy carbonate sequence, to which he informally applied the name

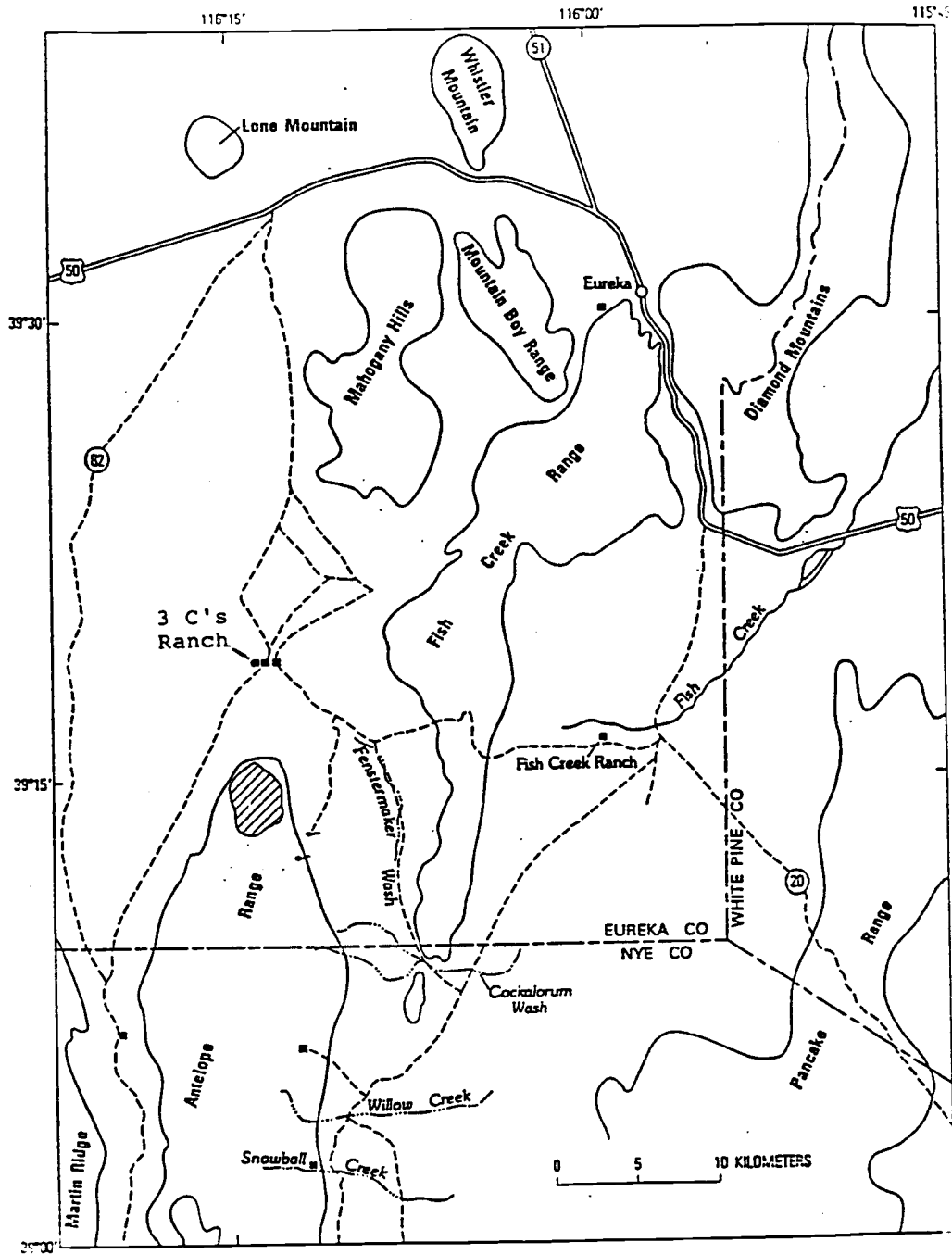


Figure 1. Location map of the northern Antelope Range (hachures) showing accessibility from Eureka. Modified after Hose and others (1982).

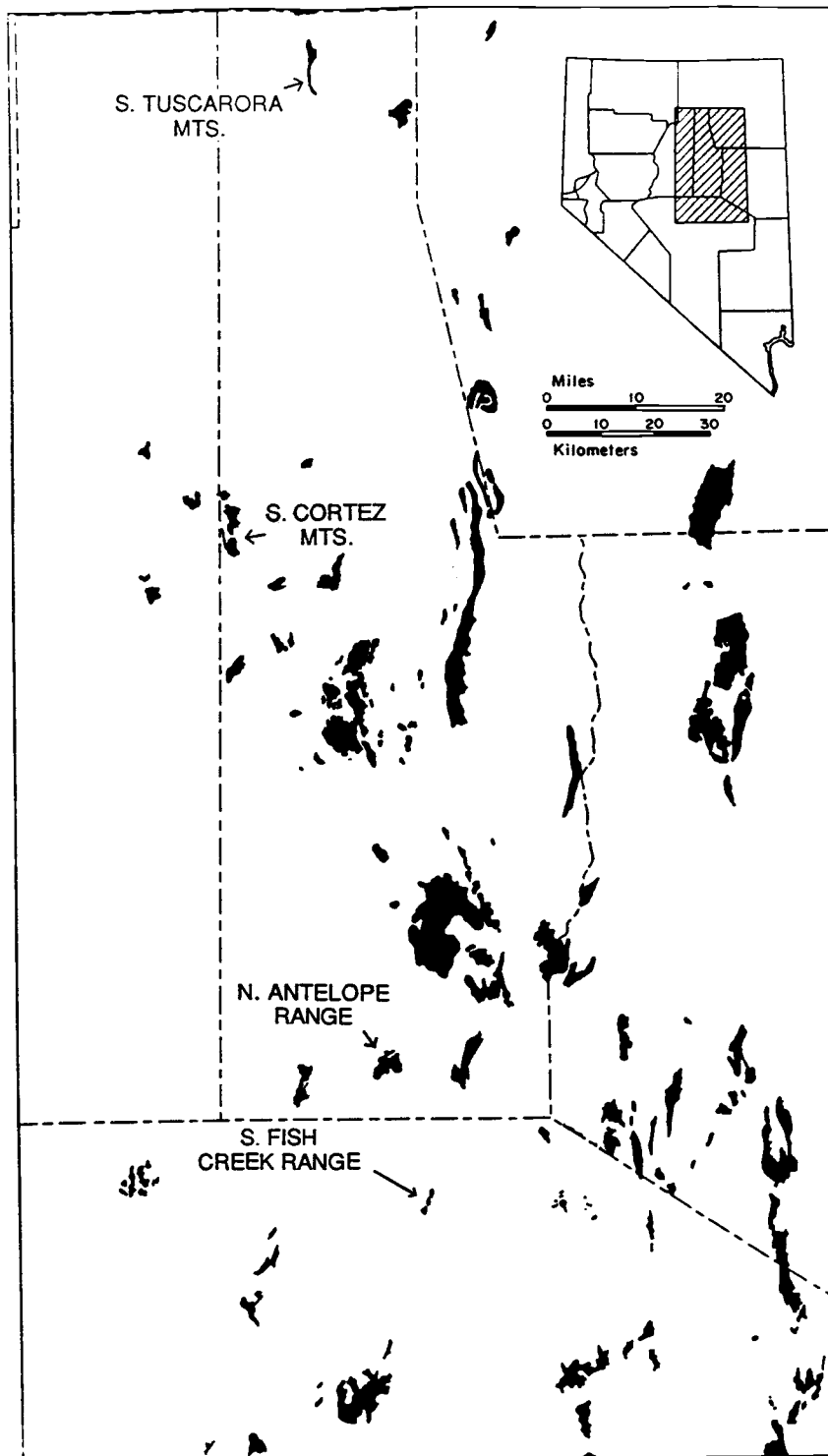


Figure 2. Index map of central Nevada. Inset in upper right shows area covered. Devonian outcrops in black. Modified from Johnson and Murphy (1984).

Devonian Sandstone. The sequence in question is partially shown as the uppermost unit in Trojan's (1978) sections TA III and IV (Fig. 3), in depositional contact with the underlying Denay Limestone. The name Devonian Sandstone will not be retained as it shares the name of a geologic time period, and the unit is more accurately described as a sandy limestone than a sandstone. Trojan's faunal collections continue to be studied and referenced, as they represent some of the most complete biostratigraphic collections of Middle Devonian rocks in western North America. Johnson and others (1980, 1986) discuss the brachiopod and conodont biostratigraphy of the northern Antelope Range.

Trojan (1978) described the Devonian sequence (Figs. 3, 4) of the northern Antelope Range as consisting of the uppermost 500 ft (152 m) of the Siluro-Devonian Lone Mountain Dolomite, overlain by the Lower Devonian McColley Canyon Formation (Kobeh, Bartine, and Coils Creek Members; 583 ft (178 m) thick, as revised by Johnson and others, 1986). The McColley Canyon Formation is in transitional contact with the overlying Denay Limestone (approximately 1395-1585 ft thick (425-483 m)). The upper part of the Upper Denay Limestone is in transitional contact with the overlying Fenstermaker Limestone (revised and restricted herein), which varies across the field area between 167 ft (51 m) thick and approximately 240 ft (73 m) thick. The Devonian sequence is capped by a Mississippian flysch-molasse sequence (Davis Spring Formation at the base; Hose and others, 1982). Nineteen conodont zones are unrepresented at the top of the Devonian sequence between the Fenstermaker Limestone and the Lower Mississippian Davis Spring Formation. Trojan recovered conodonts assigned to the Frasnian Uppermost *gigas* Zone from near the top of the formation (equivalent to the *linguiformis* Zone of Sandberg and others, 1988b).

John Graham (then of Amoco Production Co.), aided by Heidi Hoffman (then of Oregon State University, working on her M.S. thesis) measured and collected three biostratigraphic sections (ANA I, II, and III) in the northern Antelope Range during the

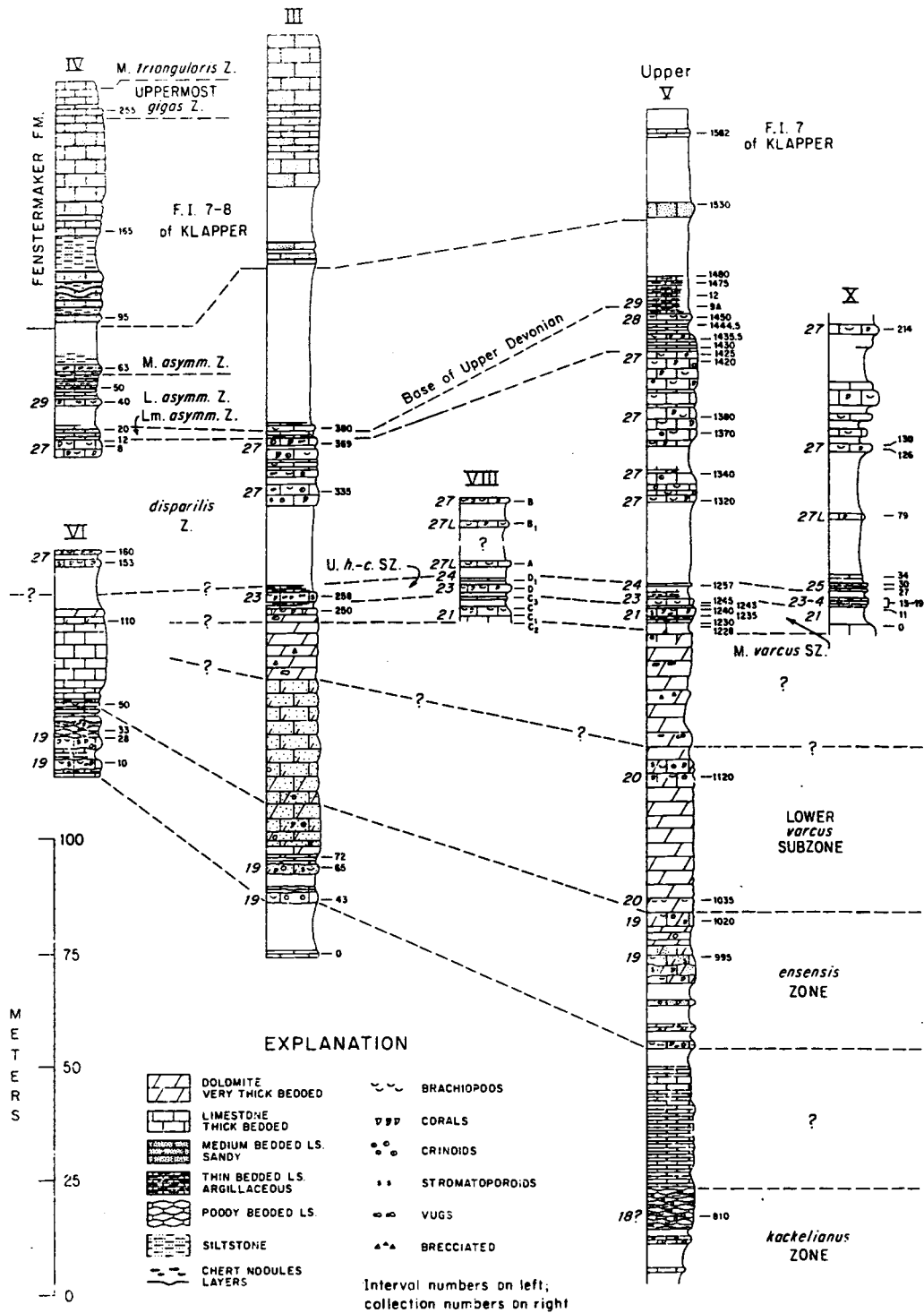


Figure 3. Northern Antelope Range stratigraphic sections (incomplete) showing part of the Fenstermaker Limestone at top (labeled "Fenstermaker Formation"). Modified from Johnson and others (1980).

summer of 1985. They recognized that Trojan's (1978) TA IV section, which contains a "jog" to the east at TA IV 142, could be subdivided into two sections, ANA II and ANA III. Their collections, integrated with Trojan's measurements, indicated that carbonate rocks of Famennian age (Middle *triangularis* Zone; ANA III 126) are present on the dip-slope above what seems to be the top of the cliff (Fig. 5), above Trojan's highest sample, TA IV 255. The discovery of Famennian strata in the northern Antelope Range spurred new interest in the Fenstermaker Limestone (Trojan's Devonian Sandstone), because it spans the controversial Frasnian-Famennian boundary and the associated Late Frasnian mass-extinction event.

Hose and others (1982) described the geology of the northern Antelope Range, applying the name Fenstermaker Wash Formation to rocks equivalent to the upper part of the type lower Denay Limestone (Murphy, 1977) through Devonian Sandstone (Trojan, 1978) sequences. Although Hose and others (1982) mapped and described the Fenstermaker Wash Formation in depositional sequence above the Denay Limestone, the basal contact they chose for the formation was placed well within the lower member relative to the type Denay as measured and mapped in the Roberts Mountains (Murphy, 1977; Murphy and others, 1978). The usage of Hose and others (1982) is inappropriate and is not consistent with the work of previous workers on the Denay (Fig. 6). Herein (and as suggested by Johnson and others, 1989, p. 178), the name Fenstermaker Limestone is restricted to the sequence of Frasnian-Famennian sandy limestone in the northern Antelope Range (and probably in two southern Fish Creek Range slide blocks) that overlies the upper member of the Denay Limestone, and underlies the Davis Spring Formation.

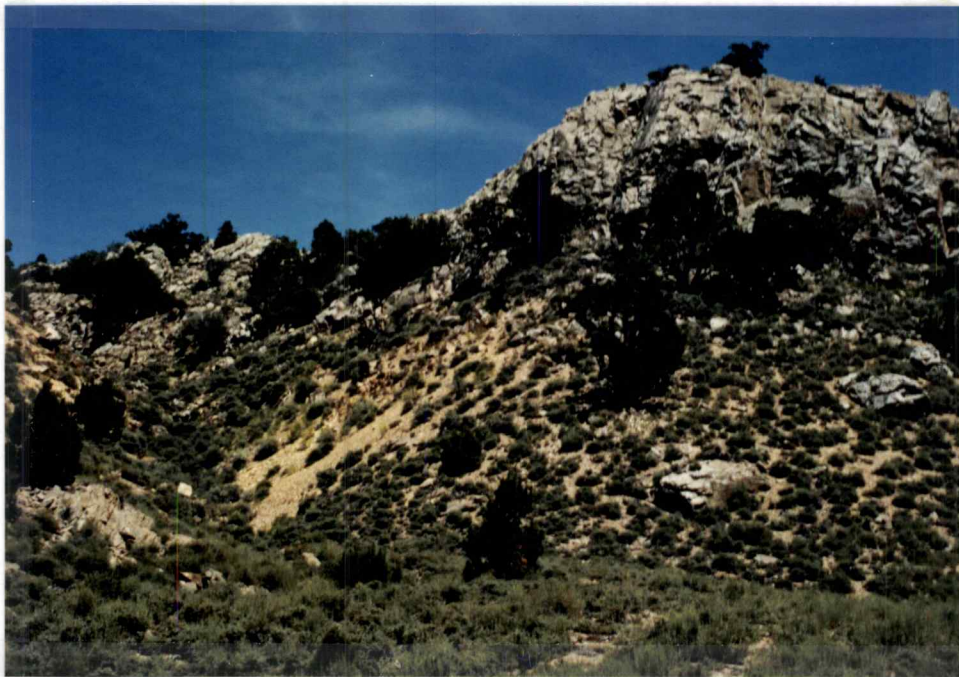


Figure 5. View east of main sandy limestone cliff in section ANA III. Dip slope is above cliff and out of view. For scale, cliff is approximately 75 ft (23 m) high.

CONODONT C ZONE	BRACH. FAUNA	E V E N T	SHOSHONE RG.- TOQUIMA RG. (SVN, TOQ; 10, 21)	BADGER SPRING ADOBE RANGE (AD)	NORTHERN ANTELOPE RG. (NAR; 1, 2)	DEVILS GATE (DVG; 35)	LITTLE 1/2 MI. CYN. CONFUSION RG. (CON; 36)	NORTH GILSON MTS. (NGM; 35)	SALT LAKE CITY AREA (BECK)
<i>praesulcata</i>	<i>Syring.</i>	17					LEATHAM MEMBER		
<i>expansa</i>	<i>Paur.</i>	16	BEDED BARITE	UNNAMED CHERT AND OOL. UNIT			LOWER FITCHV.	LOWER FITCHV.	
<i>postera</i>		15					UPPER PIN. PK.	PINYON PEAK LS.	UPP. MBR.
<i>trachytera</i>	<i>C. dev.</i>	14							LOWER MBR.
<i>marginifera</i>		13	BEDED BARITE	No data					
<i>rhomboides</i>	<i>C. retic.</i>	12							
<i>crepida</i>		11							
<i>triangularis</i>	<i>Eapar.</i>	9							
<i>gigas</i>	<i>Tawatripa</i>	8	SLAVEN CHERT (pt.)		Limestone and sandy ls.	8			
<i>A. triangularis</i>	<i>Col. Cary.</i>	7		Unnamed chert unit (pt.)	Upper part of DENAY LIMESTONE	DEVILS GATE LS. (pt.)	GUILMETTE FORMATION (pt.)		
<i>asymmetrica</i>	<i>Allanella</i>	4						GUILMETTE FM.	
		3							

Figure 6. Correlation chart of Upper Devonian stratigraphic nomenclature in western U. S. Fenstermaker Limestone is indicated as "Limestone and sandy limestone" above Denay Limestone. From Sandberg and others (1989).

Southern Fish Creek Range

Merriam (1967, 1973) noted rocks of Devonian age in the southern Fish Creek Range, applying the name Cockaloram Wash Formation to a mixture of autochthonous and allochthonous rocks that crop out between Cockalorum Wash and Willow Creek, although he did not comment on the stratigraphic or structural relationships of these rocks. Hose (1978) produced a preliminary geologic map of the Cockaloram Wash quadrangle showing the distribution of Cockaloram Wash Formation outcrops. Later workers (Johnson and Pendergast, 1981; Poole and others, 1983; Hose, 1983; Sans, 1986; Lee, 1989) have reassigned the outcrops of the Cockaloram Wash Formation to the Devils Gate Limestone, Pilot Shale, Woodruff, Antelope Range, and Webb Formations.

Sans (1986) mapped the southern Fish Creek Range in detail, describing the lithology and structural relationships of the allochthonous blocks. Three of his mapped blocks (blocks A, B, and C) are of interest here. Conodont biostratigraphy (Sans, 1986) has shown that block B (collection SS60) is of Frasnian Upper to Uppermost *gigas* Zone age (Montagne Noir Zone 13), and that block A (collection SS27) is of early Famennian age. Block C was not sampled by Sans (1986), although it shows field and petrographic relations to blocks A and B. The assignment of these blocks to the Devils Gate Formation (Merriam, 1973; Hose, 1978, 1983) is reasonable, but because of petrologic similarity, the present study reassigns two of these blocks (blocks A and B) to the Fenstermaker Limestone.

Southern Cortez Mountains

The first detailed mapping in the southern Cortez Mountains was accomplished by Gilluly and Masursky (1965) during which they assigned all Devonian rocks in the Cortez window to the Wenban Limestone and Pilot Shale. D. B. Johnson (1972) mapped the area, dividing the "Wenban" package of Devonian rocks into Windmill Limestone, Rabbit Hill Limestone, McColley Canyon Formation, Denay Limestone, and "Pilot Shale" (his quotation marks). He integrated conodont biostratigraphy into the work, and his formation assignments are compatible with those employed in the adjacent Simpson Park Range (Johnson, 1965) and in the Roberts Mountains (Murphy and others, 1978).

Southern Tuscarora Mountains

Little geologic work has been published about the Tuscarora Mountains. Studies focusing on aspects of regional Eureka County geology (Lehner and others, 1961; Roen, 1961; Roberts and others, 1967) have included the Lynn Window of the southern Tuscarora Mountains. More recently, Evans (1980) has described the geology of the area in more detail, using the name Popovich Formation, first assigned by Hardie (1966, p. 77), to the Devonian carbonate assemblage above the Roberts Mountains Formation. The stratigraphy of the Popovich has recently been studied by Ettner (1989).

METHODS

The bulk of the field work was completed during the summer of 1986, with follow-up excursions during the summers of 1987 and 1988. This included the description and measurement of three biostratigraphic sections in the northern Antelope Range (ANA II/ANA III, WNA I, and WNA II; Fig. 4, Plate 1), one section in the Cortez Mountains (CW I, Fig. 33), one section in the Tuscarora Mountains (WRC I; Plate 1), and sampling of three slide blocks in the southern Fish Creek Range, located in Eureka County and northernmost Nye County (Fig. 2). A total of 56 conodont samples, weighing 5-8 kg each, were collected from new sections (WNA I, WNA II, CW I, WRC I, WFC 1-3) and 6 were resampled in existing sections (ANA II/ANA III), along with numerous lithologic samples. An additional 7 conodont samples collected in the Tuscarora Mountains (WRC I and II), proved unsuitable for formic acid dissolution. All footages are painted on the outcrop in yellow (Amoco footages are red in ANA II and III), except WRC I and II which are not painted, as they are located on Newmont Mining property. Section measurements utilized a Jacobs staff with attached Abney level and a Brunton compass.

At Oregon State University, conodont samples were crushed and weighed before being dissolved in a dilute formic acid solution. Formic acid residues were dried and conodonts picked and glued onto microfossil slides by Claudia Regier. Large residues (in particular, those with a high abundance of quartz sand) were separated in tetrabromoethane until the nontoxic polytungstate solution became available during 1987. Conodont species lists and age determinations were compiled in tables (Tables 2-4, Pl. 2) and each species compared to an Upper Devonian conodont age-range chart, prepared by G. Klapper, for reworking and depositional environment studies. Brachiopods recovered were identified by J. G. Johnson, Oregon State University.

Radiolaria from ANA II 111 were sent to A. R. Ormiston, Amoco Production Co., for identification.

The quartz sand fractions of formic acid residues were weighed and compared to original sample weights, in order to determine quartz sand percentages. Of those, 27 were chosen for ro-tap grain-size analyses. Calculated grain-size statistics were then plotted on cumulative frequency curves, grain-size histograms (Figs. 35-39), and Friedman plots (Friedman, 1961, 1967; Figs. 40-43), as an aid in the determination of depositional environment and quartz sand provenance. Grain-size characteristics were then compared to those of the Oxyoke Canyon Sandstone (sample Dno), Lower Denay Limestone (TA V 0) and other possible quartz sand sources.

A total of 52 thin-sections were made and examined under a petrographic microscope and were assigned carbonate rock names using both the Folk (1962) and Dunham (1962) classifications. Of these, several were chosen for photomicrograph study. Porosity was observed and described in thin section, but because of its general absence, was not quantitatively determined. Additional thin sections were produced from sample WRC I 237 and point-counted to quantify formational thickness loss through stylolitization.

A few acetate peels were made, but these were soon shown to be unsuitable for the majority of rock types represented.

Stratigraphic sections were drafted (Fig. 33, Pl. 1) and compared with related published and unpublished sections.

During the spring and fall of 1989, depositional environment, provenance, paleogeographic, and biostratigraphic interpretations were formulated and the manuscript written. The thesis was presented during the winter of 1990.

REGIONAL GEOLOGY

Central and eastern Nevada rocks are divided into three distinct facies assemblages: (1) an eastern assemblage of shallow-water limestone, dolomite, and quartz sandstone deposited on the carbonate platform; (2) a siliceous and carbonate transitional assemblage deposited on the flanks and within an outer-shelf basin (Matti and others, 1975); and (3), a western assemblage of deep-basinal shale, bedded chert, and rare limestone (Smith and Ketner, 1968). The northern Antelope Range is located near the gradational facies boundary between the eastern and transitional assemblages (Trojan, 1978). A variety of platform, shelf-edge, and outer-shelf-basin lithofacies are repeated in adjacent fault blocks, and a Devonian shelf-to-basin transect is exposed (Johnson and others, 1980). Distribution and sedimentation of these rocks was controlled mainly by eustatic change and epeirogenic uplift (Sandberg and others, 1983). The Devonian rocks of the northern Antelope Range are part of a north-trending limestone belt across Eureka County (Johnson and Sandberg, 1977; Johnson and others, 1980).

From late Llandoveryan time to about the end of Middle Devonian time, shelf sedimentation occurred on a broad, shallow-water inner and middle shelf and in a narrower, outer-shelf basin (Johnson and Murphy, 1984). During the Middle Devonian, the basinal Denay Limestone transgressed the carbonate shelf edge twice in the Eifelian and once during the late Givetian Taghanic onlap (Johnson and others, 1985). During this time, the dolomite front followed the shelf edge cratonward during onlaps, and basinward during a Middle Devonian regression (Johnson and Murphy, 1984). Deposition of the thick Frasnian and lower Famennian sequence began during inundation by the Taghanic onlap (Johnson, 1970; Sandberg and Poole, 1977).

In the Roberts Mountains, the top of the Denay Limestone is placed at the base of a massive bed of bioclastic packstone of the Devils Gate Limestone (Murphy, 1977; Johnson and others, 1980). In the northern Antelope Range, upper Denay Limestone deposition occurred relatively farther offshore, where basinal and allodapic sedimentation continued for some time (Johnson and others, 1980). During Frasnian time, western uplift, associated with early movements of the Antler orogeny, caused sedimentation to shift eastward (Johnson and Sandberg, 1977; Sandberg and Poole, 1977; Johnson and others, 1985). This led, in late Frasnian time, to the formation of the lower Pilot Shale basin, which received limestone turbidites (Sandberg and Poole, 1977).

The formation of the lower Pilot Shale basin isolated Devils Gate Limestone deposition in Eureka County to a narrow north-trending shelf (Johnson and Murphy, 1984). Frasnian to early Famennian sedimentation was characterized by three rapidly deepening events, one of which is probably related to Antler foreland subsidence (Johnson and others, 1985); the deeper water may have provided species with paths of communication across former barriers (Johnson, 1970). Upward-deepening characteristics of the Devils Gate Limestone (Sandberg and Poole, 1977) indicate that shoals of the Devils Gate Limestone were probably drowned, and that Pilot Shale deposition joined Woodruff Formation deposition to the west, on top of the Roberts Mountains allochthon (Johnson and Murphy, 1984).

Continued foreland uplift during Famennian time ended shelf sedimentation in the area, and caused the shelf edge to shift into western Utah (Johnson and Murphy, 1984). This regressive phase continued into an episode of widespread erosion, which lasted until at least the end of the Devonian in many areas (Sandberg and Poole, 1977).

UPPER DEVONIAN CONODONT ZONATION

Upper Devonian conodont zones were redefined by others while this thesis was in preparation.

Ziegler (1962) originally proposed the 29-zone worldwide standard Late Devonian conodont zonation and subsequently made revisions (Ziegler, 1971). Ziegler's standard zonation has been employed widely by workers in both North America and Europe. The Famennian part of the zonation has since been subdivided by Sandberg and Ziegler (1984) to include 21 zones. Revisions to the Famennian part of the standard conodont zonation are not of concern here, with the exception of the *triangularis* Zones above the Frasnian-Famennian boundary, and are discussed elsewhere. Sandberg and Poole (1977) estimate the average length of Upper Devonian conodont zones at approximately 0.5 m.y., based on the thicknesses of biostratigraphic sections in North America and Europe, with the exception of the *Ancyrognathus triangularis* Zone, which may represent as much as 1 m.y. (Sandberg and Poole, 1977, p. 149).

In their paper dealing with the causes for a Late Frasnian mass-extinction event, Sandberg and others (1988b) have replaced the name Uppermost *gigas* Zone (highest conodont zone of the Frasnian; Fig. 7) with *linguiformis* Zone, which is employed where appropriate throughout this work. The base of the *linguiformis* Zone is defined as the first occurrence of *Palmatolepis linguiformis*, and the upper limit is defined by the first occurrence of *Palmatolepis triangularis* (base of the Lower *triangularis* Zone).

Presently, disagreement exists between conodont workers regarding the taxonomy of *Ancyrodella rotundiloba* (see Sandberg and others, 1988a; Klapper, 1988; Johnson, 1989), a species with biochronologic importance regarding the placement of both the base of the Lower *asymmetricus* Zone and the base of the Upper Devonian

Series at Montagne Noir, France. Klapper (1989) has published a temporary Frasnian conodont zonation, subdivisions of which are referred to as Montagne Noir Zones 1-13. Klapper identified all conodonts for this study, and his Montagne Noir zonation is employed throughout. Direct correlations with the standard conodont zonation of Ziegler (1962, 1971) are not yet possible, although Klapper (written comm.) has indicated that the upper part of Montagne Noir Zone 13 correlates directly with the Uppermost *gigas* Zone (*linguiformis* Zone). The Montagne Noir zonation increases the number of subdivisions of the early Late Devonian; therefore each conodont zone may represent less than the estimated 0.5 m.y. suggested by Sandberg and Poole (1977). Figure 7 compares the various Frasnian conodont zonation schemes (Ziegler, 1971; Sandberg and others, 1988b; Klapper, 1989).

Ziegler and Sandberg (in prep.) are revising the Frasnian portion of the standard conodont zonation. Their work is separate from Klapper's, and correlation is presently uncertain between their conodont zones and the Montagne Noir zones of Klapper (1989).

CONODONT ZONE

Ziegler
(1971)Sandberg
and others
(1988)Klapper
(1989)

FAMEN- NIAN	<i>triangularis</i>			U — M — L
	Uppermost <i>gigas</i>	<i>linguiformis</i>	upper part of M. N. Zone 13	
FRASNIAN	<i>gigas</i>		U — L	M. N. Zone 13 — ? —
	<i>A. triangularis</i>			M. N. Zones 6-12
	<i>asymmetrica</i>		U — M — L	M. N. Zone 5 — M. N. Zones 1-4
	Lowermost <i>asymmetrica</i>			
GIV.				

Figure 7. Comparison chart of Frasnian (Upper Devonian) conodont zonation schemes. M. N. = Montagne Noir.

FENSTERMAKER LIMESTONE

NOMENCLATURE

Hose and others (1982, p. 9) named a northern Antelope Range sequence of rocks the Fenstermaker Wash Formation. Their assignment of rocks to that formation included those reported on here, as well as a significant portion of the underlying Denay Limestone (Johnson and others, 1989, p. 178). The base of this new formation would have been equivalent to a level well within the lower member of the Denay Limestone in the Roberts Mountains (Murphy, 1977; Murphy and others, 1978) and as mapped and described earlier in the northern Antelope Range (Trojan, 1978). Hose and others' (1982) usage of the name Fenstermaker Wash Formation is unacceptable (Johnson and others, 1989) to describe rocks above a decapitated Denay Limestone and below the Mississippian Davis Spring Formation in the northern Antelope Range.

Trojan (1978) mapped and described the Devonian rocks of the northern Antelope Range, informally assigning the name Devonian sandstone (Dss) to those rocks stratigraphically above the upper member of the Denay Limestone and below the Davis Spring Formation. Subsequent work on the Denay by geologists of Amoco Production Co. has included remeasurements and additional conodont collections from section TA IV (now ANA II/ANA III) and the addition of a new Amoco biostratigraphic section ANA I, both of which include Trojan's (1978) Dss unit.

The name Fenstermaker Limestone is revised and restricted herein to include only those rocks stratigraphically at and above ANA II 88 in sequence above the top of the upper Denay Limestone (Plate 1) and below the Davis Spring Formation. Its stratigraphic position in the Upper Devonian outer-shelf sequence is shown in Figure 8. The name Fenstermaker remains as the only geographic name close to the map area that

is acceptable in terms of the North American Stratigraphic Code (1983), taking its derivation from Fenstermaker Wash located just east of the area.

The type section for the Fenstermaker Limestone is section ANA II/ANA III (Fig. 5; Plate 1). This section is chosen both for its completeness and because it represents the only locality at which the lower contact of the Fenstermaker with the upper Denay Limestone is well exposed. In this section the lower contact of the Fenstermaker Limestone is chosen approximately 72 ft (22 m) below the contact chosen by Trojan (1978), and includes dip-slope beds above TA IV 255.

THICKNESS AND DISTRIBUTION

The Fenstermaker Limestone is generally well exposed in NNW- and NE-trending outcrop bands in secs. 16, 20, 21, 29, and 30, T. 16 N., R. 51 E. of the northern Antelope Range, southern Eureka County, and in at least two slide blocks adjacent to Cockalorum Wash in the southern Fish Creek Range, northern Nye County, Nevada. Figure 4 indicates the outcrop distribution of the Fenstermaker in the northern Antelope Range and shows the location of measured biostratigraphic sections. Trojan (1978) shows the Fenstermaker (his Dss) at the top of sections TA III and IV. The Fenstermaker is approximately 173 ft thick (53 m) in ANA II/ANA III (Plate 1), thickening to 194 ft thick (59 m) in WNA I and 213 ft thick (65 m) in WNA II to the NW and WNW respectively.

Structural mapping and interpretation of the northern Antelope Range was presented by Trojan (1978). His map indicates strikes within the Devonian section generally N to NW, with dips 19°-35° E. Structure within the Devonian section is

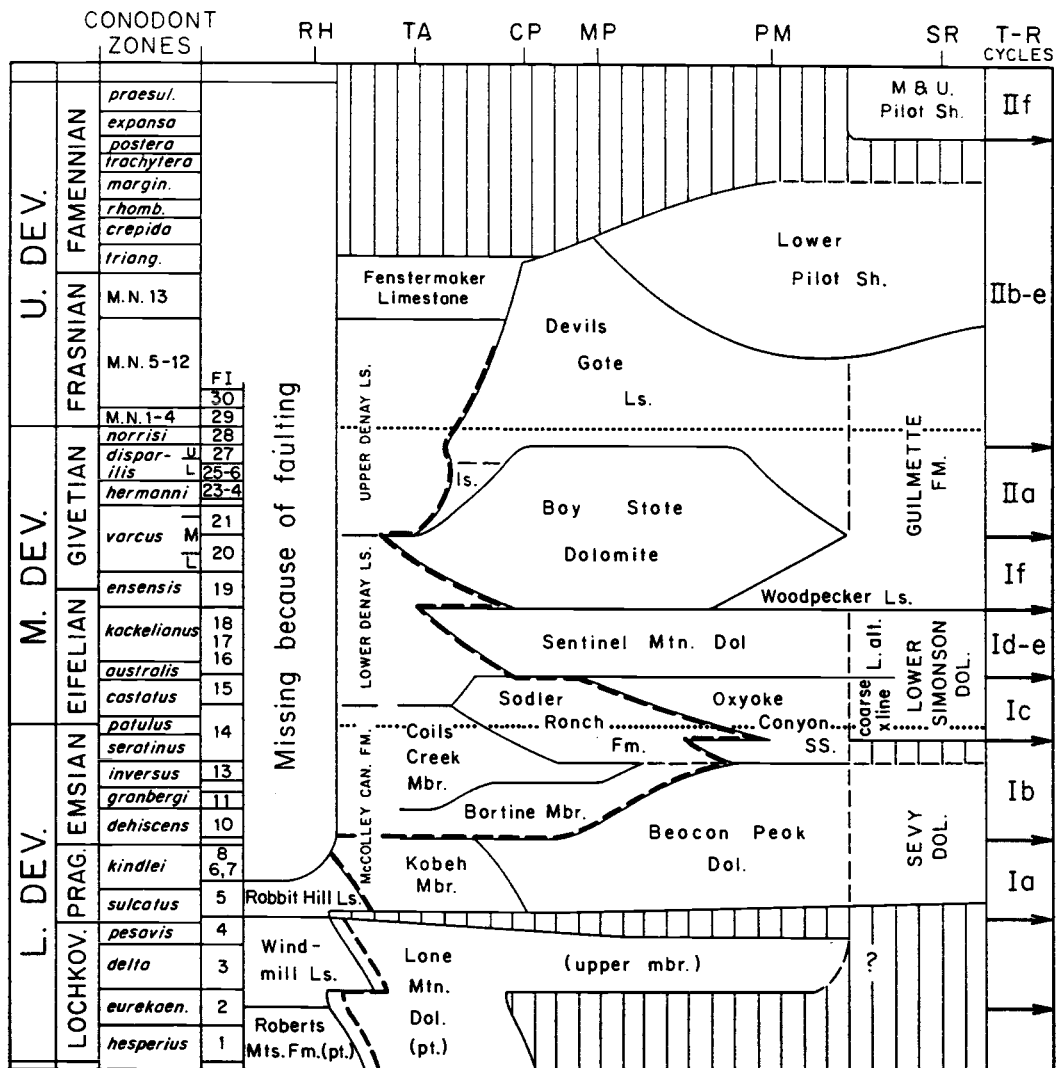


Figure 8. Time-rock transect across Siluro-Devonian outer continental shelf of central Nevada. Heavy dashed line corresponds to carbonate shelf edge. Modified from Johnson and Murphy (1984).

similar to that produced by Tertiary block faulting at other locations within the Basin and Range Province. Of interest here are the dip slopes that occur near the top of the Fenstermaker (Fig. 9) above the main cliff-forming outcrops and below the contact with the overlying Mississippian Davis Spring Formation throughout the map area. Fossil collections made by Trojan (1978) did not include samples above these cliffs, and it was not until John Graham, then of Amoco Production Co., collected and remeasured sections in 1985 that the continuous upsection nature of the dip slopes was discovered. Prior to that discovery the Fenstermaker was not known to span the Frasnian-Famennian boundary.

MEASURED SECTIONS

Two new sections were measured, described, and sampled for fossils in the northern Antelope Range (WNA I, II; Plate 1). In addition, three established sections were studied and new samples taken (ANA I-III). Two slide blocks containing partial Fenstermaker sequences were studied and collected from the southern Fish Creek Range (WFC 1, 3). These outcrops and samples of Fenstermaker Limestone were compared and correlated (Plate 1) with samples taken from other Upper Devonian formations in the southern Tuscarora Mountains (WRC I), southern Cortez Mountains (CW I; Fig. 33), and a published section at Devils Gate (DVG; Sandberg and Poole, 1977), as an aid in the interpretation of paleogeographic relationships and deposition environments.

ANA I was first described and measured by Amoco Production Co. geologists in 1985 (Plate 1). The section is located in the SE 1/4 of sec. 20. Their measurement of the section included 10 fossil collections and short stratigraphic descriptions. ANA I is approximately 290 ft (88 m) thick, extending onto the dip slope above the main cliff-



Figure 9. Dip slope above ANA III 96 cliff showing 30 ft segment of trench dug to expose beds. Upsection is downhill and to the right. Note rock hammer in trench for scale.

forming unit of the Fenstermaker, but ends just short of the Frasnian-Famennian boundary. The lower 175 ft (53 m) of the section is almost entirely covered, and lithologic samples only were collected from the section for this study.

The combined ANA II/ANA III biostratigraphic section represents an integration of Trojan's (1978) TA IV section (8 of his TA IV samples), collections made in 1985 by Amoco (25 samples), and 20 new and recollected samples from this study. ANA II 142 (=ANA III 0) is a laterally traceable wavy (erosional) limestone bed that joins the top of ANA II with the base of ANA III (Fig. 10). The entire combined thickness of the sections is 265 ft (81 m), plus an additional 102-ft (31-m) unzoned interval at the base measured by Heidi Hoffman. ANA II/ANA III is located about 1/4 mi (0.4 km) SSE of ANA I in the NE 1/4 of sec. 29 and is generally well exposed throughout. The combined section is of particular interest because (1) it provides a type section for the Fenstermaker Limestone, displaying a well-exposed, gradational contact with the underlying upper Denay Limestone; (2) a 60-ft (18 m) trench (one-foot sample intervals) was constructed on the dip slope between ANA III 106 and ANA III 126 in an attempt to expose and better document the Frasnian-Famennian boundary; (3) biostratigraphic control (mainly by conodonts) for the Fenstermaker is unrivaled in other sections; and (4), carbonate sedimentary structures are well developed.

WNA I is a new biostratigraphic section with 14 fossil collections; it is approximately 417 ft (127 m) thick and is located along the western range front in the SW 1/4 of the SW 1/4 of sec. 16. It represents the thickest section of Fenstermaker Limestone, although its lower contact with the upper Denay Limestone is not exposed. The basal 168 ft of the section is poorly exposed, but becomes entirely exposed between WNA I 168 and WNA I 331 (main sandy limestone cliff of the Fenstermaker). Exposure is poor to good on the overlying dip slope above the cliff. Although the section includes the Frasnian-Famennian boundary, a fault at the top of the section has



Figure 10. ANA II 142 sandy limestone bed, equivalent to ANA III 0. It is highly undulatory, and scours the underlying thin-bedded mudstone layers.

removed the contact with the Davis Spring Formation.

WNA II is a new biostratigraphic section with 12 fossil collections, and is 409 ft (125 m) thick. Although the lower 196 ft (60 m) of the section are almost entirely covered, the main sandy limestone cliff, as well as the dip slope above, are well exposed (Fig. 11). WNA II is of interest because of the abundant quartz sand layers visible at the base of the main Fenstermaker cliff (\approx WNA II 196-203).

Other measured sections and localities (CW, WBH, WIC, WFC, WRC) are discussed in subsequent sections.

LITHOLOGY AND CONTACTS

The lower contact of the Fenstermaker Limestone is transitional with the upper Denay Limestone. This lower contact is taken at the base of ANA II 88, representing both a horizon just above a large faunal break (discussed below), and the base of a sequence of alternating silty shale and sandy limestone beds (Plate 1). Fossiliferous limestone of the upper Denay, generally below ANA II 63, is not present within the Fenstermaker. Trojan (1978) placed the lower contact at TA IV 163, above the uppermost shale beds. In other northern Antelope Range sections containing the Fenstermaker (ANA I, WNA I, II), the base of the formation is generally covered by upper Denay shale or sandy limestone talus, and the Fenstermaker is first recognized by the appearance of a prominent sandy unfossiliferous cliff-forming limestone, which in the ANA II/ANA III section is located at approximately ANA III 47. This horizon is well within Montagne Noir Zone 13.

The upper contact of the Fenstermaker Limestone with the overlying Lower Mississippian Davis Spring Limestone is concealed everywhere within the study area.



Figure 11. Typical exposure of Fenstermaker Limestone beds in upper WNA II section (foreground), above the main cliff. Hills in background are of overlying Mississippian Davis Spring Formation. Assistant for scale.

In general, the upper 10-20 feet (3-6 m) of the Famennian dip slope is covered by scree from the overlying formation. The stratigraphic transition from Fenstermaker Limestone to Davis Spring Formation is abrupt and readily recognized in the field both by a change from medium gray, medium to thick-bedded sandy limestone to light brown to dark yellowish orange, very thin-bedded mudstone and shale, and by a change from dip-slope topography to an uphill-rising section. The contact between the Fenstermaker and the Davis Spring is believed to be erosional, based on missing conodont zones and equivalent Upper Devonian-Lower Mississippian eastern-assemblage sequences in east-central Nevada.

In outcrop, the Fenstermaker Limestone is mainly light olive gray to medium gray on weathered surfaces, and medium gray to medium dark gray on fresh surfaces. Nearly all outcrops emit a noticeable fetid odor on breakage.

The formation is composed almost entirely of sandy limestone which crops out as prominent cliffs and ledges throughout the study area, except in the lower part of the formation (ANA II 88-ANA III 47), where the number and thickness of sandy limestone beds progressively increase upwards and replace shale. In the southern Fish Creek Range, it forms low, rounded outcrops. Thick to massive bedding (2-3.5 ft (0.61-1.1 m) thick) is revealed as a series of amalgamated beds (0.5-1 ft (0.15-0.3 m) thick) where bioturbation has not destroyed the alternating sequence of quartz-rich and peloid/intraclast-rich layers. This rhythmic bedding is preserved between WNA II 196-203 and to the north and south of WNA II along the western range front, as well as in isolated occurrences between ANA I and ANA II/ANA III (Fig. 12). Abundances of iron-stained quartz sand are also preserved in stylolites which trend both parallel to, and at high angles to, bedding planes. Moderate yellowish brown to grayish orange quartz-sand rich layers weather in relief over the peloid-rich layers. The laminated nature of these beds suggests sorting of the quartz-sand fractions during deposition.



Figure 12. Rhythmically alternating beds of quartz-rich limestone and peloid-intraclast-rich limestone between ANA I and ANA II/ANA III. Quartz-rich beds are darker and weather in relief.

Selected quartz-sand percentages for the Fenstermaker Limestone are given in Table 1. One large hand sample from WNA II 196 contains a few quartz-sand layers which suggest low-angle cross-laminations (Fig. 13). Rarely, faint laminations resembling dish and flame structures are observed.

Of particular interest is the ANA II 142 (=ANA III 0) "wavy" bed (Figs. 10, 14). This laterally traceable bed scours into the limy mudstone layers below, demonstrating some current energy during deposition of the formation. The bed is not the product of structural folding or slumping because it clearly scours underlying strata, and siltstone layers above the bed are parallel to those below. Aside from these few megascopic features, most outcrops lack carbonate sedimentary structures.

In section ANA II/ANA III, where the lower part of the Fenstermaker is exposed, limestone beds separated by limy mudstone and siltstone layers identical to those of the upper Denay, are bounded by dusky red to dark reddish brown chert layers 1-3 inches (2.5-7.6 cm) thick. Only a few beds above ANA III 47 show this relationship. These chert layers are secondary diagenetic features, and chert nodules, up to about 4 inches in diameter, are common in the sandy limestone cliffs just south of ANA I (Fig. 15) and at a few localities in the western range front, suggesting a deeper water depositional environment.

Iron-oxide-rich calcite veins are common throughout as are isolated iron stringers, both of which are considered to be diagenetic in origin.

Megafossils are rare to absent in most hand samples. Some fragments of thin-shelled brachiopods and tabulate coral (probably *Favosites* sp.) were observed. An exception is ANA III 126, which has yielded at least three species of brachiopods, as well as coral and algal fragments. More rarely, small fragments of stromatoporoids are observed.

TABLE 1. SELECTED QUARTZ SAND WEIGHT PERCENTAGES

SECTION	SAMPLE	% QTZ. SAND	SECTION	SAMPLE	% QTZ. SAND
ANA I	0	15.65	ANA III	0	15.61
	175	13.78		8	19.12
	189	13.64		22	14.61
	235	13.73		33	13.67
	245	15.57		47	13.81
	255	13.14		56	13.74
	265	13.94		66	11.33
	275	16.29		76	10.65
	280	10.21		96	15.06
	286	14.56		106	14.94
	290	14.37		107	5.06
				108	4.27
ANA II	98	21.33		110	14.11
	103	18.11		111	2.91
	142	10.72		112	5.41
WNA I	334	0.78		114	6.62
	339	0.69		115	3.55
	344	0.55		116	5.55
	352	0.72		117	15.99
	354	0.41		123	0.18
	389	0.11		126	12.93
	395	0.11		133	10.76
	417	0.11			



Figure 13. Large, oriented hand sample from WNA II 197. Light-colored laminations are quartz-sand rich and weather in relief. Note possible cross-bedding defined by quartz sand.



Figure 14. Erosional scouring by ANA II 142 thick sandy limestone bed into underlying thin-bedded mudstone layers. This feature cannot be produced by slump folding or tectonic folding as mudstone layers are truncated.



Figure 15. Secondary chert nodules in sandy limestone cliff just south of the ANA I section.

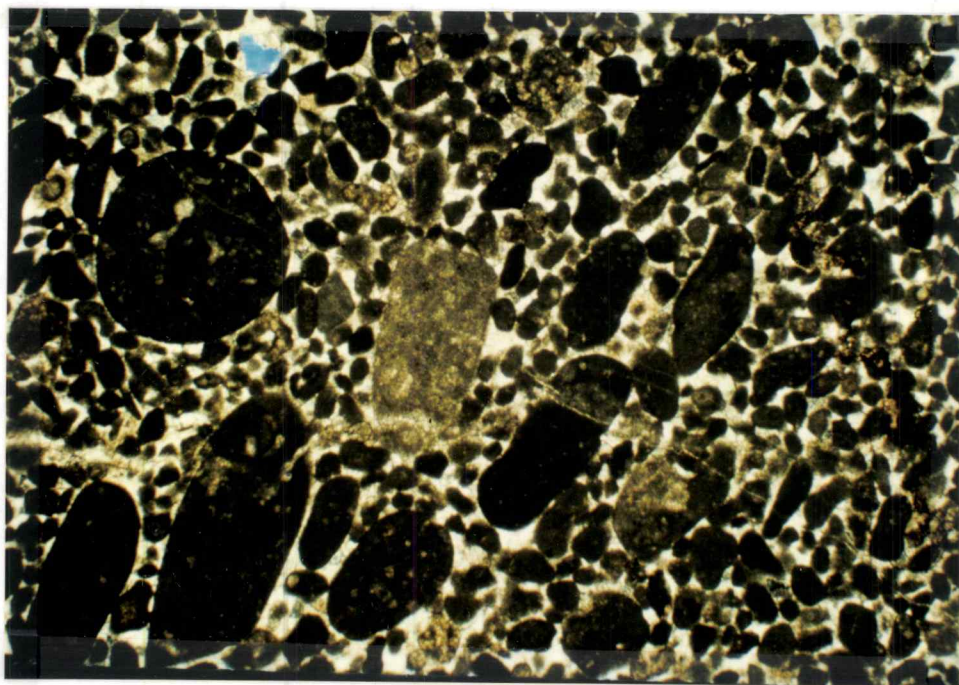
PETROGRAPHY

A total of 52 thin sections from the Fenstermaker Limestone were examined as an aid in determining microfacies, depositional environments, and diagenetic relationships. With the notable exception of silty calcareous shale that is interbedded with sandy limestone in the lower part of the Fenstermaker, all studied samples are classified as sandy intrapelsparites (*sensu* Folk, 1962). Rocks of this type may be classified as microclastic limestones (*sensu* Plumley and others, 1962) or sandy peloidal packstones and grainstones (*sensu* Dunham, 1962).

Small spherical to elliptical grapestone intraclasts, generally 0.5-2 mm in maximum dimension, are seen in thin section to be composed of partially-lithified clumps of peloids which were eroded and redeposited as a nongraded mixture of peloids and quartz sand. Intraclasts of this type have been attributed to an origin as "miniresediments" (Wilson, 1969) and compose 5-75% of samples examined (Fig. 16A). This interpretation contrasts with the more commonly observed peloidal grapestone (see Illing, 1954; Taylor and Illing, 1969) in which patches of spar are "trapped" between lithified bunches of peloids. Grapestones attain their rounded shape from being rolled back and forth in a shallow, moderate-energy wave or current environment. Individual peloids averaging 0.1-0.5 mm in long dimension are probably fecal pellets, as opposed to micritized skeletal or oolitic grains, as the majority contain inclusions of calcispheres and quartz silt (Fig. 16A). Furthermore, there is no indication that peloids "developed" around central nuclei. Polychaete worms were probably responsible for much of the observed fecal material (Bathurst, 1975, p. 138).

Calcispheres of unknown affinity constitute 1-6% of the rock (mainly as inclusions within pellets and intraclasts) and represent the majority of observed allochems. Most appear as single-walled non-spinose forms and are spherical to

A.



B.

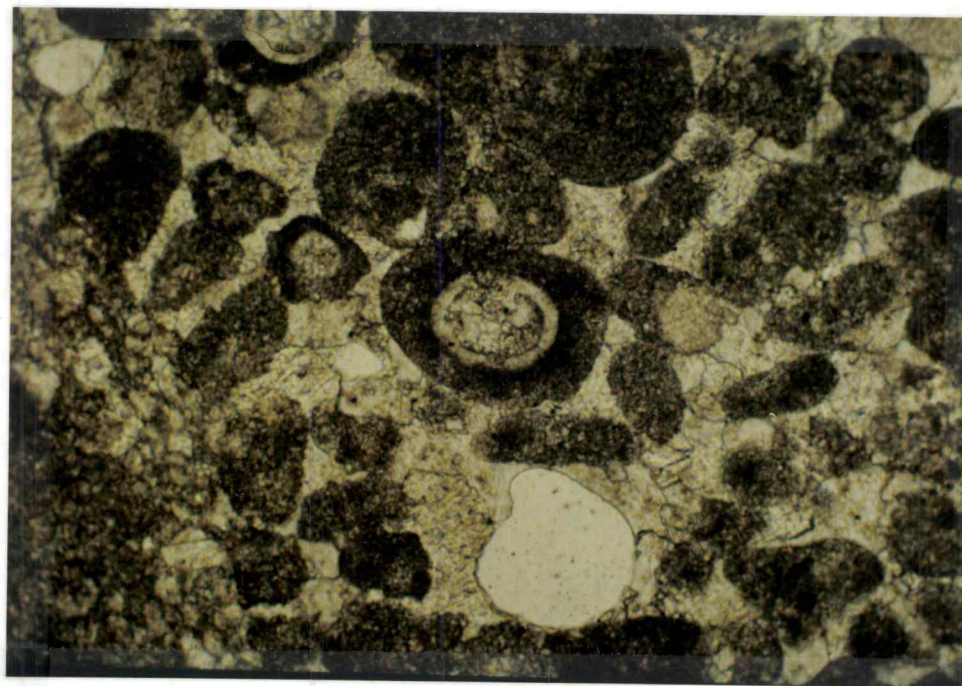


Figure 16. A) Photomicrograph of ANA I 0 showing typical mixture of pellets and intraclasts. Detrital quartz grain upper left (crossed polars; field of view approx. 6.7 mm). B) Photomicrograph of ANA III 116 showing double-walled calcispheres in peloids (plane light; field of view approx. 1.3 mm).

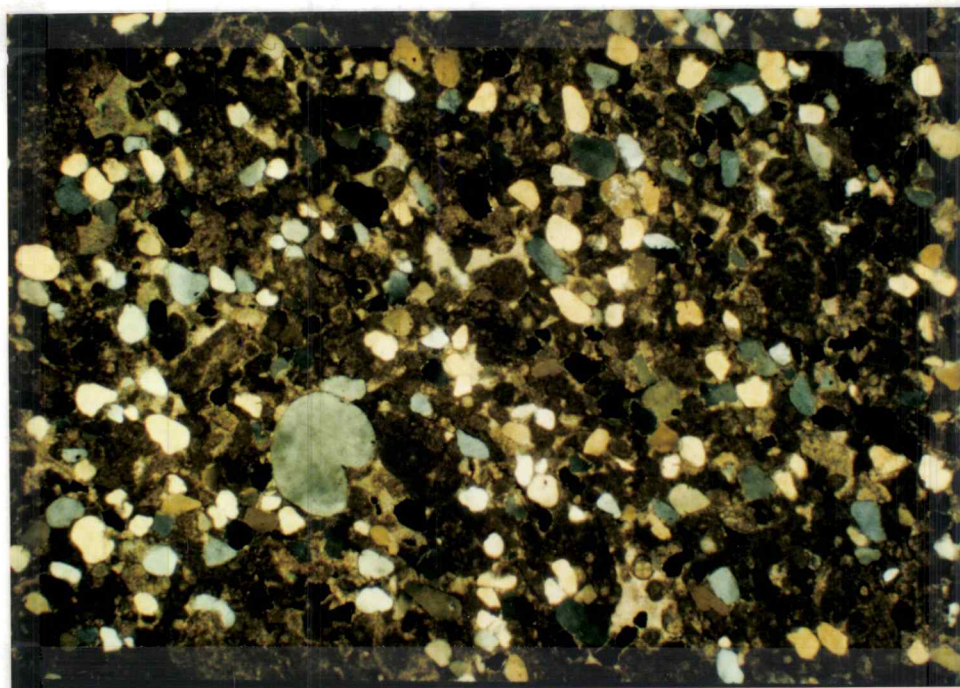
slightly oval. In sections displaying a lesser degree of neomorphism, calcispheres are seen to be composed of a double-walled structure (Fig. 16B) with radiating calcite between the walls and a blocky microspar core. Nearly all calcispheres display a pseudouniaxial cross under crossed polars. Rupp (1967) noted the similarity between calcispheres and the fruiting cases of the living dasycladacean alga *Acetabularia*, which originates in water depths averaging 3-5 m, but no deeper than 12-15 m (Ginsburg and others, 1971).

Detrital quartz sand constitutes 1-22% of all samples (Table 1) as determined by weighing silicic formic acid residues and confirmed through thin-section estimates. Utilizing Powers (1953) classification scheme, individual quartz sand grains are subrounded to well-rounded (Fig. 17A) and range between low and high degrees of sphericity. A tendency toward a bimodal distribution of these grains is noted, and the significance of this bimodality as well as other grain-size parameters is discussed in a subsequent section.

Crinoid fragments with large syntaxial calcite overgrowths are present in nearly all thin sections (<1-1%). The presence of echinoderms in these samples indicates that final Fenstermaker depositional environments must have been in well-circulated, normal marine water (Fig. 17B). The remaining allochemical constituents in these rocks are rare brachiopod (<1%) and coral (<1%; Fig. 18A) fragments. Conodonts, although common to abundant in formic acid residues, were not observed in thin section.

These rocks are entirely calcite; no primary or secondary dolomite was noted, either in alizarin-red-stained slabs or in thin section.

A.



B.

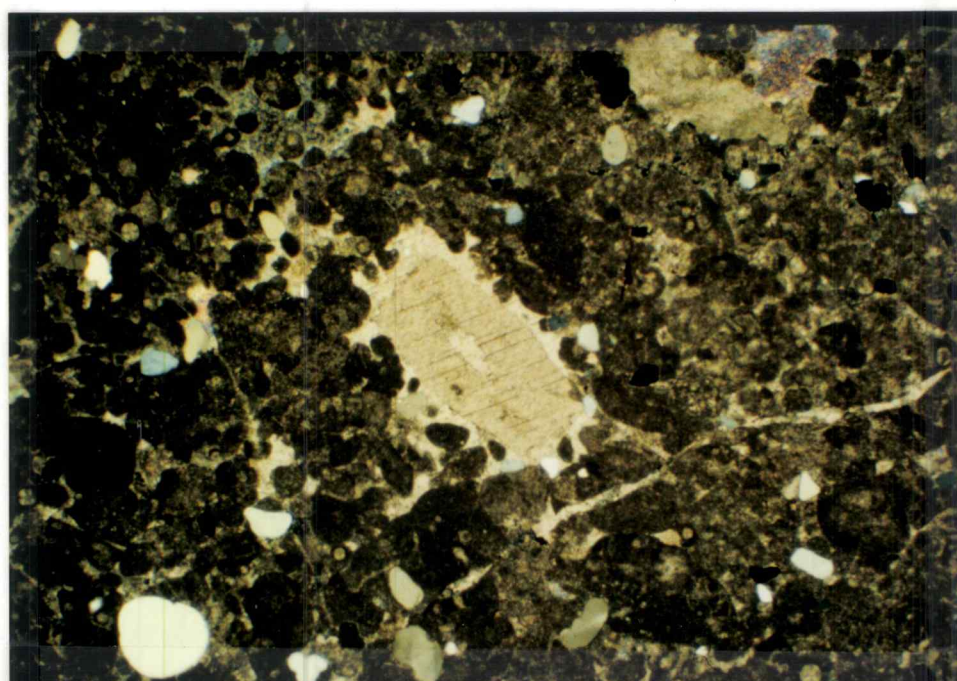
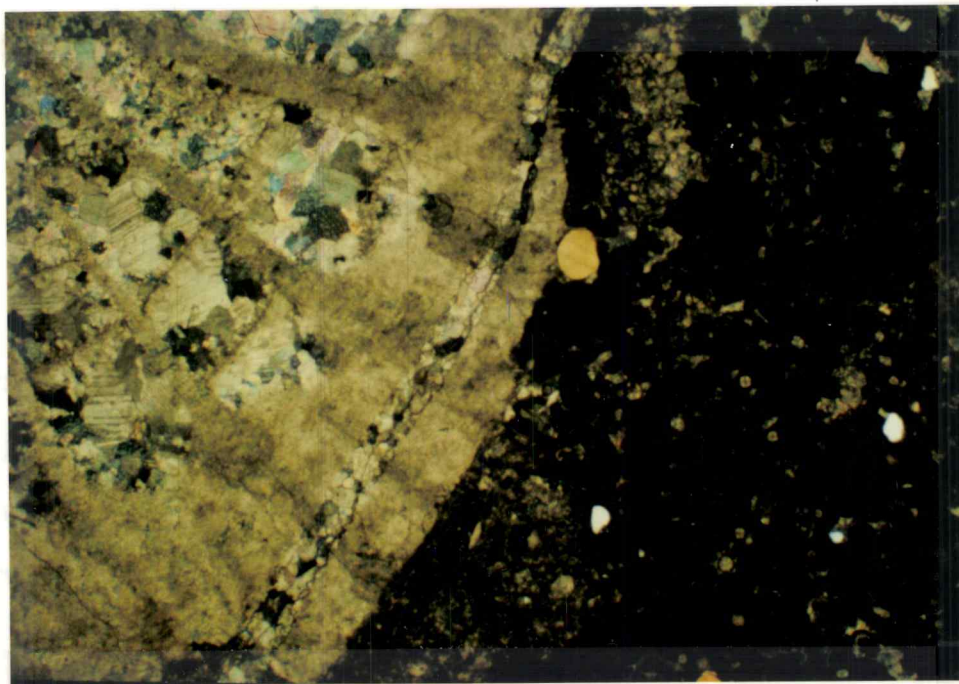


Figure 17. A) Photomicrograph of TA IV 185 showing unusually high detrital quartz-sand percentage (crossed polars; field of view approx. 6.7 mm). B) Photomicrograph of crinoidal fragment with syntaxial rim cement (ANA III 107; crossed polars; field of view approx. 6.7 mm).

A.



B.

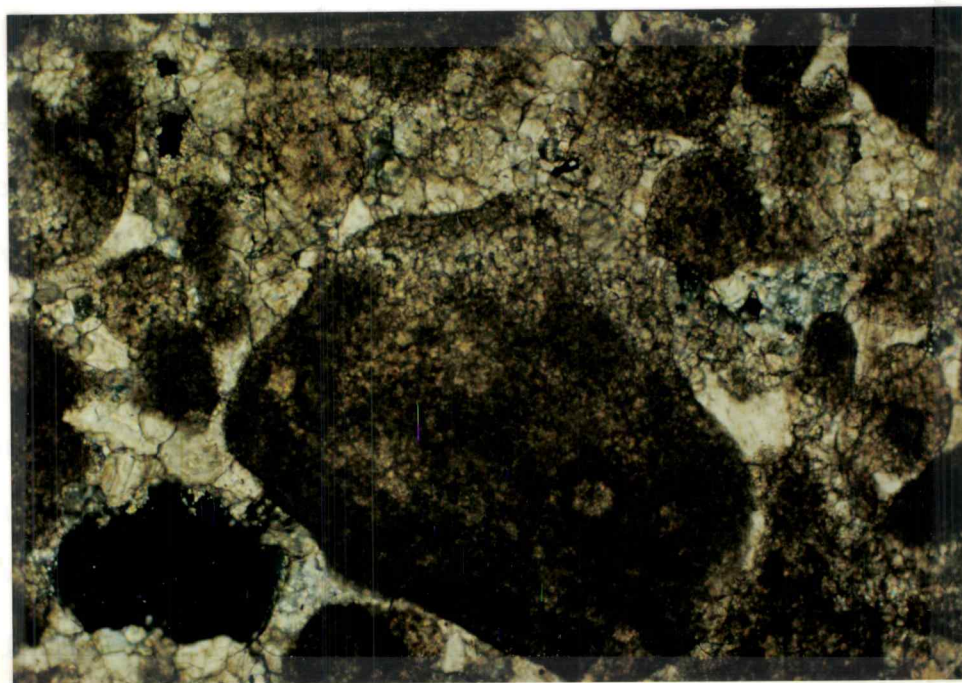


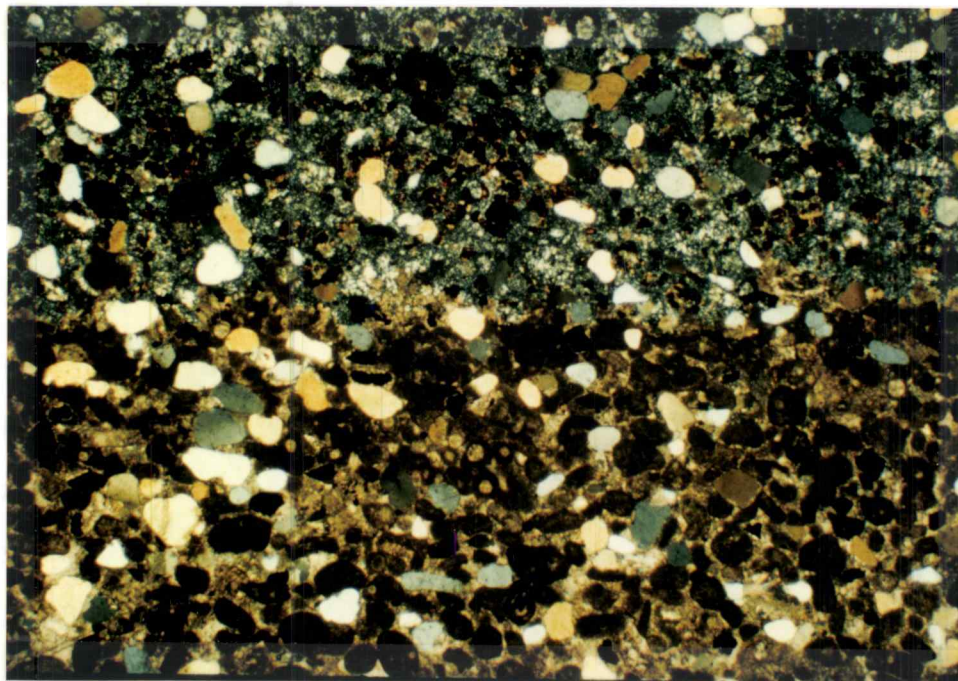
Figure 18. A) Photomicrograph of coral from ANA I 280 with intraparticle sparry calcite cement fill (crossed polars; field of view approx. 6.7 mm). B) Photomicrograph of WNA I 2 showing incipient neomorphism (to microspar) of peloids/intraclasts (crossed polars; field of view approx. 1.3 mm).

DIAGENESIS

The majority of Fenstermaker Limestone samples have been winnowed of micrite mud and cemented with sparry calcite. Samples having retained a higher percentage of micrite between peloids and intraclasts are cemented by neomorphic microspar and, to a lesser extent, pseudospar. Neomorphism (both porphyroid and coalesive; Folk, 1965) has obscured internal peloid and intraclast components and grain boundaries (Fig. 18B) in many samples.

In outcrop, limestone beds in the lower part of the formation (visible between ANA II 88 and approximately ANA III 22) that are interbedded with calcareous shale layers are bounded on top and bottom by 1-3 inch thick (2.5-7.6 cm), reddish brown chert layers. In thin section, these chert layers are clearly secondary in origin (Fig. 19A), because depositional products such as detrital quartz sand and peloids straddle limestone-chert boundaries. These chert layers are probably the result of siliceous sponge spicule and radiolaria dissolution and silica migration from intervening shale or mudstone beds, and indicate deeper-water deposition (Wilson, 1969). Both sponge spicules and radiolarians were recovered from the shale bed ANA II 111 (Appendix A). Chert layers are enriched in iron-oxide blebs and stringers, but retain identical quartz-sand percentages as in the unaltered parts of sandy limestone beds. This iron oxide is probably siderite (FeCO_3 ; Fig. 19B) as suggested by its characteristic optical properties, brown color, and perfect rhombic form. Bissel (1959) believed that an increase in chert per unit volume of sediment occurred in miogeosynclinal carbonates with increasing distance from the craton. Ogren (1961, p. 24) described thin limestone beds in the Mississippian Fayetteville Shale in which the upper and lower bed surfaces were near the craton margin, replaced by chert, and as in the lower Fenstermaker, the

A.



B.

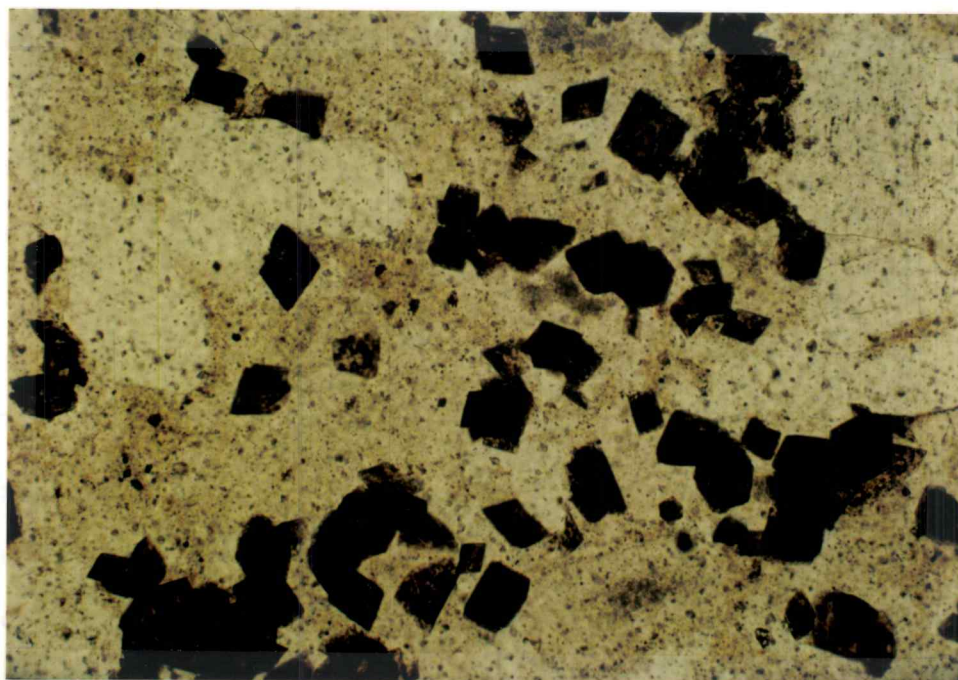


Figure 19. A) Photomicrograph of TA IV 100 showing contact between chertification front (above) and unaltered sandy limestone (crossed polars; field of view approx. 6.7 mm). B) Close-up of (A) showing iron-oxide rhombs, probably siderite, in chert layer (plane light; field of view approx. 1.3 mm).

centers of the beds were unaltered limestone. His study showed an increase in limestone silicification basinward, with complete chertification occurring only in deep-water miogeosynclinal beds.

Quartz sand grains recovered from formic-acid residues show pitting and frosting similar to that observed on surfaces of eolian-transported sand. Thin-section analysis reveals a diagenetic etching origin for the pitting and frosting (Fig. 20), as nibbling and embayment of the grains by neomorphic microspar.

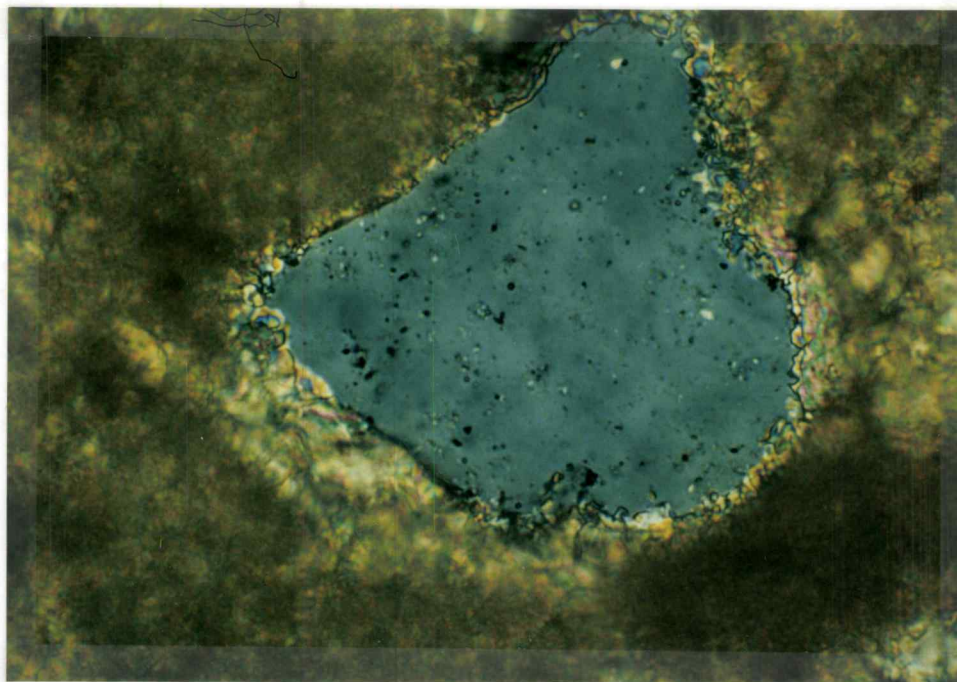
Porosity is generally nonexistent ("tight") or constitutes $<<1\%$ in all studied samples, both in outcrop and in thin section. Conversely, one sample (WNA I 2) displays patchy cement-reduced eogenetic mesopore intercrystalline porosity (crSe-smsBP($\leq 5\%$)-in the Choquette and Pray, 1970 classification scheme), as a result of incomplete calcite cementation between peloids.

Randomly-oriented veins of mosaic sparry calcite are common, but not abundant, and transect all allochemical rock constituents.

Quartz-sand and iron-oxide stylolites (Fig. 21A) are a common pressure-solution feature, representing a significant loss of depositional thickness through carbonate dissolution. Elsewhere, stylolites are believed to be responsible for thickness reductions up to 20-35% (Bathurst, 1975, p. 460), and the carbonate thus released may account for much late-stage diagenetic calcite cement. Bathurst recognizes that stylolites must have been formed after initial (first generation) cementation (p. 470), as they transect cement. This relationship is observed in Fenstermaker stylolites. In a few samples (e.g. WNA I 12; Fig. 21B) iron-oxide stained stylolites and "seams" transect post-cementation calcite veins, thereby demonstrating stylolite formation prior to calcite-vein emplacement.

Thin-section evidence described above indicates that peloid micritization and ongoing post-depositional neomorphism (including diagenetic quartz-grain etching) was

A.



B.

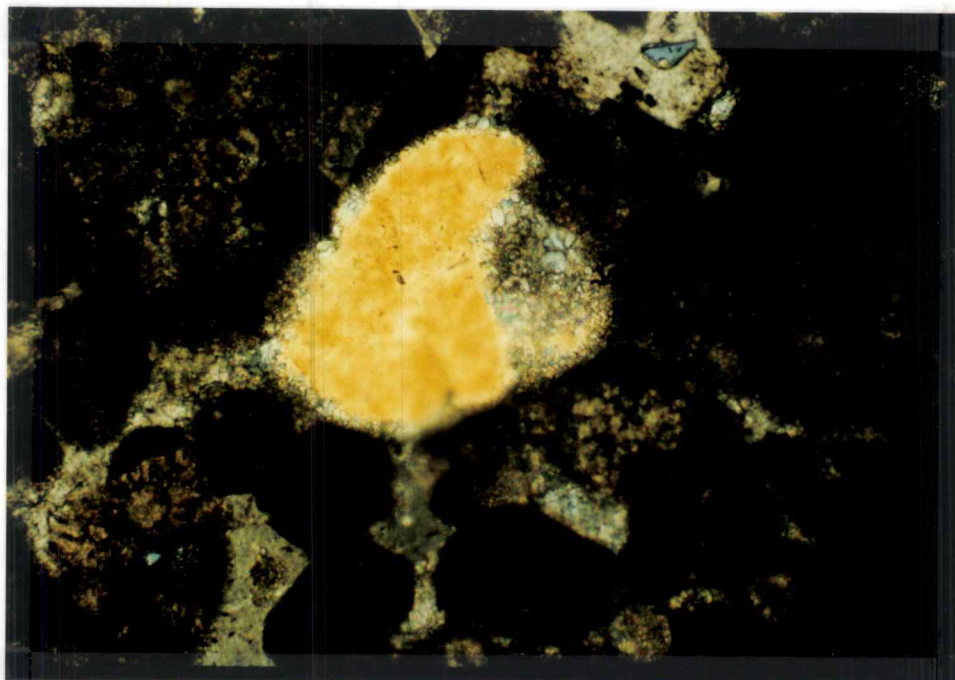
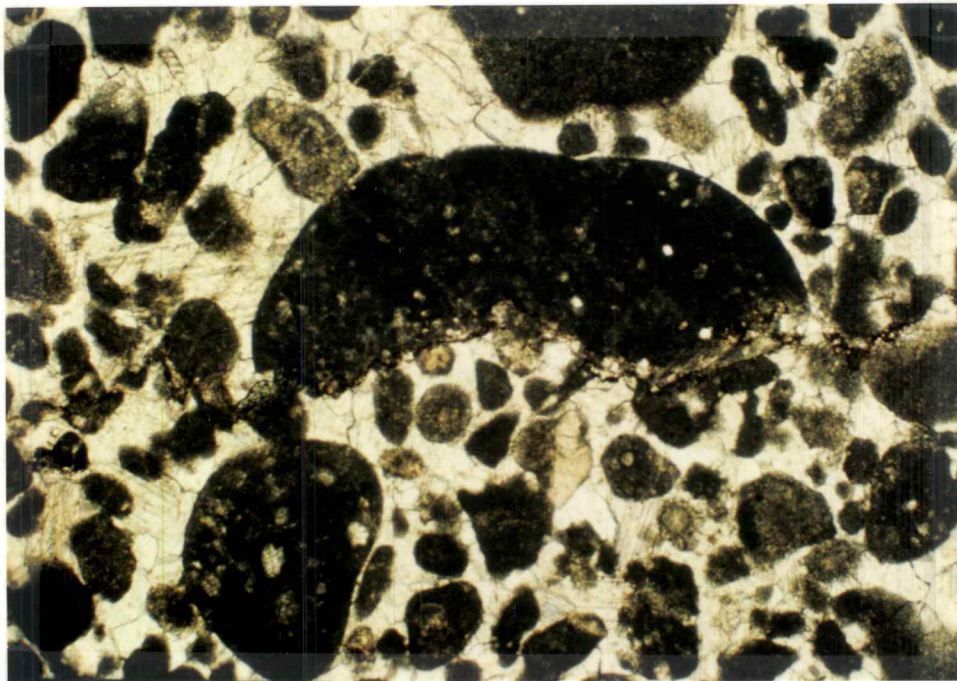


Figure 20. A) Photomicrograph of detrital quartz grain from WNA I 6 demonstrating diagenetic etching by neomorphic microspar (crossed polars; field of view approx. 1.3 mm). B) Photomicrograph of ANA I 286 showing partial replacement of detrital quartz grain by neomorphic microspar (crossed polars; field of view approx. 1.3 mm).

A.



B.

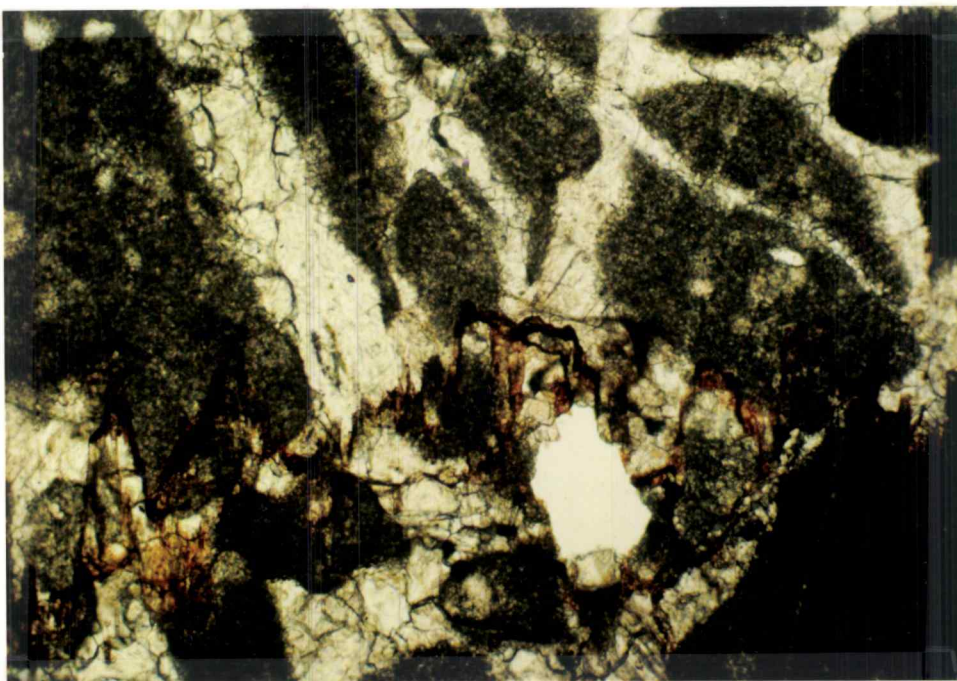


Figure 21. A) Photomicrograph of ANA III 122 iron-oxide-rich stylolite truncating intraclast (plane light; field of view approx. 3.3 mm). B) Photomicrograph of WNA I 12 showing stylolite crossing sparry calcite vein (plane light; field of view approx. 1.3 mm).

accompanied by early (eogenetic) intergranular sparry calcite cementation in at least two stages, the second stage being more iron-oxide rich. Syntaxial rim cementation of crinoidal fragments seems to have preceded or was simultaneous with sparry calcite pore filling. Cementation was followed by calcite-vein emplacement, and finally stylolite growth, in response to pressure solution at depth. There is no indication that these rocks have undergone hardground, vadose zone, or early submarine cementation. Partial chert replacement of these beds probably occurred (as elsewhere) prior to rock consolidation (Harris, 1958), although no visible evidence substantiates such a conclusion.

BIOSTRATIGRAPHY

CONODONT BIOSTRATIGRAPHY

The way in which conodont zones of the Upper Devonian are divided was undergoing major revision during the present study. Klapper's (1989) Montagne Noir zonation scheme (Fig. 7) is employed here, as Klapper performed all conodont identifications and zonal assignments pertaining to this work. A more thorough description of these changes is given under an earlier heading.

The Fenstermaker Limestone ranges in age from Upper Devonian (Frasnian) Montagne Noir (M. N.) Zone 13, or possibly the highest part of M. N. Zone 12, through the lower part of the Famennian Middle *triangularis* Zone, as indicated by numerous conodont collections from sections ANA I-III and WNA I-II. Plate 1 is a stratigraphic correlation chart based on these collections employing the entry of *Palmatolepis linguiformis* (base of the upper part of M. N. Zone 13) as a datum. Conodont collections are listed in Appendix A, and species checklists are given in Tables 2-4 and Plate 2.

Conodont sampling in combined sections ANA II/ANA III (originally TA IV) is the most complete, integrating samples from Trojan's (1978) work in the northern Antelope Range, with those of Amoco Production Co. (collected by J. Graham in 1985) and many new collections from this study (53 total collections). At least 86 species of conodonts have been recovered from the combined sections thus far (Appendix A). All footages of beds sampled for conodonts are painted on the outcrop; ANA footage numbers are in red, Trojan's (TA IV, 1978), as well as footage numbers from this study, are in yellow.

TABLE 2. ANA I CONODONT CHECKLIST

ANA I Collection	175	189	235	245	255	265	275	280(A)	280(B)	286	290
Feet in section	175	189	235	245	255	265	275	280	280	286	290
An. nodosa	X							X	X	X	
Pa. sp. indet.	X	X					X				X
P. sp. indet.	X	X					X				
Pa. aff. Pa. coronata		X	X	X	X		X	X	X	X	X
Pa. sp. T		X	?	X	X			X			
An. sp. indet.		X	X	X		X					
P. lodinensis		X	X	X	X		X	X	X	X	X
I. spp.		X						X		X	
Pa. rhenana			X			X		X	X	X	X
Pa. winchelli			X						X		X
An. ioides			X					X			
An. nodosa -> An. ioides			X		X					X	X
P. imparilis group			X								
Pa. n. sp. P, form 2				X	X	?				X	X
I. alternatus					J		X		X		X
P. brevis						X					
P. imparilis						X		X	X	X	X
O. postera						X					
M. sp.						X					
Pa. rhenana morph. B								X	X		X
Pa. linguiformis								X	X	X	X
A. n. sp. (broad)								X	X		
P. brevis group								X	X		X
P. unicornis								X			
O. "confluens" homeomorph								X	X		
Pa. sp.									X		
A. n. sp. (aff. "bifurcatus")									X	X	X
P. angustidiscus									X	X	
P. brevicarina									X	?	
M. gradata									X		
Belodella spp.									X	X	
aff. Pa. n. sp. P., form 2										?	
Pa. semichatovae										?J	
Pa. domanicensis										X	
A. sp. (cf. amana)										X	
An. gigas form 3											X
An. curvata, late form											X
An. sp.											X
A. sp.											X
P. evidens											?
I. subterminus											X
Pel. planus											X
Conodont zone	?	M.N. Zone 13						Upper part of M.N. Zone 13			

TABLE 3. WNA I CONODONT CHECKLIST

WNA I Collection	168	1	2	3	4	5	6	7	8	9	10	11	12
Feet in section	168	331	334	339	344	346	349	352	354	389	395	400	417
Pa. n. sp. P, form indet.	X												
P. samueli	X												
P. imparilis	?						X	X	X		X	X	
P. lodinensis	X	X			X	X	X		X			X	
P. spp.	X								X				X
An. nodosa	X			X					X				
A. sp. indet.	X												
Pa. rhenana		?							X				
Pa. sp. indet.		X	X	X	X	X	X	X	X	X		X	X
An. sp. indet.		X										X	
P. brevis group		X					X					X	
P. sp. indet.			X	X	X	X	X	X	X				
Pa. rhenana morph. B				X	X	X							
P. unicornis					?								
Pa. winchelli						X						X	
M. spp.						X			X	X			X
Pa. sp. T							X		X				
Pa. aff. Pa. coronata							X						
Pa. linguiformis									X				
Pa. hassi									?				
Pa. delicatula										?			
I. alternatus										X	X		X
P. brevilaminus										X	X	X	X
Pa. triangularis											X		X
Pa. delicatula subsp. indet.											X		
Belodella spp.												X	X
Conodont zone	M.N. Zone 12	M.N. Zones 12-13					M.N. Zone 13			M. triangularis Zone			
							U. part of M. N. Zone 13			triangularis Zone undifferentiated			

TABLE 4. WNA II CONODONT CHECKLIST

WNA II Collection	1	170	196	227	245	289	303	323	341	363	386	409
Feet in section	1	170	196	227	245	289	303	323	341	363	386	409
Pa. disparalvea	X											
P. webbi	X	X										
P. dengleri	X											
P. dubius	X											
P. spp.	X					X						
S.? gracilis	X											
S. sp.	X											
Pa. aff. Pa. coronata		X							X			
Pa. sp. T		X							X			
Pa. rhenana		X							X		?	
Pa. winchelli		X										
Pa. n. sp. P, form 2		X		X			X					
An. nodosa		X		X		X						
An. nodosa -> An. ioides		X										
A. tsiensi		X										
Ancyrodelloides? h-morph		X							X			
P. brevis		X										
P. lodinensis		X	X		X			X	X		?	
P. pacificus		X							X			
P. decorosus		?										
P. n. sp. R		X		X								
P. imparilis		X					X		X	X		
I. alternatus		X							X		X	
Pel. planus		X										
O. sp.		X										
Belodella sp.		X										
Pa. n. sp. P, form indet.			X									
Pa. sp. indet.			X	X	X	X				X		X
P. citreumae			X									
P. sp. indet.			X	X	X		X			X		X
I. sp. indet.			X			X						X
A. sp. indet.				X					X	X		
P. unicornis				X								
An. sp. indet.								X				
Pa. linguiformis									X			
A. n. sp.									X			
An lobata									?			
Pand. insita									X			
P. n. sp.										X		
Pa. delicatula delicatula											X	
Pa. triangularis											?	
P. brevilaminus											X	
Conodont zone	Upper disparilis Zone								M.N. Zone 13		Upper part of M.N. Zone 13	M. triangularis Zone

ANA II/ANA III is approximately 265 ft (81 m) thick, but may be extended to include an additional 102 ft (31 m) below ANA II 0, as measured by Heidi Hoffman (written comm.), above a prominent Middle Devonian cliff which crops out close to the jeep trail. The base of the Fenstermaker Limestone is taken at ANA II 88 on the basis of lithologic changes at that horizon, but is nearly coincidental with the base of M. N. Zone 13. A large collection taken from ANA II 88 is M. N. Zones 12-13 in age, and a collection 10 feet (3 m) above (ANA II 98) is assigned to Zone 13. The base of the Fenstermaker is poorly exposed elsewhere in the northern Antelope Range.

The ANA II/ANA III section encompasses conodont zones from as low as the Upper *disparilis* Zone up into the Middle *triangularis* Zone. With the exception of TA IV 40 and 63, M. N. Zones 1-12 are poorly represented between TA IV 12 to ANA II 88, because most beds within this interval are composed of deep-water shale and mudstone composing a condensed sequence. Deeper water, probably outer-shelf-basin hemipelagic beds of this nature are not easily sampled for conodonts and were deposited slowly enough to account for the restriction of M. N. Zones 1-11 to a 76 ft (23 m) interval.

M. N. Zone 13 (approximately equivalent to the Upper *gigas* Zone and *linguiformis* Zone of the standard zonation (J. G. Johnson, pers. comm.)) is very thick in ANA II/ANA III, spanning at least 140 ft (43 m) between ANA II 98 and ANA III 248, and notably thicker in WNA II (Plate 1). Such a zonal expansion indicates rapid deposition for most of the Fenstermaker, and is supported by the fact that this interval contains fewer mudstone and shale beds than those below. No mudstone beds are present within the Fenstermaker Limestone above ANA III 22.

Sixteen samples were taken in a 60-ft (18 m) trench dug between ANA III 106 and ANA III 126 (partially shown in Fig. 9), in an attempt to better locate and describe lithologic and biostratigraphic changes that may have occurred across the Frasnian-

Famennian boundary. The limited information obtained from these collections, obtained at one-ft (30-cm) intervals across the boundary, is given in a subsequent section. The Frasnian-Famennian boundary, or the faunal changeover that occurred between the upper part of M. N. Zone 13 (equivalent to the *linguiformis* Zone of Sandberg and others, 1988b, and the Uppermost *gigas* Zone of an older zonation) and the Lower *triangularis* Zone occurs between samples ANA III 117.5 and ANA III 119. Conodont collections from this section, as well as other northern Antelope Range sections, demonstrate a very thin to entirely absent Lower Famennian Lower *triangularis* Zone, as has been observed elsewhere in east-central Nevada (Sandberg and others, 1989).

From the faulted base of ANA I up to ANA I 189 the section is mainly covered, the ANA I 189 collection being within M. N. Zone 13. It is a reasonable assumption that ANA I 189 occurs well above the base of M. N. Zone 13, considering its stratigraphic position below ANA I 280, dated as the upper part of M. N. Zone 13, and lithologic correlation with ANA II/ANA III (Plate 1) about 1/4 mi (0.4 km) to the southeast. A date of upper part of M. N. Zone 13 is given by the ANA I 290 collection, but the section has not been sampled to the top. The few stratigraphic meters of dip-slope on sandy limestone above ANA I 290 may straddle the boundary with the Lower *triangularis* Zone. Back-hoe trenching in the future below ANA I 235 and ANA I 175 could reveal the base of the Fenstermaker, improving the knowledge of this section.

WNA II is located about 2/3 mi (1.1 km) west-northwest of ANA II/ANA III. Although the lower 170 ft (52 m) of the section are mainly covered, a date of M. N. Zone 13 has been determined for WNA II 170. Only WNA II 341 and WNA II 386 were positively dated above (upper part of M. N. Zone 13 and Middle *triangularis* Zone respectively), but are sufficient to provide a good correlation with the ANA II/ANA III Fenstermaker type section. This correlation indicates that the sandy limestone facies of the Fenstermaker is significantly thicker along the northeast-trending range front

(sections WNA I and WNA II) than in ANA I and ANA II/ANA III. The WNA II section extends up into the Lower Famennian Middle *triangularis* Zone, with no collections recovered from the Lower *triangularis* Zone.

The WNA I section is located about 1 1/4 mi (2 km) northeast of the WNA II section. This section is poorly dated in terms of conodont zonation below the prominent sandy cliff; however, several samples on the dip slope constrain the Frasnian-Famennian boundary fairly well. This section combines both samples collected from and below a lower sandy cliff, with samples recovered above an upper, repeated sandy cliff, separated from the lower cliff by a Tertiary normal fault. The section is 417 ft (127 m) thick and ranges in age from M. N. Zone 12 at the base (within the upper Denay Limestone) through Middle *triangularis* Zone at the top.

CONODONT BIOFACIES

Lateral conodont biofacies belts were proposed by Sandberg (1976) to describe offshore to nearshore assemblages from studies of the Late Devonian Lower *expansa* Zone, and derive their names from the most abundant conodont genera. Klapper and Lane (1985) applied the conodont biofacies concept to Frasnian sequences in western Canada. Sandberg and others (1988b) used the concept of conodont biofacies shifts as an aid in identifying eustatic events associated with the Late Frasnian mass-extinction event. Conodont biofacies are not strictly determined for northern Antelope Range collections, as doing so requires conodont percentage counts; this is a labor-intensive task and beyond the scope of the present study. Qualitatively, however, the majority of Fenstermaker collections probably contain *Palmatolepis*-dominated faunas (Appendix A) indicative of offshore environments (J. G. Johnson, pers. comm.), as opposed to nearshore, inner-platform, or reefal environments.

CONODONT ALTERATION INDICIES (C. A. I.)

Epstein and others (1977), supplemented by Rejebian and others (1987), demonstrated through both field and experimental data that semiquantitative estimates of depth and duration of burial, as well as temperatures of metamorphism and hydrothermal alteration, can be given for rocks containing conodonts by observing their color. Conodont colors are compared to published color charts, and indices (conodont alteration indices, or C. A. I. values) are assigned for comparative purposes. C. A. I. values can range from 1 to 8 and reflect carbonization, followed by the loss of organic matter through oxidation and volatilization of oxides.

Conodonts from both the Fenstermaker Limestone in the northern Antelope Range and from the Denay Limestone in the southern Cortez Mountains were observed for their C. A. I. values. Fenstermaker samples are almost invariably pale yellow to very pale brown in color, correlating with C. A. I. values of 1 to 1 1/2. Their color suggests that these rocks were not subjected to temperatures above 50°-90° C, and therefore were probably not buried deeply for any significant length of time. Conversely, conodonts from the Denay Limestone, where exposed in the Cortez Mountains, are uniformly black, displaying fairly high C. A. I. values of approximately 5. Experimental temperatures of 300°-400° C (Rejebian and others, 1987) produced C. A. I. values of 5. Cortez C. A. I. values can be attributed to hydrothermal alteration associated with Tertiary igneous intrusions such as the Mill Canyon stock present in the area.

SIGNIFICANCE OF REWORKED CONODONTS

A comparison made between a new Frasnian (Upper Devonian) composite standard conodont range chart (G. Klapper, in prep.) and checklists of species collected in northern Antelope Range biostratigraphic sections (Tables 2-4; Plate 2) indicates that at least 27 species (91 occurrences) have been reworked into higher stratigraphic horizons (Table 5). Time intervals between original depositional events and the reworking of unlithified peloidal carbonate mud was, in all cases, shorter than three conodont zones (< 1.5 m.y.; see Sandberg and Poole, 1977, p. 149). Some of the specimens in question show physical evidence of reworking as well.

The reworking of northern Antelope Range conodonts provides important depositional environment information. *Palmatolepis semichatovae* occurs in several collections (Table 5) above its known upper limit in the Lower *gigas* Zone, and in M. N. Zone 11. Klapper and Lane (1985) indicate that certain species of *Ancyrodella*, *Ancyrognathus*, as well as *Pa. semichatovae* were more tolerant of water-depth changes, therefore ranging into shallower areas than the *Palmatolepis* biofacies. These occurrences suggest a reworking of shallower water carbonates into at least slightly deeper water.

Table 5 indicates that reworked conodonts from the northern Antelope Range fall into two main categories: (1) those that were deposited during Montagne Noir Zones 10-12 and reworked into M. N. Zone 13 or the upper part of M. N. Zone 13; and (2), those that were deposited in M. N. Zone 13 and reworked into the Famennian Middle *triangularis* Zone. Time intervals during which carbonate sediments were reworked (M. N. 13 and Middle *triangularis* Zones) can be shown to correspond with known regressive cycles on the carbonate platform (see Sandberg and others, 1989; Johnson

TABLE 5. REWORKED CONODONTS

Reworked Interval:	10/11->U. 13	11->13	11->U.13	12->13	12->U.13	13->M. triang.	Totals
An. gigas form 3	1b						1
Pa. Ijaschenkoae	1a						1
Pa. domanicensis		1?a	1b				2
Pa. n. sp. P form 1*		2a;1d(indet.)					3
Pa. n. sp. P form 2*		7a;3b;3d	1a;2b				16
Pa. aff. Pa. domanicensis		1a					1
Pa. semichatovae		3a	17b				4
An. curvata, early form		1a					1
Pel. planus		1a;1d	1b				3
P. evidens			17b				1
An. lobata			17d				1
Pand. insita			1d				1
I. symmetricus				2a	1a		3
P. angustidiscus				1a	2b		3
An. nodosa -> An. ioides				3a;2b;1d	2a;2b		10
P. n. sp. R				3a;2d	2d		7
An. ioides				2a;1b	1b		4
P. samueli				1a;1c			2
O. dissimilis					1a		1
Pa. rhenana						2a;17d	3
P. imparilis						4a;2c	6
Pa. winchelli						1a;1c	2
I. alternatus						5a;3c;1d	9
P. lodinensis						2a;1c;1d	4
P. unicornis						1a	1
P. brevicarina						1a	1
Totals	2	24	9	19	11	26	91

a=TA IV/ANA II/ANA III d=WNA II

b=ANA I

?=questionable i.d.

c=WNA I

*=Klapper does not differentiate between Pa. n. sp. P forms 1 and 2 on range chart.

-Klapper indicates that An. sp. indet. (ANA III 121) is probably reworked, although it is not included with those above.

-Samples ANA I 0 and ANA II 157 not represented.

and others, 1985,1986). During these regressive events, large amounts of unlithified carbonate mud were eroded off the broad, shallow carbonate platform and redeposited in a relatively deeper, outer-shelf depositional environment.

The earliest of these reworked intervals, having reworked conodonts from M. N. Zones 10-12 into M. N. Zones 13 and upper 13, roughly corresponds to a late Frasnian regressive event early in T-R cycle IId (western U. S. event 7 of Sandberg and others, 1989). This event was preceded by both earlier and later T-R cycle IId major transgressive events. During this time, platform sedimentation temporarily ended, and erosion is documented as having occurred as far east as Montana, North Dakota, and Wyoming (Sandberg and others, 1989). This T-R cycle lower IId regression is shown in Figure 23 (Johnson and others 1985).

The more recent of the reworked intervals, during which M. N. Zone 13 conodonts were reworked into the Middle *triangularis* Zone (rocks representing the Lower *triangularis* Zone are unknown to extremely thin in the northern Antelope Range), corresponds to western U. S. event 8 (Sandberg and others, 1989) and lies just below the boundary between T-R cycles IId and Ile (Johnson and others, 1985). This regression, which began within the upper part of M. N. Zone 13 (or *linguiformis* Zone) and preceded the Middle *triangularis* Zone eustatic T-starts of T-R cycle Ile, is represented in Figure 23 by sea-level falls recorded in rocks above the Matagne Shale on the Belgian platform, as well as above the upper member(?) of the Kellwasser Limestone in the German basin. Figure 23 does not, however, indicate regression on the western U. S. platform, although it is discussed by Sandberg and others (1989), having occurred between their paleobiogeographic lithofacies maps 4 and 5.

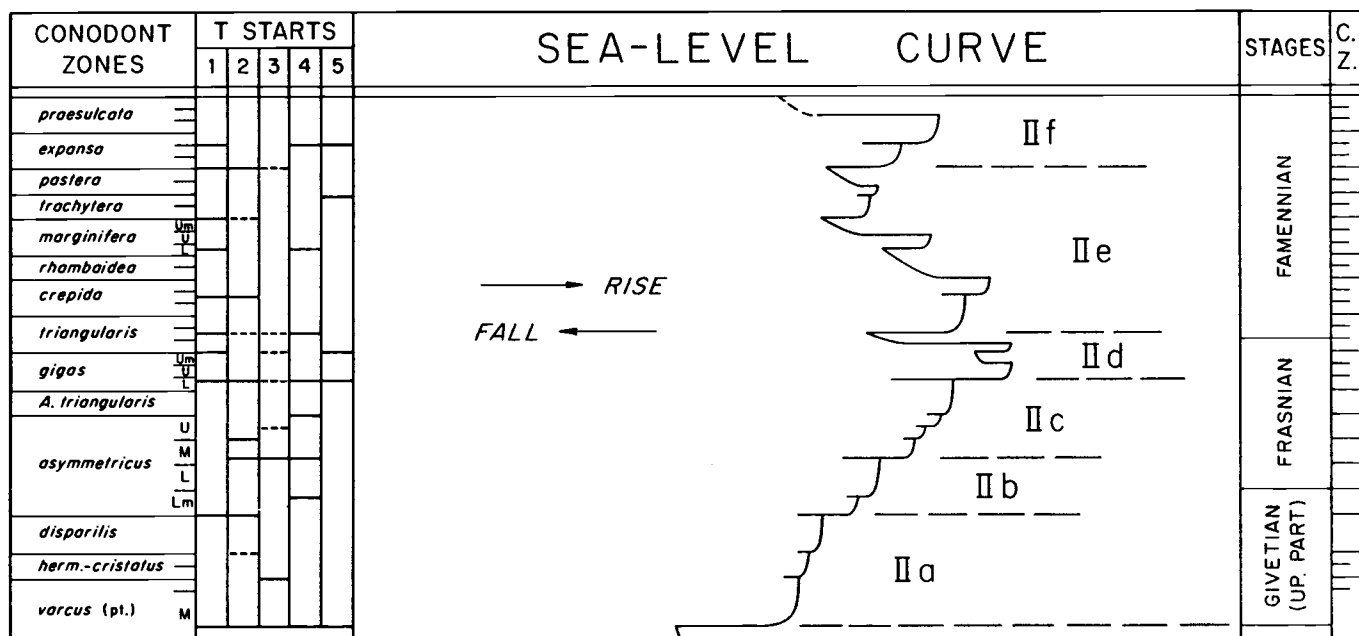


Figure 22. Upper Devonian eustatic curve in relation to Devonian conodont zones.
Modified from Johnson and others (1985).

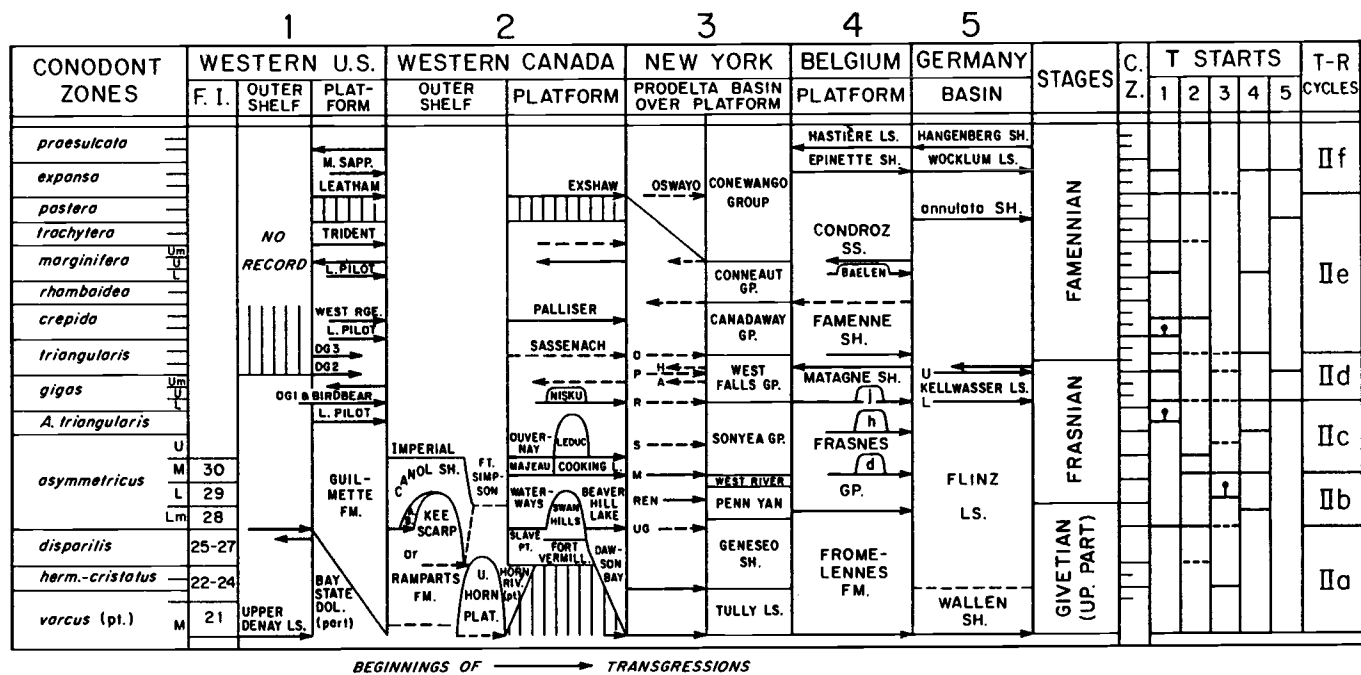


Figure 23. Time-rock chart for five regions of the Devonian Euramerican platforms, showing the principal deepening events with arrows pointing to the right. Depophases and transgressive starts are summarized on the right. Modified from Johnson and others (1985).

Figure 24 is a Devonian eustatic curve from Johnson and Sandberg (1989) in which the base of Sandberg and others' (1989) western U. S. event 9 is shown. This figure demonstrates both the relative magnitude as well as the time-rock period over which these regressions occurred. Johnson and Sandberg's (1989) figure indicates "no record" beginning in the upper two thirds of T-R cycle IId, extending to the top of the cycle, and one of the "sandy units" to the left of this hiatus is analogous to the Fenstermaker Limestone farther west in the northern Antelope Range.

Figure 25 is a comparison between depopphase II T-R cycles of Johnson and others (1985), western U. S. events of Sandberg and others (1989), and Euramerican eustatic events (Johnson and others, 1985), in terms of the Upper Devonian conodont zonation.

BRACHIOPODS

Thin-shelled brachiopods, although rare to absent in most samples, were recovered from several Fenstermaker collections and identified by J. G. Johnson, Oregon State University. Brachiopod collections and identifications are included in Appendix A. These samples indicate Upper Devonian ages for the collections, but are by their nature less accurate than the conodont determinations.

OTHER FOSSILS

Several limestone samples from the Fenstermaker Limestone contain transported solitary tetracoral fragments (ANA I 280, ANA III 112,115,116,122) and amphiporid algal fragments (ANA I 280, WNA II 303). In addition, five fish fragments were

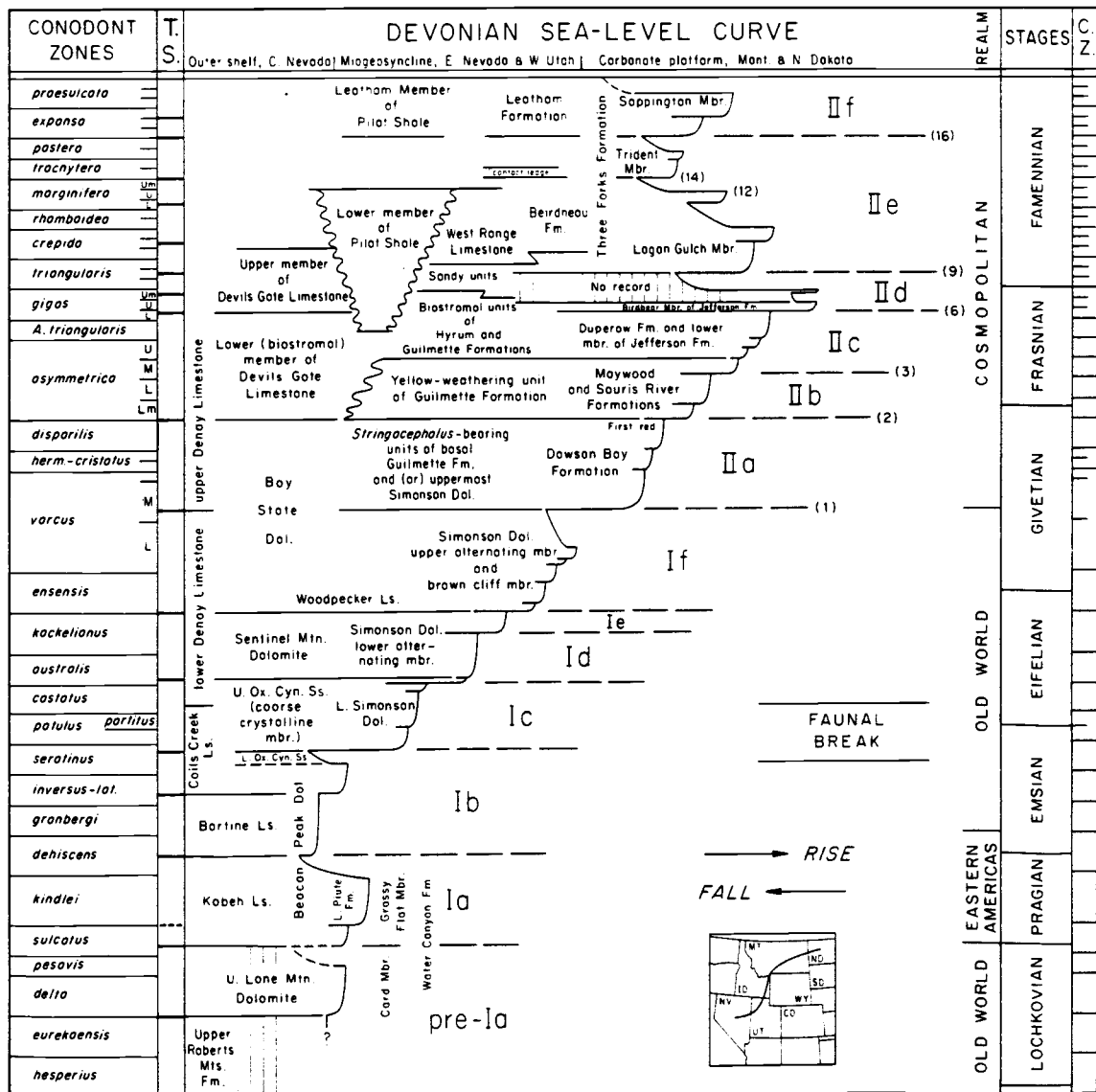


Figure 24. Devonian eustatic curve with principal stratigraphic units of western United States plotted by age and relative paleotectonic and geographic location. Numbers in parentheses indicate Late Devonian events of Sandberg and others (1989). From Johnson and Sandberg (1989).

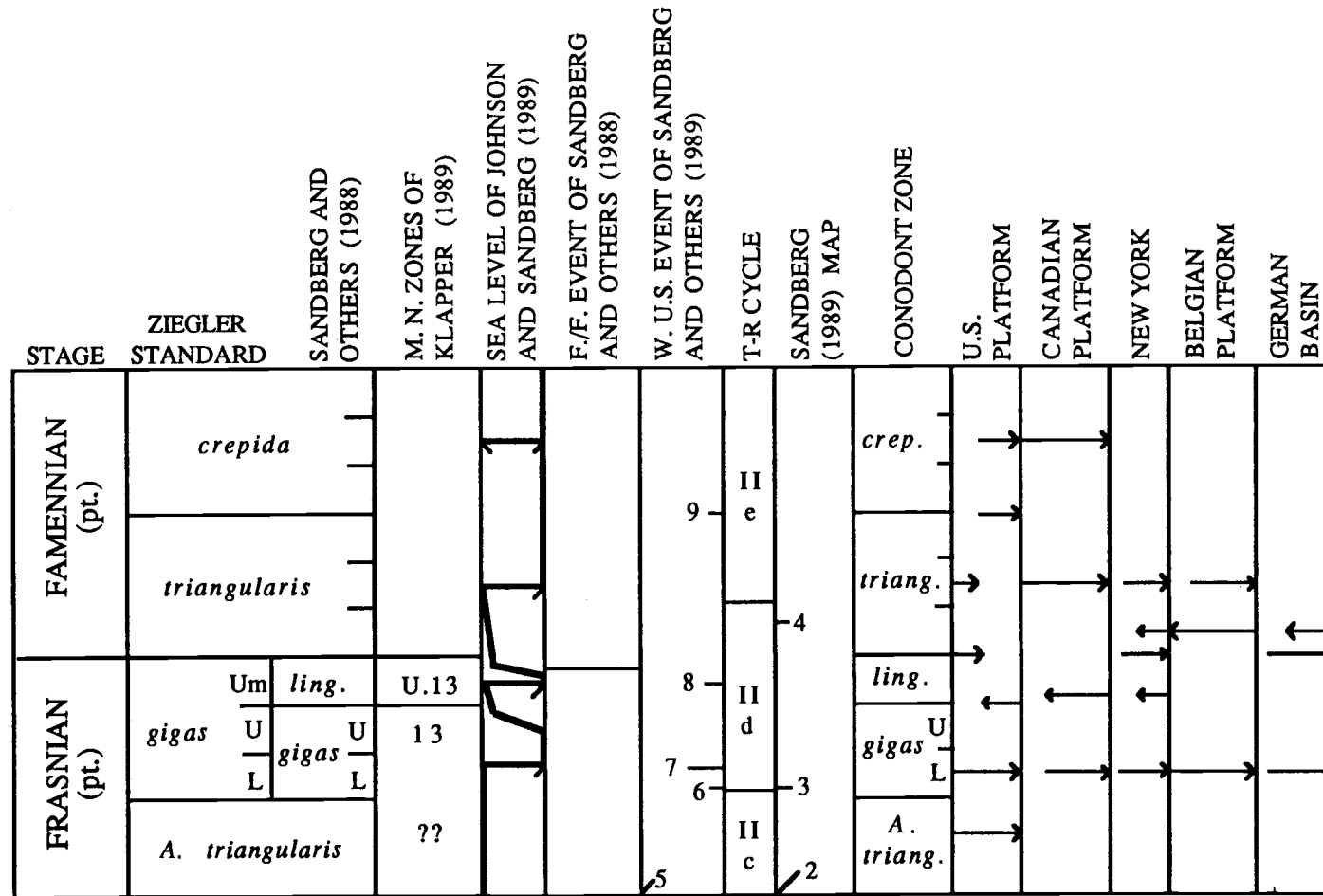


Figure 25. Comparison between depophase II T-R cycles of Johnson and others (1985), western U. S. events of Sandberg and others (1989), and Euramerican eustatic events of Johnson and others (1985), in terms of the Upper Devonian conodont zonation.

recovered from ANA I 280. Although the above fossils were not identified, their occurrences are indicated in Appendix A.

A. R. Ormiston of Amoco Production Co. identified eight species of radiolaria from ANA II 111, assigning the collection a Frasnian age. His age determination (Appendix A) is consistent with that obtained from the conodont collections.

LATE FRASNIAN MASS-EXTINCTION EVENT

The occurrence of a Late Frasnian mass extinction event (at or near the Frasnian-Famennian boundary) has been a subject of debate in the literature (see Sandberg and others, 1988b; McLaren, 1982; Johnson, 1974; Johnson and others, 1985; Sepkoski, 1982). The search for possible triggering mechanisms has been overshadowed by general confusion over the exact timing of the event, and concerning which taxa were most highly affected. Furthermore, early publication of data based on collections from horizons generally above those containing a record of the extinction, has lead to some perhaps erroneous conclusions. It now seems that the Late Frasnian extinction event may have taken place during a very short period of time (< 20,000 yr), at or just below the boundary between the Frasnian *linguiformis* Zone (equivalent to both the Uppermost *gigas* Zone of the standard zonation and the upper part of Montagne Noir Zone 13) and the Famennian Lower *triangularis* Zone (Sandberg and others, 1988b).

The Late Frasnian mass extinction event involved a reduction in both species diversity and general biomass, the later being more difficult to document (for example, see Tables 1-3 of Sandberg and others, 1988b), and is known to have involved important groups of conodonts, brachiopods, colonial corals, stromatoporoids, and other marine invertebrates (McLaren, 1982; Johnson and others, 1985).

In the northern Antelope Range, conodont biostratigraphy (especially detailed in section ANA III) shows that deposition of the Fenstermaker Limestone both preceded and continued after the Frasnian-Famennian boundary. Detailed sampling (18 samples at 0.5-1 ft intervals) across the boundary, however, indicates that it is uncertain whether Fenstermaker Limestone deposition took place *during* the extinction event, and no collections indicate deposition during any part of the Lower *triangularis* Zone. The possibility exists that rocks representing deposition during the latest *linguiformis* Zone to Lower *triangularis* Zone were eroded off the carbonate shelf during a long period of regression (Johnson and Sandberg, 1989) that began during the Late Frasnian, latest *linguiformis* Zone (Uppermost *gigas* Zone). This regression continued until interrupted by the major T-R cycle basal Ile transgression (Fig. 24) near the middle part of the Early Famennian Middle *triangularis* Zone.

The extinction has been attributed to many causes including bolide impact(s) with associated iridium anomalies (McLaren, 1985; Sorauf and Pedder, 1986), oceanic cooling (Stearn, 1987; Copper, 1986), anoxic water conditions (Geldsetzer and others, 1985), a rapid global transgression (Johnson and others, 1985), a rapid global regression (Johnson, 1974; Sandberg and others, 1988b), as well as several others.

Playford and others (1984; McLaren, 1985) discovered an iridium anomaly (Ir enrichments of about 20 times background abundances) in a *Frutexites* bed in the Upper Devonian of the Canning Basin, northwestern Australia, for which McLaren (1985) suggests a bolide impact. This hypothesis is identical to that brought forward to explain the Cretaceous-Tertiary mass extinction event (see Alvarez and others, 1980; Orth and others, 1981). Playford and others (1984) reported this bed as Upper *triangularis* Zone in age, representing strata deposited well after the timing of the main extinction event as documented by Sandberg and others (1988b). Furthermore, Playford and others (1984) did sample through what is now considered the extinction

horizon without the discovery of an iridium anomaly. McGhee and others (1984) found no evidence for iridium anomalies in three New York State sections and one section in Belgium. McLaren (1985) realized that iridium anomalies may be caused by "local chemical, physical, or biological processes", or volcanic events.

An early goal of this work was to sample the Frasnian-Famennian boundary in the northern Antelope Range for an iridium anomaly. Since that time, the thick bedded, dip-slope nature of the critical part of the section (Fig. 9; rocks dipping about 30 degrees east cropping out along a hill slope dipping about 25-30 degrees east) precluded accurate cm by cm sampling of the boundary without employing heavy equipment or explosives. Conodont biostratigraphy demonstrates that, in the northern Antelope Range, critical rocks belonging to the upper part of Montagne Noir Zone 13 (*linguiformis* Zone) and the Lower *triangularis* Zone are either very thin, or were eroded soon after deposition. The sandy pelsparites of the Fenstermaker Limestone just above the Frasnian-Famennian boundary (ANA I 0, ANA III 119, WNA I 389, WNA II 386) are lithologically indistinguishable from those just below (ANA I 290, ANA III 117.5 and 118(?), WNA I 354, WNA II 341 and 363(?)), both in hand sample, and thin section.

TIME-CORRELATIVE UNITS

SOUTHERN FISH CREEK RANGE

Two allochthonous, unidentified limestone slide blocks in the southern Fish Creek Range (see Sans, 1986, p. 31-32) are assigned to the Fenstermaker Limestone of the northern Antelope Range (blocks A and C, corresponding to conodont samples WFC 3 and 1 respectively). A third block (block B) was sampled (WFC 2), but that part of the block was determined to be older than the type Fenstermaker in the ANA II/ANA III section (Appendix A).

Sans (1986) noted two allochthonous limestone blocks (A and B) in the southern Fish Creek Range just north and south of Willow Creek. He left these blocks unassigned on the basis that they are younger than the youngest Denay Limestone, although they appeared to be structurally related to nearby Denay outcrops. A third block (C) was not assigned to a formation as no conodonts were collected from it (in Sans' text, the second line of the second paragraph on page 31 should read "...SS27, from block A,...", not "block C").

For the present study, conodonts were collected (Appendix A) and thin sections were studied from all three limestone blocks. The measurement of stratigraphic sections is not possible within these blocks because of their fragmented nature and limited exposure (Fig. 26).

The first of these samples (WFC 1), collected from block C (SW 1/4 of sec. 17, T. 14 N., R. 52 E.), yielded a conodont age of Frasnian Montagne Noir Zone 13, equivalent in age to the main sandy limestone cliff of Fenstermaker Limestone in the northern Antelope Range ANA II/ANA III section. In thin section (Fig. 27), these rocks are sandy intrapelsparites that are indistinguishable from those of the type



Figure 26. Typical exposure of southern Fish Creek Range allochthonous block C.

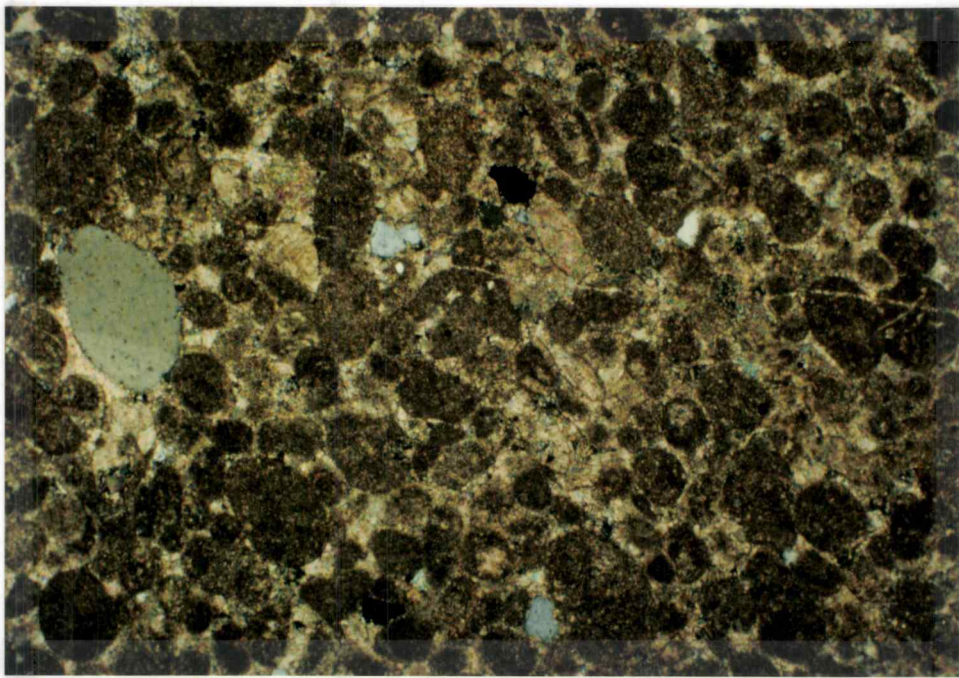


Figure 27. Photomicrograph of WFC 3 (block A) displaying typical Fenstermaker Limestone microfacies (crossed polars; field of view approx. 3.3 mm).

Fenstermaker. On the basis of the conodont age obtained, thin section observations, and bedding characteristics, allochthonous block C is assigned to the Fenstermaker Limestone of the northern Antelope Range.

Sans' (1986) block B (NE 1/4 of sec. 19, T. 14 N., R. 52 E.) was sampled for conodonts (WFC 2) and observed in thin section. Conodonts indicate a Givetian (Lower-Middle *varcus* Subzones) age for the collection, too old to be assigned to the Fenstermaker Limestone. The indicated age is in contrast with G. Klapper's age determination of Sans' (1986) SS60 collection which yielded an Upper to Uppermost *gigas* Zone age, and later reinterpreted by Klapper as belonging to Frasnian M. N. Zone 13. Thin-section evidence indicates little to no detrital quartz sand percentage and supports a conclusion that WFC 2 was not collected from the Fenstermaker Limestone. Block B may be two blocks, as Sans' (1986) sample was collected from a locality well to the north of WFC 2. Because of the age discrepancies, and lack of thin-section evidence to the contrary, block B is not assigned a unit formation name.

Block A (SE 1/4 of sec. 19, T. 14 N., R. 52 E.; collection SS27 of Sans, 1986) was sampled for conodonts and for thin sections (WFC 3, Appendix A). Collection SS27 yielded Sans an early Famennian age for the block, which G. Klapper (written comm., 1989) revised to a general Upper Devonian age because the critical fossil cf. "*Nothognathella*" *sublaevis* is apparently no longer present in the collection. Collection WFC 3 (this study) suggests a Frasnian age for the block, provided that a single specimen of *Ancyrodella* sp. indet. is not reworked. A thin section from block A (Fig. 27) is classified as sandy intrapelsparite and identical with the type Fenstermaker Limestone in the northern Antelope Range. On the basis of evidence provided by age, lithology, and petrography, block A is assigned to the Fenstermaker Limestone.

SOUTHERN TUSCARORA MOUNTAINS

Access privileges were granted by Newmont Mining Co. to briefly sample a stratigraphic section of the Popovich Formation on their Carlin Mine property in the southern Tuscarora Mountains, northern Eureka County (N 1/2 of sec. 9, T. 35 N., R. 50 E.). This reference section for the Popovich Formation has been studied and described in detail by Evans (1980), and more recently by Ettner (1989). For the purposes of this study, the section will be referred to as WRC I (see Plate 1). A second section, WRC II, was described and collected along the south wall of the leach pond near the old Carlin no. 2 mill, but its study was not pursued because these beds were too highly silicified to yield conodonts through standard acidizing methods.

Evans (1980) noted thick-bedded sandy limestone above what he described as being similar to the Denay Limestone as defined by Johnson (1966, p. 154-157) in the northern Simpson Park Mountains and in the Roberts Mountains. Conodont samples from the upper half of the sandy limestone indicated early Frasnian ages, and therefore age equivalency to Denay Limestone strata below the Fenstermaker Limestone in the northern Antelope Range, approximately 110 miles (177 km) to the south. Ettner (1989) informally applied the name Rodeo Creek unit to describe the highly silicified peloidal sand or chert beds above the sandy peloidal intraclastic limestone of an "upper" Popovich.

Johnson and others (1989, p. 178) recommended the abandonment of the name Popovich Limestone, a name which now serves to label several rock units in the area of Early through Late Devonian age. However, the name is retained by Ettner (1989) and employed here for simplicity.

Section WRC I is approximately 596 ft (182 m) thick, but only the lower 250 ft (76 m) are displayed in Plate 1. Above an 85 ft covered interval, the uppermost 261 ft

(80 m) of the section are assigned to the Rodeo Creek unit of Ettner (1989), and is highly silicified.

Four conodont samples were taken from this lower interval, two of which (WRC I 122, 212) yielded useful collections (Appendix A). The lower sample (WRC I 122) belongs to upper Montagne Noir (M. N.) Zone 3 to lower M. N. Zone 4. This collection also yielded brachiopods, the majority of which are indeterminate smooth-radiate spiriferid species and *Radiatrypa multicostellata*. J. G. Johnson assigned the brachiopods an early Frasnian age, in agreement with G. Klapper's conodont identifications. Conodonts from sample WRC I 212 can range in age from the late Middle Devonian to as high as M. N. Zone 7, but the stratigraphic position of this horizon, 90 ft (27 m) above WRC I 122, as well as the possible presence of a Frasnian specimen of *Palmatolepis* sp. suggests a Frasnian age between M. N. Zones 4 to 7. Correlations with the Fenstermaker Limestone in the northern Antelope Range based on conodont biostratigraphy are shown in Plate 1.

In this section, the lower portion of WRC I (between WRC I 0 and approximately WRC I 172) is sandy pelintra micrite to brachiopod pelintrasparite. Detrital monocrystalline quartz sand constitutes up to 55% of these rocks, which might be classified as limy sandstone as opposed to sandy limestone; but the quartz sand grains generally seem to be suspended within the peloidal matrix. Grain-size analyses of Popovich sandy limestone samples are described under a separate heading. Intraclasts that weather out in relief are a common feature, especially in the vicinity of WRC I 122, where they comprise 40-50% of the rock.

Figure 28 is a photomicrograph of a micrite intraclast (WRC I 122) in which peloid amalgamation is responsible for at least some intraclast formation. These intraclasts are structureless micrite, but many contain inclusions of silt to very

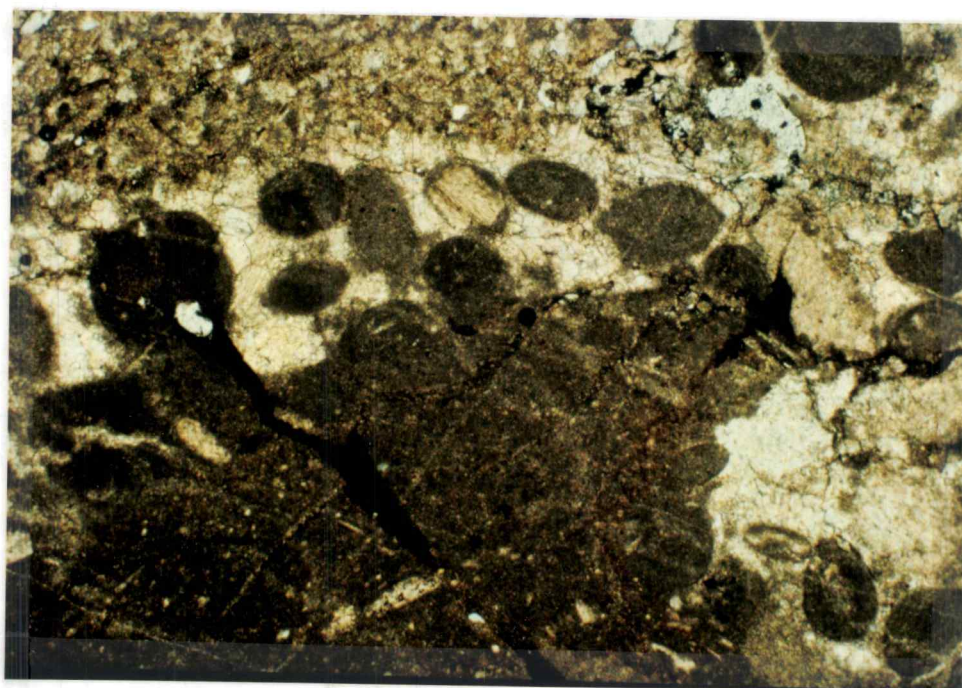


Figure 28. Photomicrograph of WRC I 122 showing peloid amalgamation in Popovich Formation micrite intraclast (crossed polars; field of view approx. 1.3 mm).

fine quartz sand. Wilson (1969) has attributed "pseudopeloids" of this type to an origin as miniresediments in deeper shelf environments. Also present in these rocks are recrystallized crinoidal fragments (2-5%) with some partial chert replacement. Iron oxides are present in most samples as small blebs (<1%) randomly distributed throughout the rock. Partial neomorphism to microspar is common, but not as prevalent as in the Fenstermaker Limestone.

Above WRC I 172 and below the Rodeo Creek unit of Ettner (1989), interbeds of silty chert-replaced limestone are common, giving way upsection to entirely chert-replaced beds at the top (above WRC I 351). Peloids, intraclasts, and bits of brachiopod shell material are visible within cherty horizons, with no silicic biotites observed. Quartz silt ranges between 3-5% to as high as 25-30% within silty chert beds (Fig. 29).

Most beds between WRC I 172 and WRC I 351 are composed of sandy intrapelsparite, similar to strata of the Fenstermaker Limestone. These rocks are composed mainly of peloids and small rounded intraclasts (75-80%), many of which contain calcisphere inclusions. Other thin-section constituents include rare crinoid fragments and brachiopod shell fragments. Figure 30 is a photomicrograph of WRC I 212 in which thin-section similarities to the Fenstermaker Limestone are visually apparent.

Of particular interest are the numerous quartz stylolites observed both below and above WRC I 237, trending both parallel to, and at a high angles to, the bedding. Stylolites, or pressure-solution surfaces, form thin zones of discontinuity within carbonate rocks (Flügel, 1982; Bathurst, 1975) and rarely in sandstone and quartzite. Experimental studies (for example, Coogan and Manus, 1975) have indicated substantial pressure-solution thickness losses, although quantification of examples in the rock record has been hampered by the lack of visible residues within the stylolite

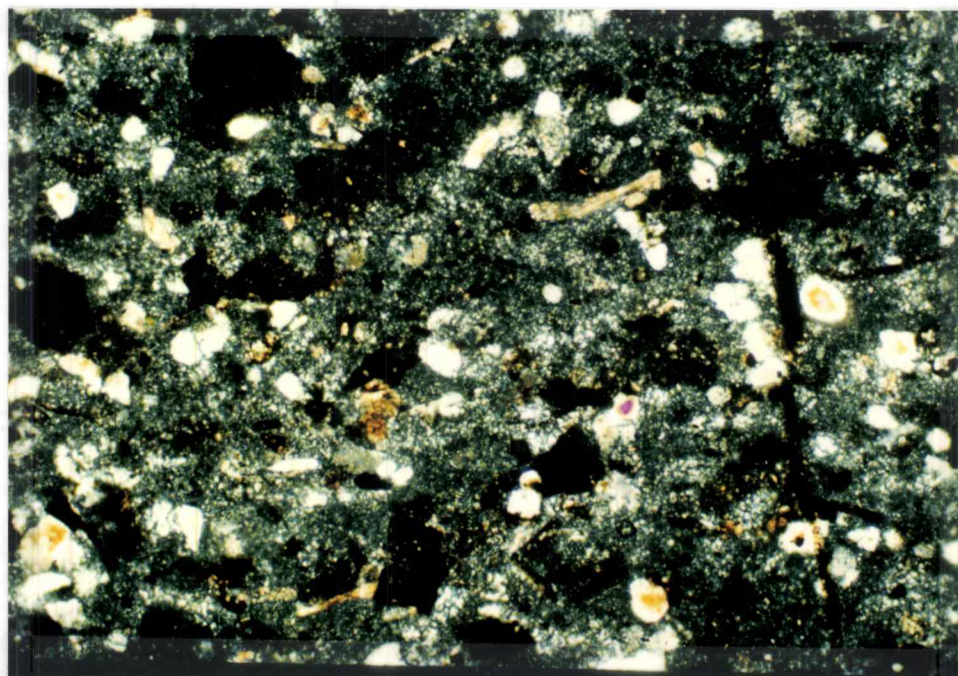


Figure 29. Photomicrograph of WRC I 172 showing typical silty chert bed in the Popovich Formation (crossed polars; field of view approx. 1.3 mm).

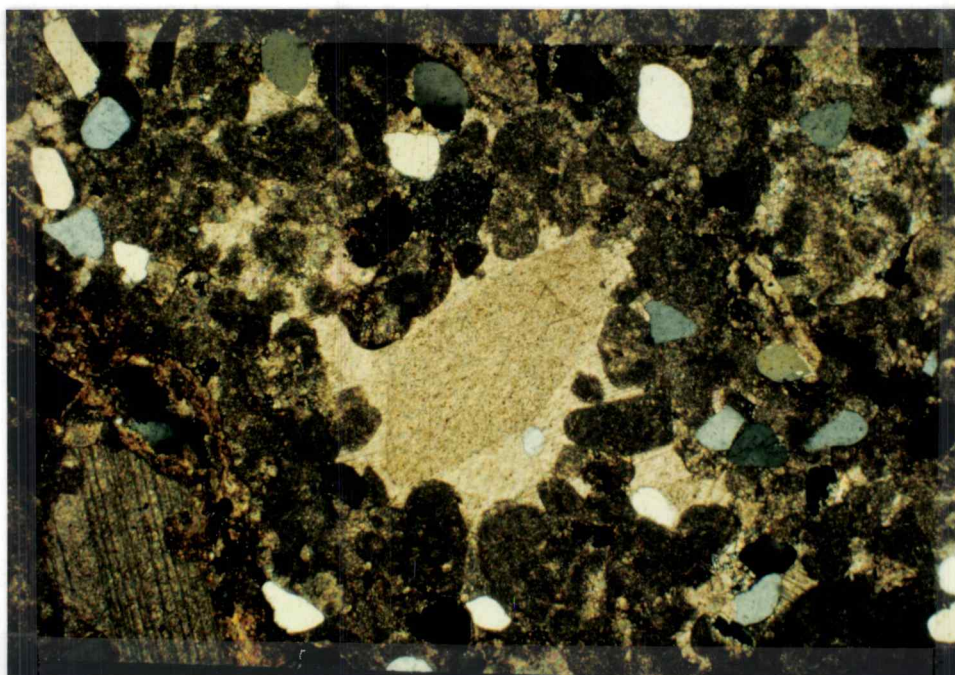


Figure 30. Photomicrograph of WRC I 212 sandy intrapelsparite. Note crinoid plate with syntaxial sparry calcite cement overgrowth (crossed polars; field of view approx. 3.3 mm).

zone itself. Delair and Leroux (1978) compared concentrations of insoluble residues within the stylolite to concentrations within the rock matrix. Bathurst (1975, p. 460) suggests that losses of 20-35% are common. Choquette and James (1987, p. 10) point out that significant reductions in thickness have been documented in many unpublished studies.

The Upper Devonian part of the Popovich Formation (Evans, 1980) in the southern Tuscarora Mountains offers a unique opportunity to quantify thickness loss through stylolitization. The Fenstermaker Limestone contains quartz-rich stylolites as well, but these generally trend at too high an angle to bedding to be quantitatively useful. In the middle part of the Popovich Formation a stylolite-rich zone exists within a sequence of sandy pelsparites (N 1/2 of sec. 9, T. 35 N., R. 50 E.; sample WRC I 237, Figs. 31, 32), in which the vertical stylolite spacing averages approximately 14 mm. Well-rounded, moderate- to well-sorted quartz sand constitutes up to about 15% of these rocks. Unaltered detrital quartz-sand grains are highly concentrated within the numerous low-amplitude stylolites, perhaps better described as multi-grain non-sutured seams (in the terminology suggested by Choquette and James, 1987, p. 14). Vertical stylolites cut across the zone as well, forming conjugate sets (Flügel, 1982, p. 93) indicating a horizontal component of compression.

The original thickness of the rock is defined as:

$$T_o = \sum_1^n T_m + T_s + T_l$$

where T_o = original rock thickness including the thickness of the stylolite

T_m = remaining unaffected thickness of rock between stylolites

T_s = final thickness of the stylolite

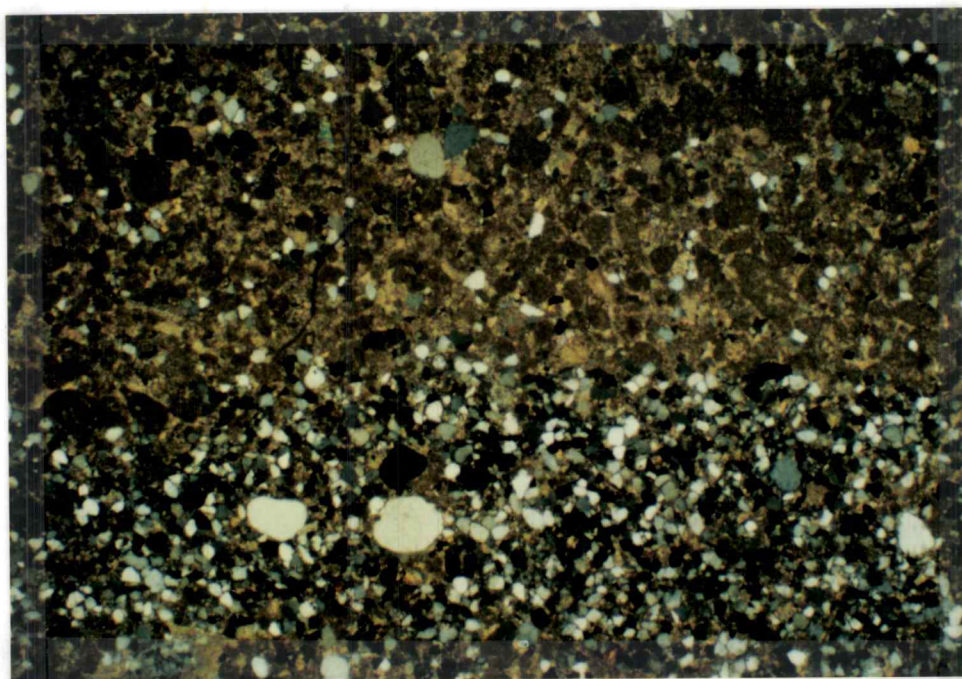


Figure 31. Photomicrograph of WRC I 237 sample used to determine percent thickness reduction during quartz-rich stylolite formation (crossed polars; field of view approx. 3.3 mm).



Figure 32. WRC I 237 quartz-rich stylolites.

T_l = thickness reduction within the stylolite.

The thickness reduction attributable to any one stylolite is:

$$T_l = \left(T_s \cdot \frac{C_s}{C_r} \right) - T_s$$

$$T_l = T_s \left(\frac{C_s}{C_r} - 1 \right)$$

where C_r = concentration of insoluble grains in the unaffected rock matrix

C_s = concentration of insoluble grains in the stylolite.

Assuming uniform grain size, stylolite spacing, and thickness, and if the number of stylolites over a given interval can be counted or estimated, the total thickness reduction is:

$$T_L = \sum_1^n T_l$$

where n = total number of stylolites within the interval.

An estimate of the percentage thickness reduction within the stylolite-rich zone ($\%T_L$) is:

$$\% T_L = 100 \left(\frac{\sum_1^n T_l}{\sum_1^n T_m + T_s + T_l} \right)$$

$$= 100 \left(\frac{\sum_{1}^n T_1}{\sum_{1}^n T_o} \right).$$

A determination of the percent lost in the stylolite-rich part of the Popovich Formation utilized 593 detrital quartz grains, 497 concentrated in the stylolite and 96 from an identically sized area in the peloidal matrix. Since the Popovich stylolites are approximately 0.5 mm thick and spaced 14 mm apart, they number approximately 71 per meter. Substituting these figures into the above equation yields an estimate of 12.6 % thickness reduction, which can be applied only to the stylolite-rich zone; the thickness of which is unknown due to limited section exposure.

Significant thickness-reduction determinations such as this suggest that pressure-solution features deserve careful examination and attention during stratigraphic section measurements and depositional environment interpretations, especially where knowledge of depositional thicknesses are a factor.

Although the rocks of the upper part of the Popovich Formation and the Fenstermaker Limestone show a high degree of similarity, they are not assigned to the same formation. The Tuscarora Mountains are approximately 110 miles (177 km) north of the northern Antelope Range, and clearly several different depositional environments existed between the two locations during that part of the Late Devonian. Furthermore, the general sequences within which these rocks were deposited are different enough to warrant separate formation names. The evidence described above suggests, however, that similar depositional environments existed in both locations during Frasnian time. Grain-size analyses support a hypothesis in which sandy limestone from both the

Popovich Formation and the Fenstermaker Limestone share the same quartz-sand provenance.

SOUTHERN CORTEZ MOUNTAINS

D. B. Johnson (1972) mapped Devonian strata in the southern Cortez Mountains, Eureka County, and was able to recognize, in ascending order, the Roberts Mountains Formation, Windmill Limestone, Rabbit Hill Limestone, McColley Canyon Formation, Denay Limestone, and the Pilot Shale in a structurally complex area. Formations between the Roberts Mountains Formation and the Pilot Shale had previously been mapped as Wenban Limestone (Gilluly and Masursky, 1965). Because the nomenclature in use in surrounding areas applies to exposures in the Cortez Mountains, J. G. Johnson and others (1989, p. 178) recommend abandonment of the term Wenban Limestone.

Johnson (1972) collected conodonts from several sample localities, including one from a breccia at the top of the Denay (J-26-71) and one from a limestone bed within the Pilot Shale (J-70-71). Klapper assigned a late Upper Devonian *triangularis* Zone age to the Pilot collection, and a lowest Upper Devonian age to the Denay breccia sample. For the present study, an attempt was made to locate these sample localities in order to document any rocks similar to the Fenstermaker Limestone of the northern Antelope Range. The exact localities of Johnson's (1972) samples were not identified, nor was the limestone bed within the Pilot Shale. Instead, a short section of the uppermost Denay was measured and sampled for conodonts (Fig. 33). Of the five collections (CW I 1, 2, 10, and 15; Appendix A), two were dated in terms of the Montagne Noir Frasnian zonation. Conodonts from CW I 2 indicate an M. N. Zone 4 age, and a large fauna recovered from CW I 15 (at the contact with the Pilot shale)

CW 1
S.E 1/4 SEC. 21
S. CORTEZ MTS., EUREKA COUNTY, NEVADA

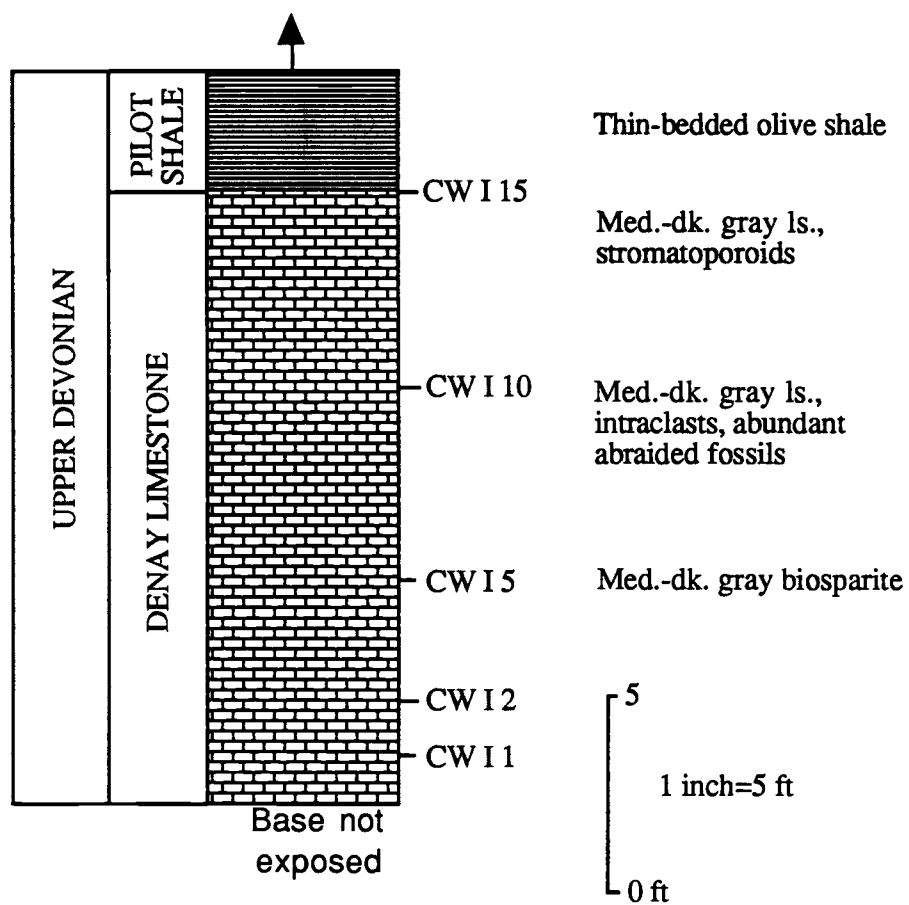


Figure 33. CW I stratigraphic section, southern Cortez Mountains.

yielded an M. N. Zone 5 date. Further study of the southern Cortez Mountains rocks was not undertaken because no rocks of Fenstermaker Limestone age were recognized.

GRAIN-SIZE ANALYSIS

Grain size analyses were performed on the quartz sand fraction of 29 limestone samples from all studied sections (Appendix B), as an aid in unit comparisons and in interpreting depositional processes, environments, and provenance for the Fenstermaker Limestone. These analyses indicate that the majority of analyzed samples were probably sorted in a high-energy wave-dominated clastic beach environment before being deposited in a carbonate lithotope. Bimodality is a prominent feature of the sand, and was probably the result of intensive bioturbation. Furthermore, the siliciclastic subpopulations show that the Fenstermaker Limestone is closely similar texturally to equivalent Upper Devonian sandy limestones to the north and east, suggesting a similar provenance or source area for these sands.

Grain-size analyses included 20 Fenstermaker samples (18 from northern Antelope Range sections ANA I-III and WNA I, II; southern Fish Creek Range samples WFC 1,2), one from a Middle Devonian southern Fish Creek Range block (WFC 3), and sample TA V 0 from near the top of the Coils Creek Member of the McColley Canyon Formation, where exposed in the northern Antelope Range. Additional grain-size samples were obtained from measured section WRC 1, Popovich Formation, southern Tuscarora Mountains, Eureka County (two samples), the Oxyoke Canyon Formation, Oxyoke Canyon, Eureka County (one sample), and the Guilmette Formation (section WBH 1e-f), southern Burbank Hills (SW 1/4, SE 1/4, NE 1/4 Sec. 22, T.23S., R.18W.), Millard County, Utah. Figure 34 shows the biostratigraphic levels from which samples WBH 1e-f were collected. Sample WIC 1 was collected from 5 m of limy sandstone to sandy limestone at the base of a 15-m-thick debris flow, turbidite, and flow-roll unit near the base of the Famennian section (see Sandberg and others, 1989, fig. 11), in the lower tongue of the Lower Member of the Pilot Shale (locality WIC 1) where exposed in Indian Creek, Cherry Creek Range (NE 1/4 Sec. 19, T.26N.,

WBH 1

SOUTH BURBANK HILLS
SW 1/4, SE 1/4, NE 1/4 Sec. 22, T.23S., R.18W.
Millard County, Utah

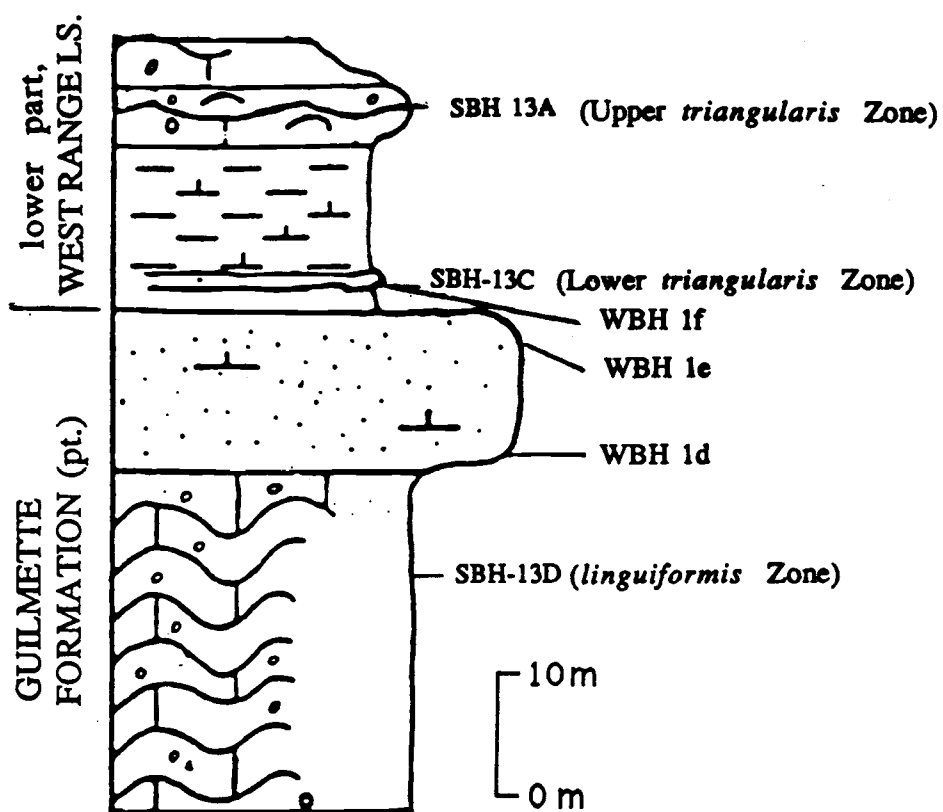


Figure 34. Combined SBH and WBH stratigraphic section, south Burbank Hills, Utah.

R.64E.), White Pine County (one sample).

As these analyses were performed on only the siliciclastic fraction of these sandy limestones, their usefulness as indicators of depositional environment in the sense of Friedman (1961, 1967) may be limited, unless it is assumed that the quartz-sand fractions inherited their textural parameters prior to final deposition in the carbonate lithotope. This is probably a safe assumption, as quartz grains only constitute <1-22% of the whole rock. Depositional environments from which these grains acquired their sorting and size characteristics were probably adjacent to shallow-marine carbonate environments in which they were later deposited, that is, if the quartz sand grains were first sorted in a siliciclastic beach environment and later transported into a relatively deeper water carbonate depositional environment during a period of regression. Conversely, grain-size analyses of this type show promise, in conjunction with heavy-mineral analyses, for regional stratigraphic correlation. Samples that display similarities in grain-size parameters and heavy mineral assemblages may have originated in the same source area.

The majority of sand samples analyzed from the Fenstermaker Limestone are well sorted and have platykurtic distributions (Appendix B). The apparent contradiction between the terms "well sorted" and "platykurtic" is illusory, reflecting the fact that these well-sorted sands plot close to the division between well and moderately sorted (0.51 avg.), and many platykurtic samples are nearly mesokurtic. Moderately sorted sand is also present, but is more common in time-equivalent strata east and north of the northern Antelope Range. A slight increase in sorting to the west could reflect increased time spent on the shelf as recycled quartz sand moved relatively westward across the carbonate megaplatform. Skewness values range from very negative (-0.34) to very positive (+0.35), displaying wide variations in departure from symmetry.

Histograms were constructed for all analyzed samples (Figs. 35-39), and log-normal subpopulations observed on plotted cumulative frequency curves (Visher, 1969). These graphs indicate a definite bimodality in 17 of the 29 sand samples (59%), occurring between the 2 and 3 phi-size classes (medium and fine sand). Bimodality is also evident as a break in slope on plotted cumulative frequency curves (not shown) of Visher (1969). Grain-size analyses of the Oxyoke Canyon Formation and Coils Creek Member of the McColley Canyon Formation (Fig. 36) show no such tendency toward bimodality, but only a single sample was run from each of those locations. Bimodality is discussed by Folk (1968) in reference to quartz-cemented quartz sandstones in which bimodality is probably the result of wind-lag deflation. Burrowing organisms as well as the simple mechanical infiltration of fine-grain sizes deposited directly above much coarser sediment can also be the cause of bimodality (Blatt, 1982, p. 134). Of these three processes, both wind deflation and infiltration can probably be ruled out. Eolian bimodal wind-lag deposits are most easily recognized in pure quartz sandstone in which there has been little net transport from the eolian environment to that of a shallow transgressive sea. Conversely, these analyzed sandy limestones were, as determined through other independent criteria, deposited in deeper water and during episodes of late Frasnian and early Famennian regression. Simple mechanical infiltration processes require that the underlying sediment be much coarser than the overlying sediment in order for fine grains to settle into the pore spaces between the larger grains. This process is clearly not possible during the deposition of a sandy limestone, as intergranular spaces are assumed to be occupied by carbonate mud. Mixing of sand sizes through bioturbation is the most plausible cause of the bimodality observed in these samples. Extensive bioturbation is indicated (discussed elsewhere in this report) by the general lack of sedimentary structures and lamination (probably destroyed) and by the high percentage of peloids that constitute the rock matrix. Conversely, the

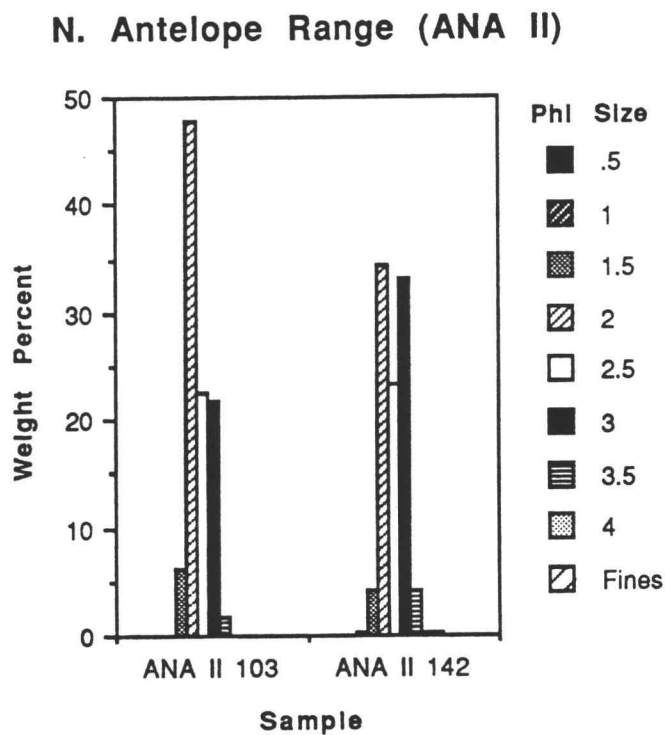
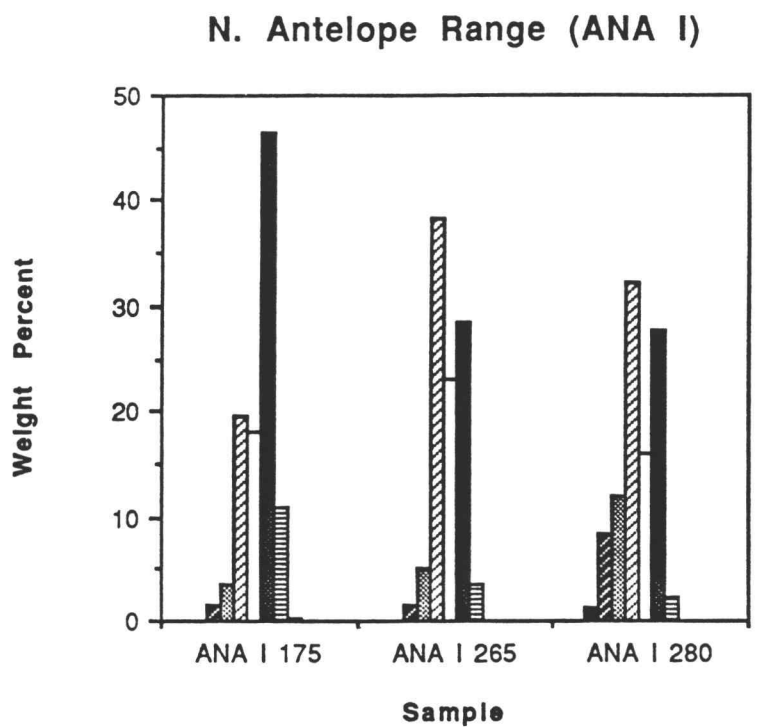
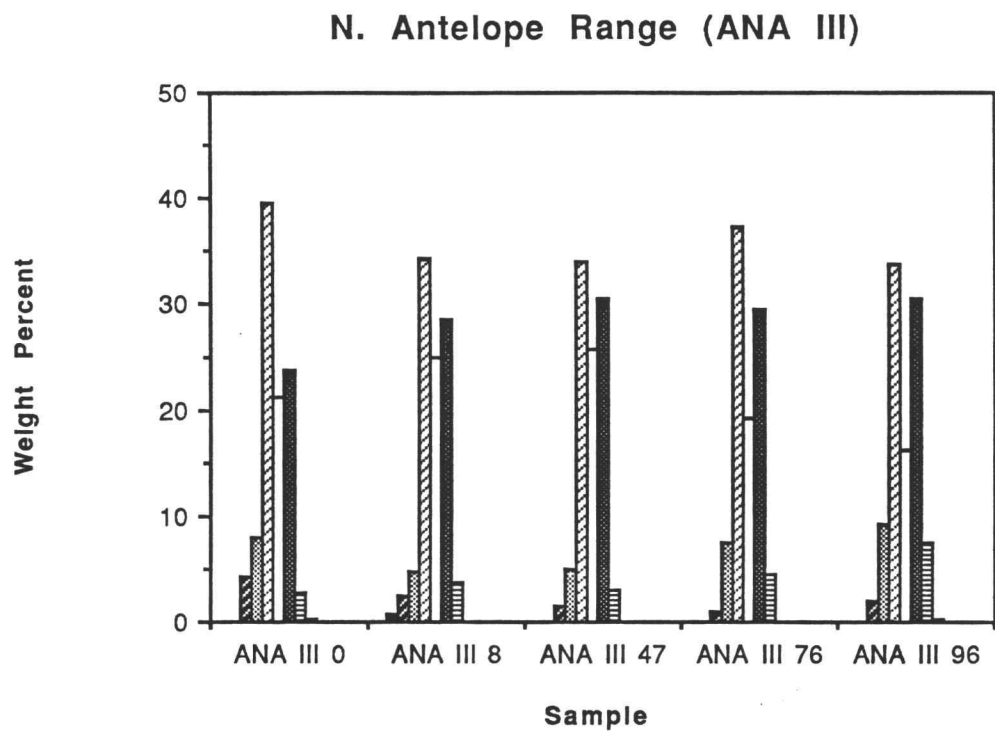
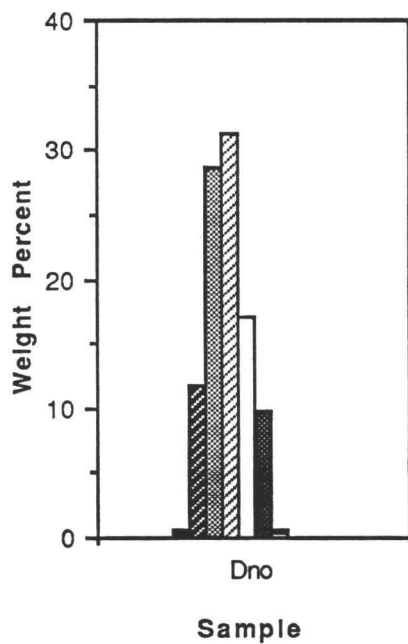


Figure 35. ANA I and ANA II grain-size histograms.



Oxyoke Canyon (Dno)



N. Antelope Range (TA V)

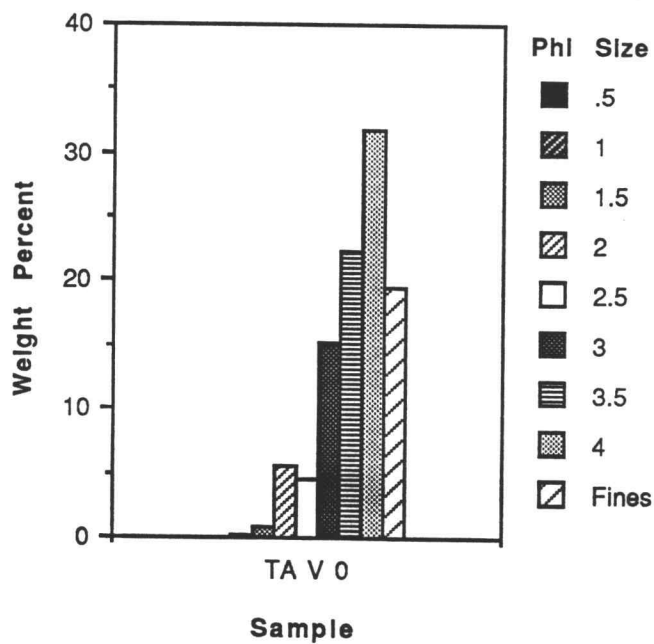


Figure 36. ANA III, Oxyoke Canyon (Dno), and TA V grain-size histograms.

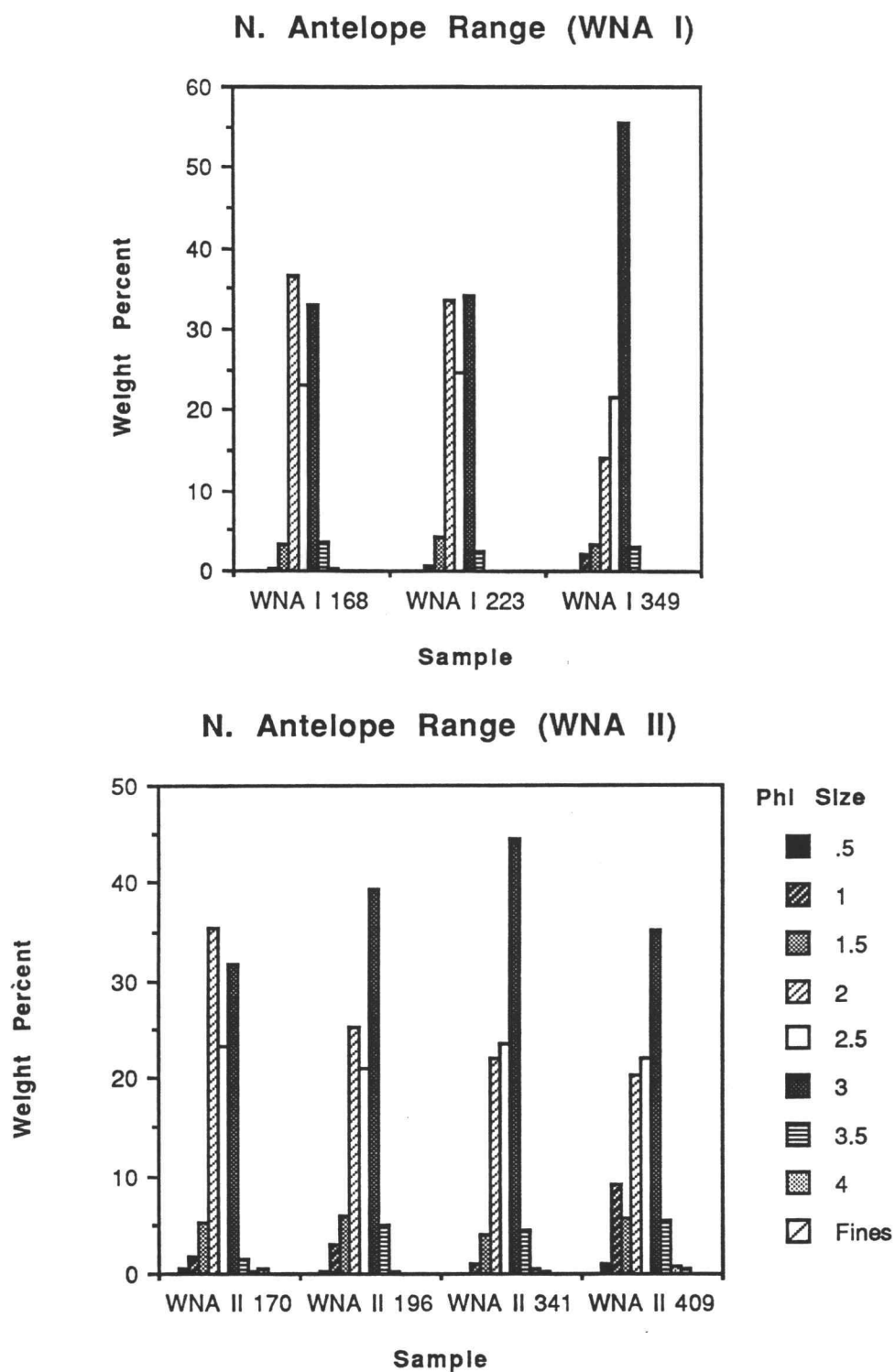
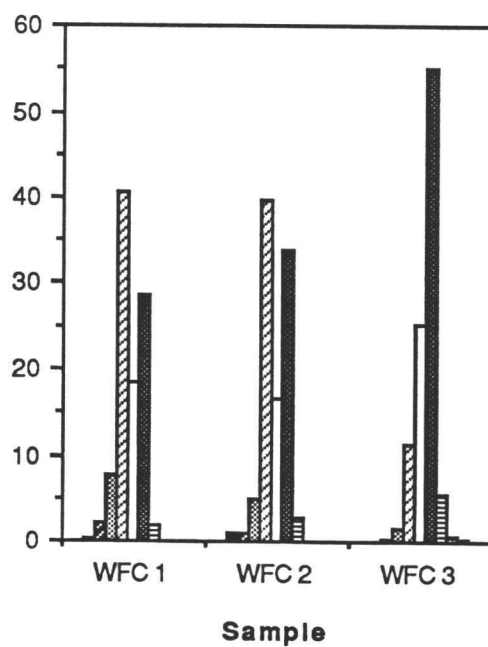


Figure 37. WNA I and WNA II grain-size histograms.

S. Fish Creek Range (WFC)



S. Tuscarora Mountains (WRC I)

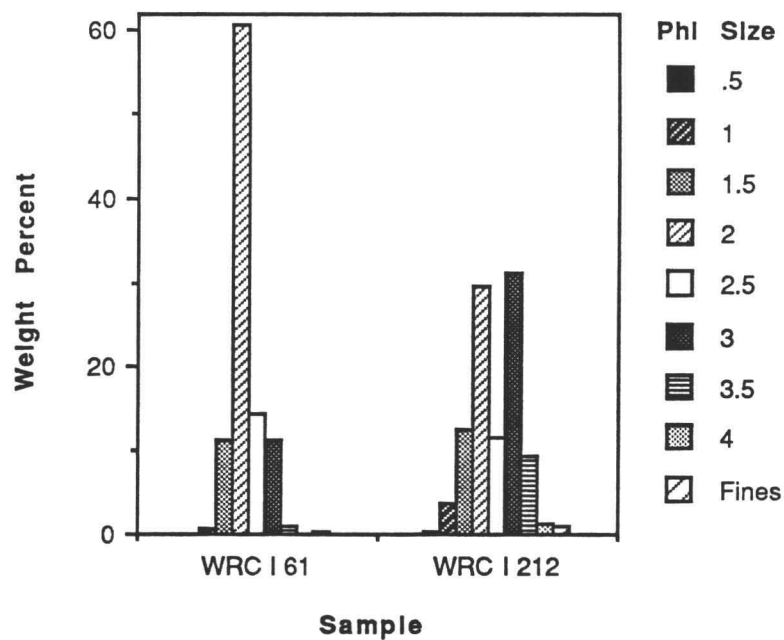


Figure 38. Southern Fish Creek Range (WFC) and southern Tuscarora Mountains (WRC I) grain-size histograms.

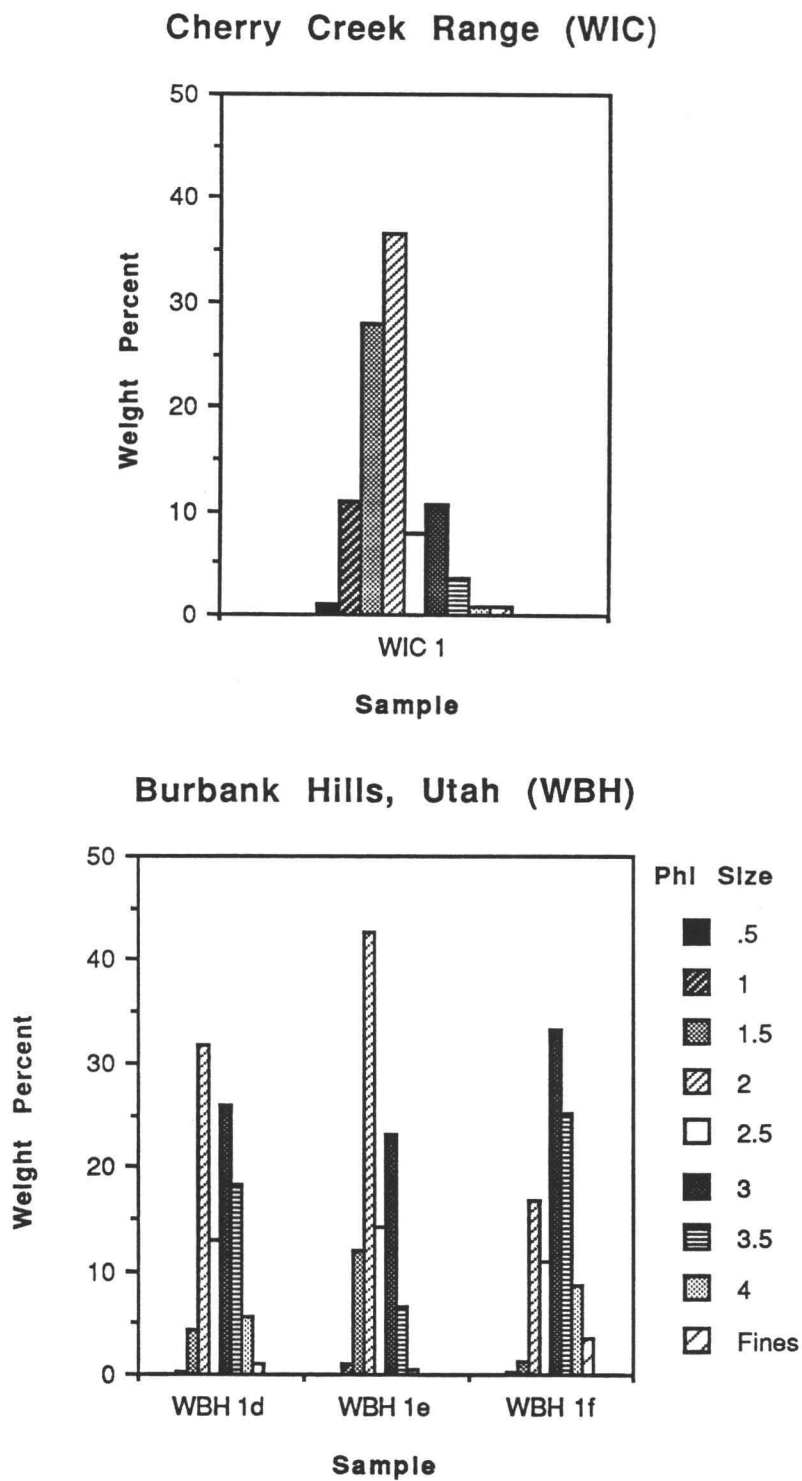
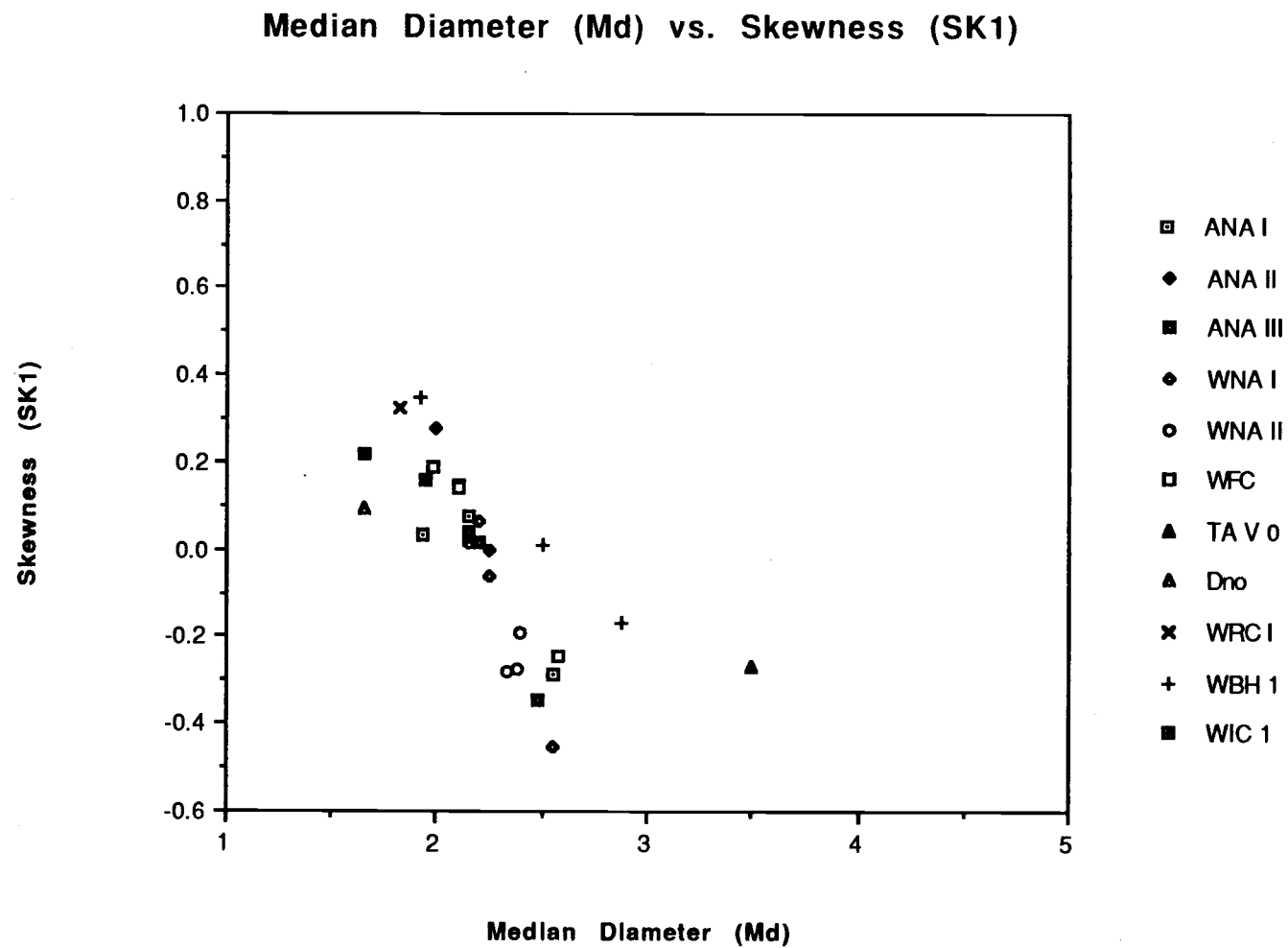


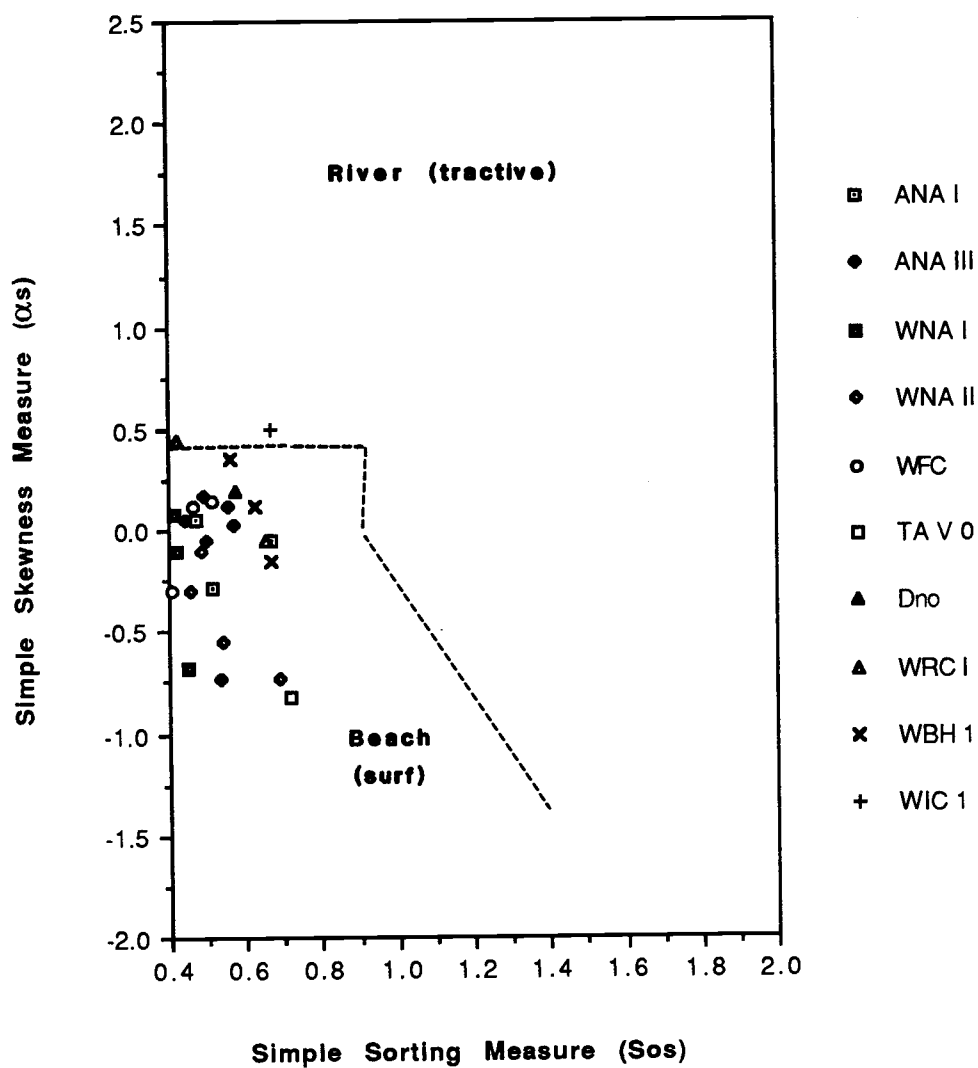
Figure 39. Cherry Creek Range (WIC) and south Burbank Hills, Utah (WBH), grain-size histograms.

bimodality of these sands may be inherited.

Four bivariate graphs of the type utilized by Friedman (1961, 1967) were constructed (Figs. 40-43). Friedman defined fields on these graphs which have been used to distinguish such depositional environments as river, dune, and beach. Such fields are not displayed on the graphs presented herein, as an assumption that the quartz-sand fraction of sandy limestone reflects the last clastic sedimentary lithotype before deposition into a carbonate depositional environment is probably invalid. Comparison of this nature is useful, however, if restricted to affinities between adjacent formations and facies. Conversely, on a binary plot of simple sorting (So_s) vs. simple skewness (α_s) (Fig. 41) employed by Friedman (1961) to distinguish beach vs. river (surf vs. tractive) environments, nearly all analyzed samples (27 of 29) fall within the field of beach environment. Independent lines of evidence such as rounding also suggest a previous beach environment, and the observed sand seems likely to have been cycled through a beach environment and subsequently shifted by longshore currents into shallow carbonate depositional environments, before being transported farther offshore during a series of Late Devonian regressions discussed elsewhere in this report. Furthermore, this plot (Fig. 41) indicates that simple skewness and sorting characteristics of all the studied Upper Devonian sandy limestones fall into a well-defined range of values, suggesting similar source areas for the quartz sand fractions. Similarly, a bivariate plot of inclusive graphic standard deviation (sorting; s_1) vs. mean (M_z) (Fig. 43) shows that most samples fall within a fairly narrow range of values. A notable exception on all four bivariate plots is sandy limestone sampled from the Cherry Creek Range (WIC 1) and from the southern Burbank Hills, Utah (WBH 1), whose values appear to differ significantly from the other localities. Bivariate plots of median diameter (M_d) vs. inclusive graphic skewness (SK_1) (Fig. 40), and one of inclusive graphic standard deviation (s_1) vs. inclusive graphic skewness (SK_1) (Fig. 42) both



Simple Sorting (S_{os}) vs. Simple Skewness (α_s)



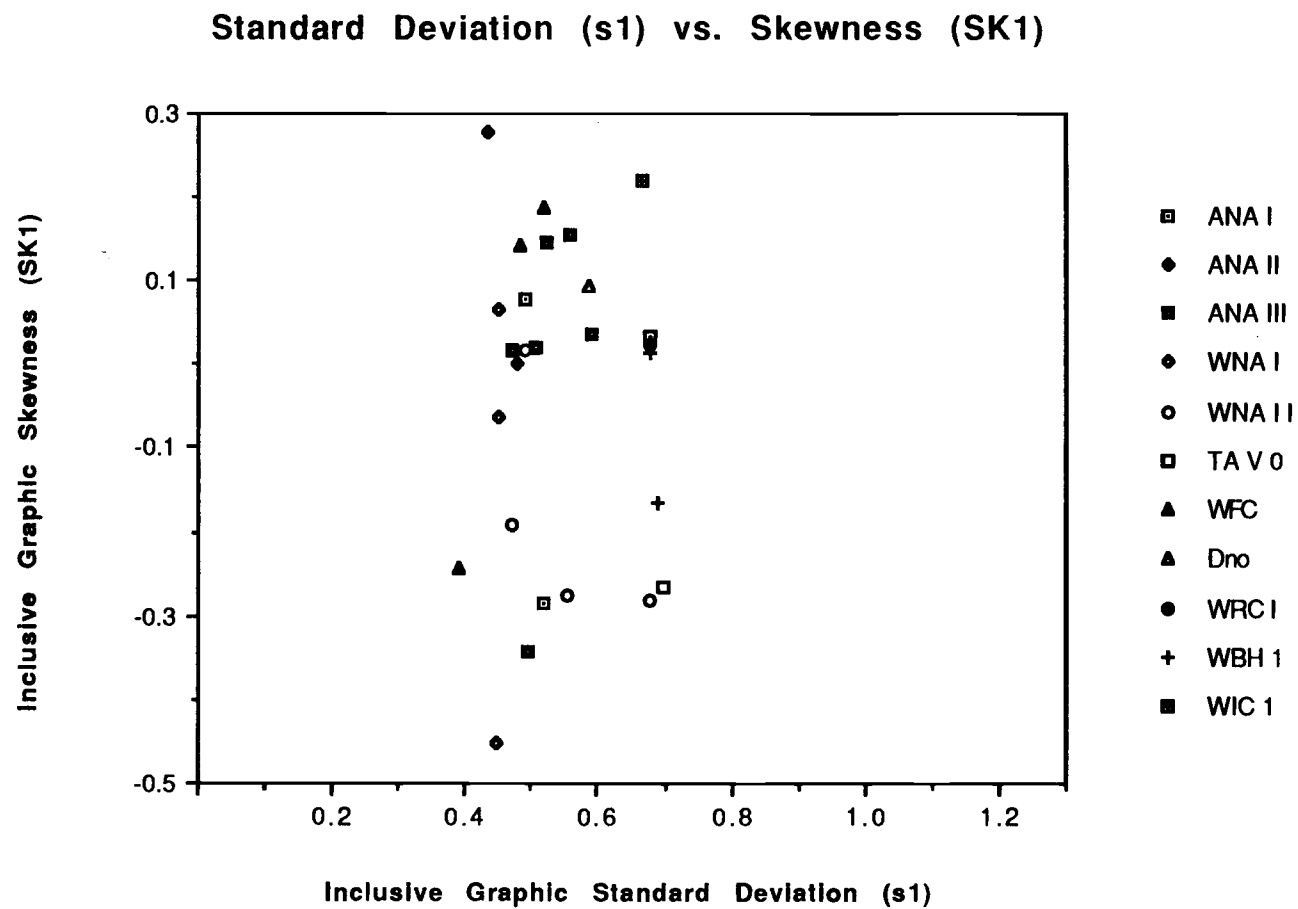


Figure 42. Friedman (1961, 1967) bivariate graph of inclusive graphic standard deviation versus inclusive graphic skewness.

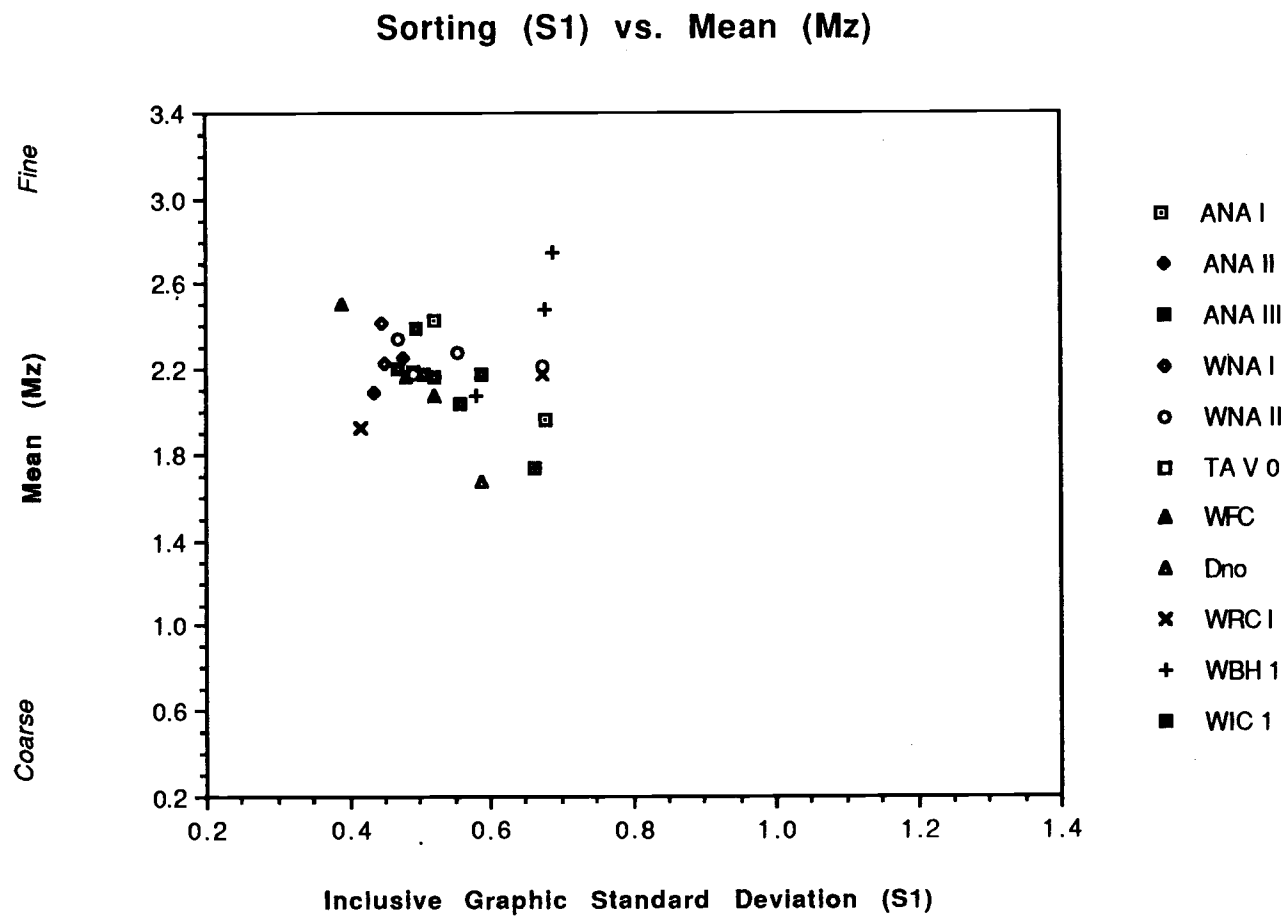


Figure 43. Friedman (1961, 1967) bivariate graph of inclusive graphic standard deviation versus mean grain size.

show general linear trends, although an interpretation of these based upon what little is understood about the hydrodynamics of quartz grains in carbonate depositional environments may be misleading.

A CM graph (Passega, 1957) was created (Fig. 44), which stresses hydrodynamic processes of the coarsest 1% and median grain size as opposed to the depositional environment graphs of Friedman (1961, 1967). In agreement with Friedman (1961) simple skewness vs. simple sorting plot (Fig. 41), most of the analyzed samples plot within a beach-process field (VII). A sample from the southern Tuscarora Mountains (WRC 1) and one from section ANA II plot close to the field IV minimum, interpreted by Passega (1957) as indicative of minimum turbulence at the bottom of the current.

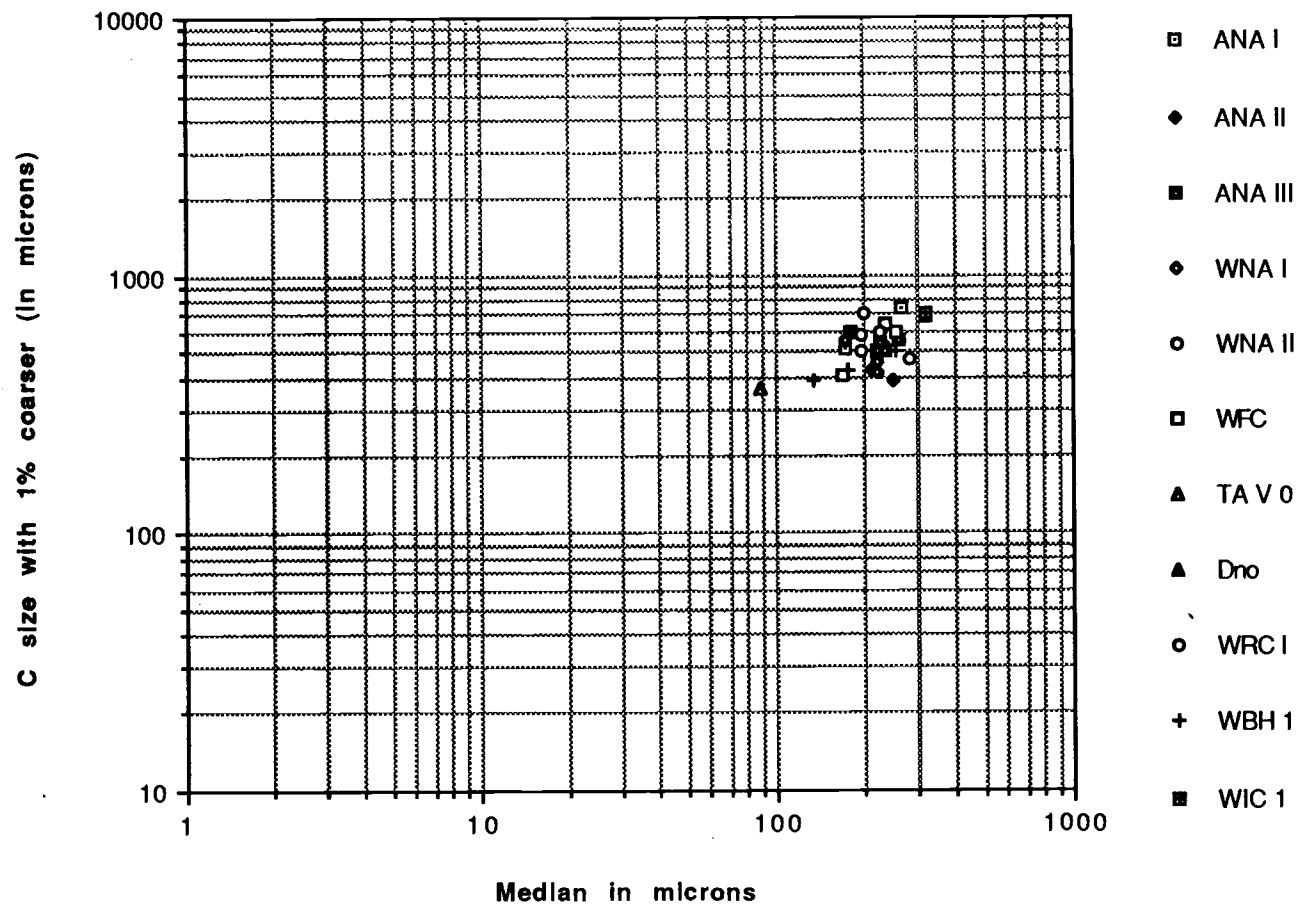


Figure 44. Coarsest one percentile (C) versus median diameter (M). Modified after Passega (1957).

DEPOSITIONAL ENVIRONMENTS

Sandy limestone of the Fenstermaker Limestone in the northern Antelope Range, and in two allochthonous blocks in the southern Fish Creek Range, was probably deposited by sediment gravity flows onto a ramp or gently inclined slope into an outer-shelf basin in response to emergence and erosion on the inner and/or middle platform. Deposition by reciprocal sedimentation accounts for the observed upward-thickening sequence of interbedded shale and sandy limestone in the lower Fenstermaker in combination with incipient outer-shelf basin filling.

QUARTZ SAND PROVENANCE AND MIXING

Provenance for detrital quartz sand fractions was probably to the southeast or north of the northern Antelope Range. A combination of cratonic and older sandy limestone/sandstone sources are indicated by the both the high degree of rounding attained by the majority of sand grains (2nd-4th cycle) and a lack of westerly, eugeosynclinally derived grains such as detrital chert.

Grain-size analyses of detrital quartz sands suggest that quartz grains attained their sorting characteristics in a high-energy wave-dominated siliciclastic beach environment prior to dispersal into the adjacent carbonate shelf environment. In a Friedman (1967) graph of simple sorting versus simple skewness (Fig. 41), quartz sand fractions from five ranges in east-central Nevada plotted well within the beach depositional environment field. The viscous nature of carbonate oozes precludes such a degree of quartz-sand sorting (and rounding) once mixed into the carbonate lithotope.

The mixing of carbonate and siliciclastic sediment has been recognized as a major sedimentary process along both in modern and ancient shelf margins. Modern

carbonate-clastic depositional environments in which detrital quartz sand constitutes a significant percentage include the Gulf of Elat in the Red Sea and along the coast of the Java Sea (Friedman, 1988), as well as throughout most of a 270,000 sq. km mixed system associated with the Great Barrier Reef (Belperio and Searle, 1988). Holmes (1988) noted that a greater volume of siliciclastic sediment enters the carbonate environment of southwest Florida during extreme lowstands of sea level, which supports Hine's (1983) suggestion that sand is deposited off bank margins for short intervals during transgressive starts and during pre-emergence eustatic lowering of sea level. Shanmugam and Moiola (1982) discussed an increased frequency in turbidite deposition during lowered sea level, as well as an increase in the occurrence of winnowed turbidite deposits as a result of strong basinal contour currents. Fenstermaker sandy pelsparites are winnowed as well, and deposition probably occurred during T-R cycle IId regressions, discussed in a previous section. The extent to which carbonate deposition was reduced during T-R cycle IId regressions is clearly indicated on Sandberg and others (1989) paleobiogeographic lithofacies maps of the Lower *gigas* Zone and Lower *triangularis* Zone (Figs. 45, 46).

Mount (1984) has described and classified four major carbonate-siliciclastic mixing models. These models are termed punctuated mixing, facies mixing, in situ mixing, and source mixing. Of these, only elements of the punctuated-mixing and source-mixing models seem to be applicable to the Fenstermaker depositional environment.

In the punctuated-mixing model, mixing of siliciclastic and carbonate sediment occurs during "rare, high intensity sedimentation events" in response to storm-surge ebbs and wind forcing. In the Fenstermaker Limestone, no evidence exists for periodic

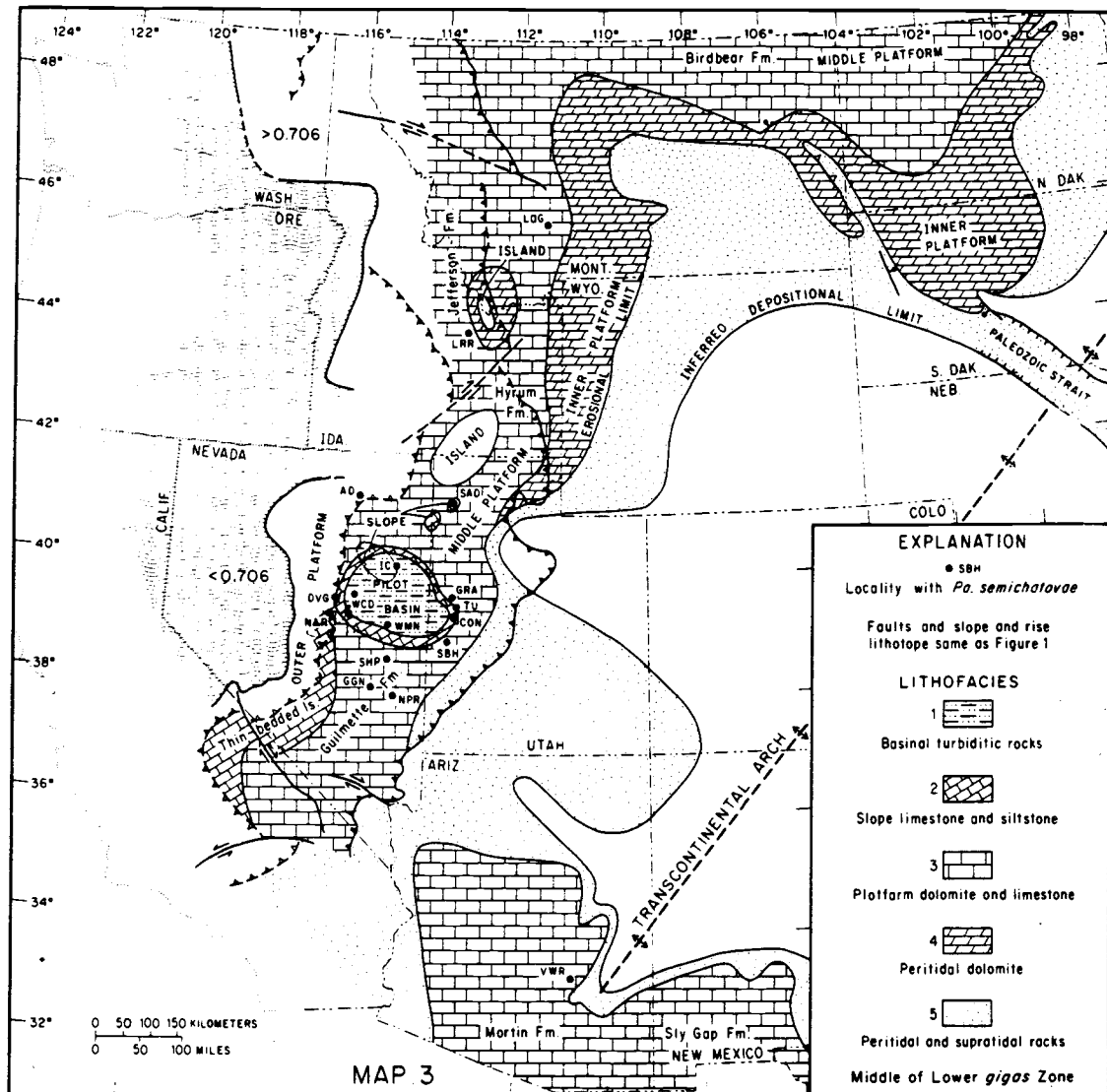


Figure 45. Paleobiogeographic lithofacies map of the Lower *gigas* Zone during maximum transgression (T-R cycle lower IId). NAR=northern Antelope Range. From Sandberg and others (1989).

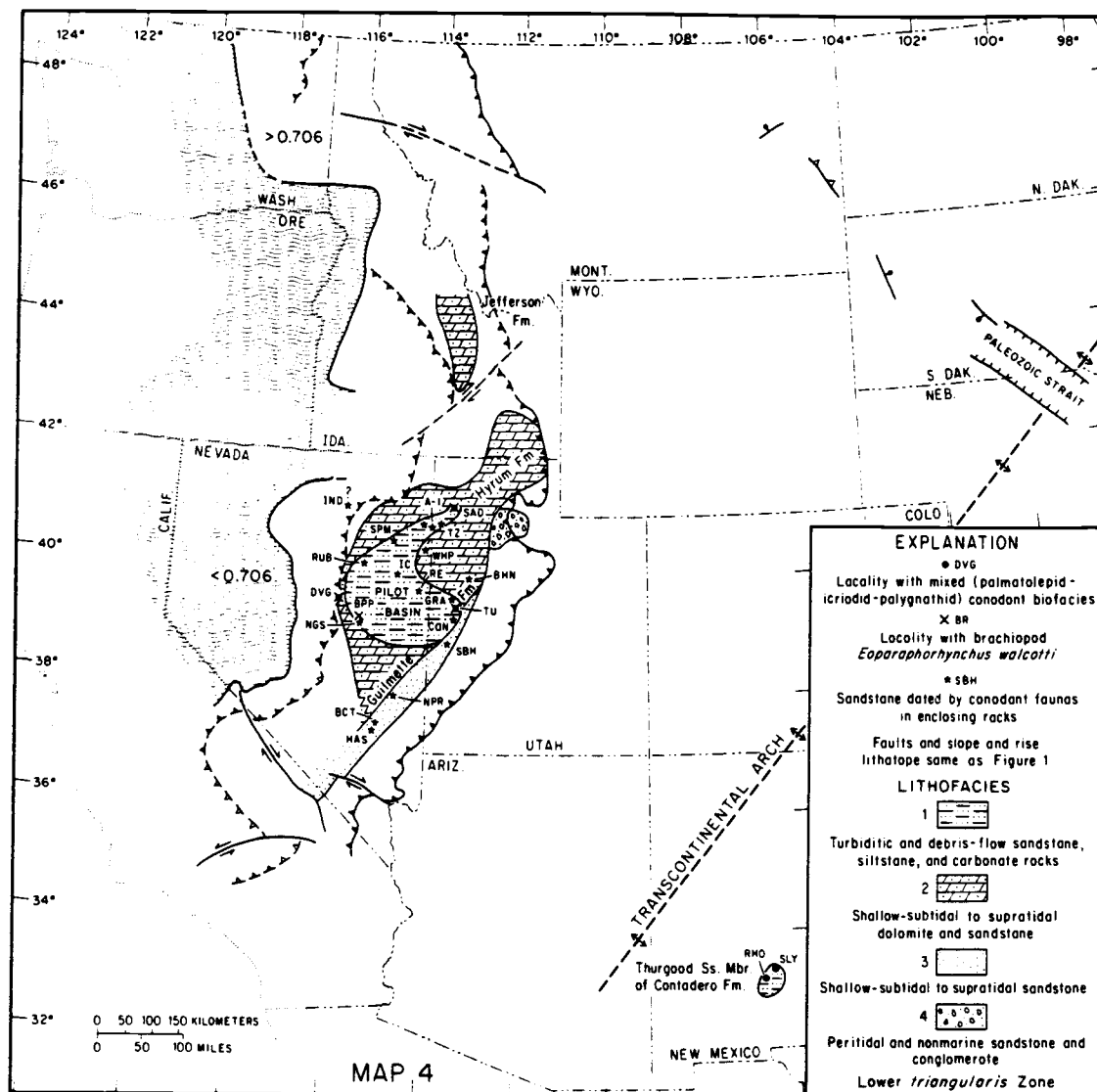


Figure 46. Paleobiogeographic lithofacies map showing greatly reduced areal distribution of lowest Famennian (T-R cycle upper IId; Lower *triangularis* Zone) rocks. From Sandberg and others (1989).

sand influx in the form of sand-rich or sand-poorer layers. Instead, quartz sand seems to be rather uniformly mixed throughout the beds, except where rhythmic sand layering is present at the base of allodapic beds (near ANA I, WNA II 196, and an equivalent horizon in the main Fenstermaker cliff in WNA I). However, carbonate-siliciclastic mixing could have occurred sporadically, with quartz sand and peloid admixtures being produced as high-energy channels carried mixed sediment across the carbonate platform.

The source-mixing model is attractive because it accounts for emergence and erosion of older carbonate source terranes, but it produces admixtures of carbonate clasts in basically siliciclastic environments, dissimilar to observed Fenstermaker (and other east-central Nevada Upper Devonian) lithotypes. A variation of this model, however, in which quartz sand and sandy limestone was eroded into a dominantly carbonate shallow-shelf environment seems plausible, and Mount (1984) points out that his models do not account for all possibilities.

The most likely explanation for carbonate-siliciclastic mixing in the Fenstermaker Limestone is by longshore transport of sorted siliciclastic beach sand (Bowen, 1969; Komar, 1976, p. 183-200) into an area shoreward of the restricted Fenstermaker shoals. Significant terrigenous influx during uppermost Denay deposition in response to platform emergence and erosion east of the northern Antelope Range may have led to decreased carbonate production on the shelf and therefore restriction of the Fenstermaker biota to a pellet-forming infauna, with rare patches of brachiopods and crinoids. With erosion dominant over deposition and over carbonate production on the platform, siliciclastic influx would not have a significant influence on carbonate depositional environments.

Interfingering wedges of carbonate and siliciclastic deposits have been termed reciprocal (Wilson, 1967; Rose, 1976). Products of reciprocal sedimentation need not

necessarily be beds of pure limestone and sandstone, but as in the case of the Fenstermaker Limestone, the product is interbedded sandy limestone and outer-shelf-basinal calcareous mudstone (Fig. 47). In response to sea-level fluctuation, variation in subsidence rate, or regional uplift, a carbonate shelf environment can be flooded by craton-derived terrigenous detritus. Transport of detrital matter across the shelf is rapid and often complete to the extent that emergent phases may not be recognized within the shelf sequence (Rose, 1976).

DEPOSITIONAL MODELS

From early in the Frasnian *asymmetrica* Zone until at least the Famennian Middle *triangularis* Zone, an outer-shelf basin existed along the collapsed shelf edge (Matti and others, 1975; Matti and McKee, 1977; Johnson and Trojan, 1982; Johnson and others, 1989; Fig. 48). Although Figure 48 depicts the general trend of this basin, its actual shape and extent remains unknown (J. G. Johnson, pers. comm.). Matti and McKee (1977) postulated that in the Early Devonian this basin possessed a seaward edge, which they termed the Toiyabe Ridge. However, Johnson and others (1989) point out that the few observed shallow-water buildups of the Tor Limestone do not justify an interpretation which includes a continuous ridge.

The floor of this outer-shelf basin was probably "starved" at times. The concept of starved basins was presented by Rose (1976), where he noted that calcareous basinal sediment can be 1/2 to 1/10 as thick as coeval shelf carbonate and realized that most of this basinal sediment was derived from the adjacent shelf. In his discussion of pelagic and hemipelagic carbonates, Cook (1983) recognizes the starved-basin facies. He attributes starved basins of the Paleozoic to a combination of high biotic diversity, but low total abundances in the pelagic realm. Paleozoic deeper water carbonate deposits

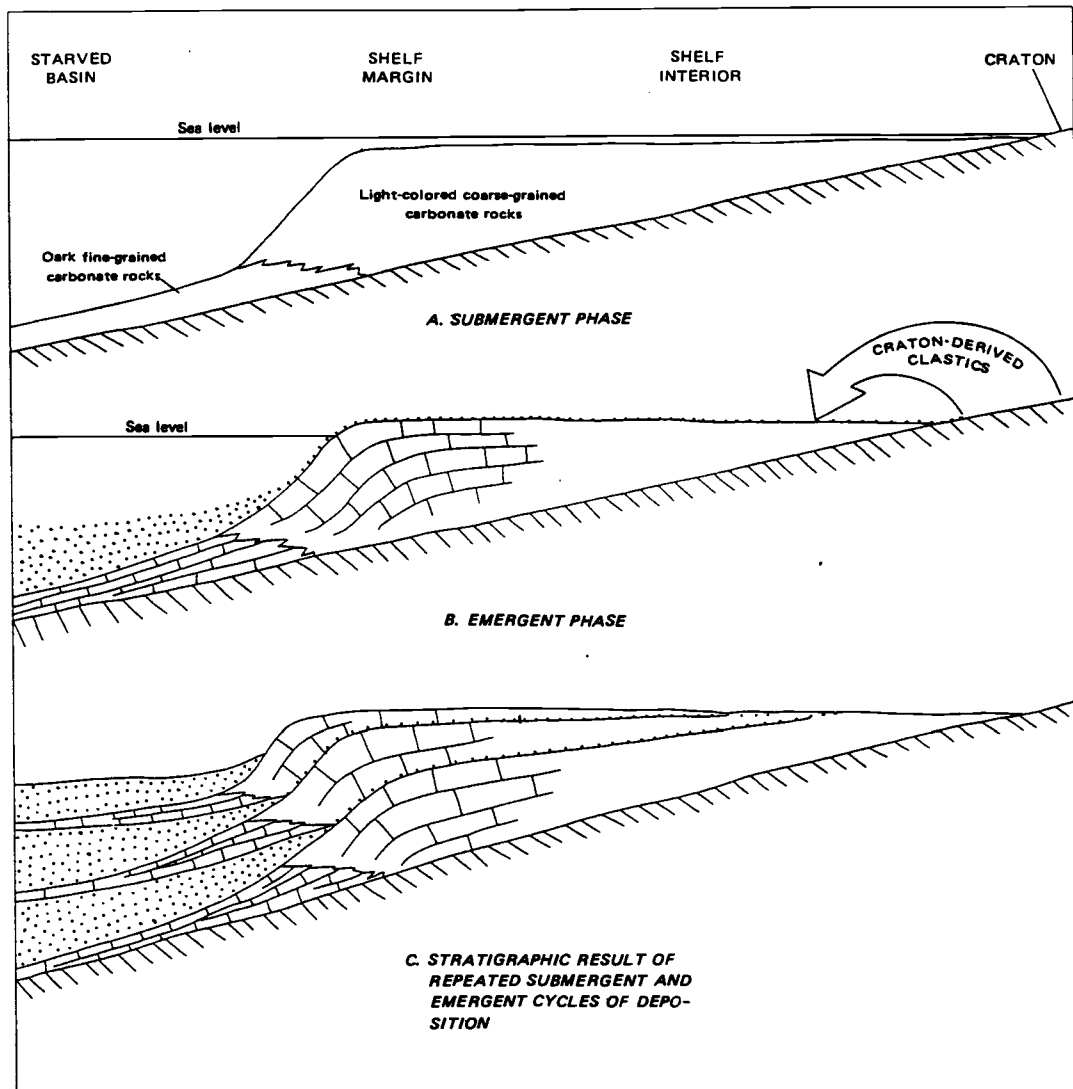


Figure 47. Reciprocal sedimentation model. Dotted clastic products can be sandy limestone (as with Fenstermaker Limestone) From Rose (1976).

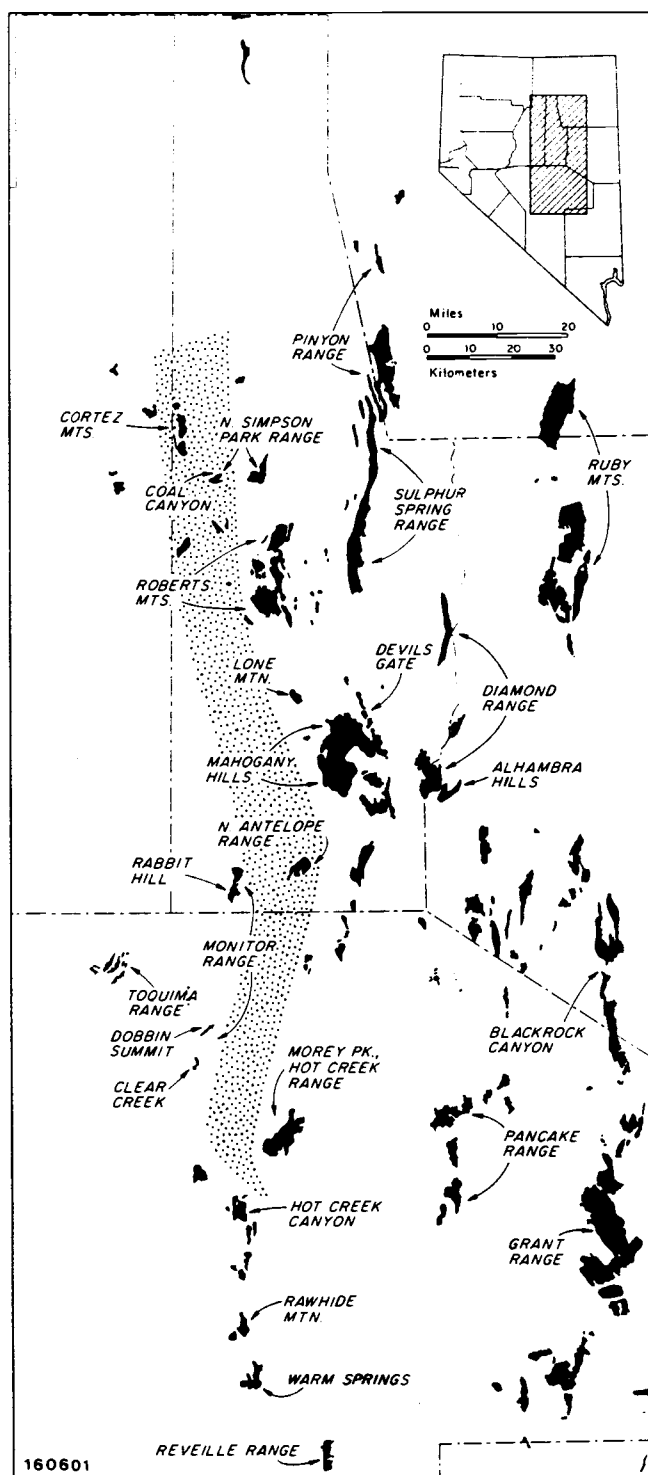


Figure 48. Inferred position of outer-shelf basin (dotted strip) that existed west of the broad carbonate shelf from the *asymmetrica* Zone through at least the Middle *triangularis* Zone. Devonian outcrops are in solid black. From Johnson and Trojan (1982).

consist mainly of platform-derived sediment, with low pelagic contributions.

Conversely, deeper-water carbonate environments of mid-Mesozoic (and later) ages are highly populated with pelagic forms (for example, forams and coccoliths), which greatly increase the pelagic contribution to these sediments (Cook and Egbert, 1983).

The Fenstermaker Limestone was deposited as a deeper water apron (sensu Mullins and Cook, 1986; Cook, 1983) along the outer-shelf-basin margin. Although these rocks display several of the same microfacies and bedding characteristics as shallow-water shelf limestones, compelling evidence suggests a deeper water depositional setting. Fenstermaker sandy limestone beds are clearly interbedded with deeper water spiculitic, radiolarian-rich mudstone in the ANA II and lower ANA III sections and are bounded by diagenetic chert layers at these horizons. Conodonts are mainly of the deeper-water *Palmatolepis* biofacies (Sandberg, 1976; Plate 1), with a contribution of shallow-water and reworked shallow-water conodont species. Rocks of this type have been termed peri-platform oozes (Schlager and James, 1978), which most often consist of shallow-water lime mud, pelagic constituents from open-marine environments, and terrigenous clastics (Cook, 1983).

In assigning these rocks to a deeper water carbonate lithotope, an apparent contradiction might seem to be the light color of both the Fenstermaker sandy limestone beds and the lower interbedded shale and mudstone. Light-colored, deeper water limestone of marginal-cratonic and intracratonic-basinal origin has been observed (Wilson, 1969). The Fenstermaker Limestone was probably deposited at depths of 150 m or less, within the zone of aerobic and dysaerobic water layering (Byers, 1977). Further evidence that these rocks were deposited in an aerobic or dysaerobic environment, as opposed to an anaerobic environment, is provided by the general lack of sedimentary structures, probably the result of intense bioturbation by a burrowing infauna. Byers (1977) presents an example from the Upper Devonian of New York

State (Sawmill Creek Shale) which was deposited in the dysaerobic zone (50-150 m water depth) in which all sedimentary structures have been destroyed, and as with the Fenstermaker, lacks a shelly fauna.

Allochthonous slope carbonate is well known from central and east-central Nevada. The Ordovician lower Hales Limestone of Nevada was deposited in a similar setting on the carbonate slope (Cook and Taylor, 1977), and it also contains transported quartz sand. At Copenhagen Canyon, Lower Devonian beds (for example, the Rabbit Hill Limestone) are allodapic, grain-supported, graded and nongraded, skeletal and nonskeletal calcarenites (Matti and others, 1975) that were transported out into basinal environments. Allochthonous facies are recognized in the McColley Canyon Formation (Mullins and Cook, 1986), Denay Limestone (Trojan, 1978; this study), and others as well.

In terms of microfacies and textures, the sandy limestone of the Fenstermaker Limestone most resembles the "boundary limestone" studied in detail by McIlreath (1977), which was shed off the thick Cathedral Formation escarpment as a flanking wedge against the interfingering and overlying basinal Stephen Formation. In this shelf by-pass setting, peloidal muds were deposited in thin- to massive-bedded intervals as heterogeneously mixed wackestone to grainstone. Major differences between the "boundary limestone" and the Fenstermaker Limestone are that the former are not bioturbated, do not contain detrital quartz sand, and include numerous intraformational truncation surfaces.

Throughout the relatively brief period of Fenstermaker Limestone deposition, the outer-shelf-basin shelf edge was probably a ramp, or a shelf-slope break of low angle ($<40^\circ$). The carbonate-ramp model was presented by Read (1982, 1985), and the Persian Gulf is a good example of a modern carbonate ramp (Wilson and Jordan, 1983). Although Read (1982, 1985) presents several different ramp models,

Fenstermaker outcrops provide insufficient information to make reliable distinctions between them. Evidence for a very gentle slope into the outer-shelf basin is suggested by the lack of megabreccias (in the sense of Cook and Egbert, 1981; Cook, 1983) and intraformational truncation surfaces, which are features normally observed at steeper slope aprons.

DEPOSITIONAL MECHANISMS

Sandy limestone of the Fenstermaker Limestone were probably deposited as sediment gravity flows toward the distal end of a outer-shelf-basin carbonate ramp, or very low-angle carbonate slope.

Allodapics, or carbonate turbidites, were defined by Meischner (1964), who pointed out the major differences between carbonate and siliciclastic turbidites (in the sense of Mutti and Ricci Lucchi, 1972). Important differences between these two basic types of shelf-slope resedimentation processes and the geometry of the deposits they produce have been stressed by several authors (Colacicchi and Baldanza, 1986; Matti and others, 1975; Mullins and Cook, 1986; Cook and others, 1972).

The most significant difference between carbonate and siliciclastic turbidites is the areal distribution of the deposits. Siliciclastic turbidites are usually fed from a point source, such as the head of a submarine canyon, and therefore create fan deposits. Conversely, allodapic flows tend to be fed from a line source, with many smaller feeder channels, resulting in a wedge-shaped apron deposit (Mullins and Cook, 1986; Colacicchi and Baldanza, 1986). Multiple canyon heads which feed sheet-flow allodapic systems can be observed along Little Bahama Bank. Apron deposits are classified as slope aprons or base-of-slope aprons (Mullins and Cook, 1986), depending upon the nature of the platform rim and the slope angle. Allodapics of the

Fenstermaker Limestone were deposited on an shoaling-upward ramp apron, but this ramp may have extended only up to a platform-margin peloidal shoal. Figure 49 is a model depicting probable Fenstermaker depositional environments.

Whether or not classical Bouma (1962) sequences can be observed in allodapics, as well as the depositional mechanisms through which these deposits are transported, has been the subject of some debate (for example, Colacicchi and Baldanza, 1986; Matti and others, 1975). Commonly, a few sedimentary structures typical of Bouma sequences are observed, but rarely are most characteristic features present in any one deposit. Sequences are base-cut-out and/or missing- T_d sequences. True T_e sequences are generally absent or unrecognizable (Colacicchi and Baldanza, 1986). The different areal distribution of allodapics, as well as the lack of recognizable sedimentary structures, has been attributed to a lack of mud in these flows (heavily loaded), creating low transport efficiency and a rapid loss of kinetic energy, differences in the feeding system, and commonly, tectonic control by syndimentary fault systems which continually rejuvenate the escarpment (Scaglia Formation examples of Colacicchi and Baldanza, 1986). Depositional mechanisms for allodapics have been variously described as sediment gravity flows (Mullins and Cook, 1986), hybrid sediment gravity flows (Hopkins, 1977), and grain flows and modified grain flows (Matti and others, 1975). Several mechanisms may work together during allodapic transport (Cook and others, 1972).

Fenstermaker Limestone allodapics were likely deposited by one of the processes discussed above. Sedimentary structures are generally absent, with the exception of crude, concave-upward lamination resembling dish structure observed at one location, a feature associated with siliciclastic grain flows (Stauffer, 1967), and a bed displaying possible flame structure. Parallel laminations are observed within quartz-sand-rich horizons and are probably the result of differential settling rate during

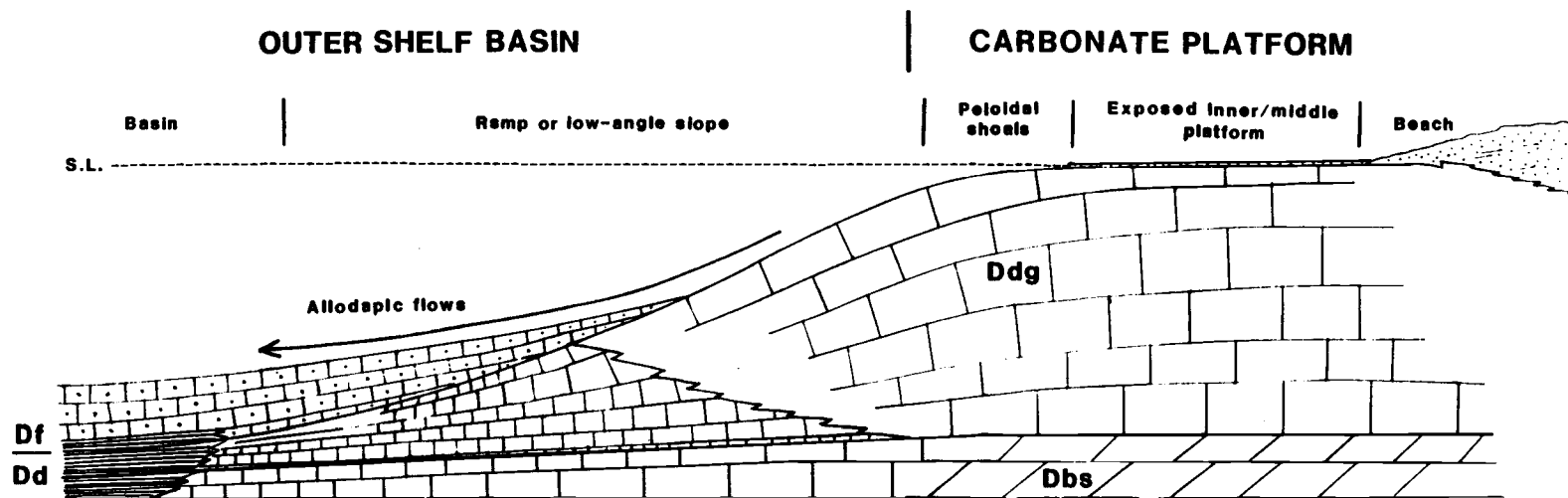


Figure 49. Deposition model for the Fenstermaker Limestone. Vertical thicknesses greatly exaggerated, but reflect measured thickness relationships between Devils Gate pass and the northern Antelope Range. Dbs=Bay State Dolomite; Dd=Denay Limestone; Ddg=Devils Gate Limestone; Df=Fenstermaker Limestone.

turbidite deposition. Peloids initially possess a high internal porosity and would be expected to settle above denser detrital quartz sand grains of the same size (H. E. Cook, pers. comm.). Conversely, well-hardened peloids may settle at rates comparable to quartz grains 70-100% of their size (Wanless and others, 1981).

These allodapic sheets are nongraded, and might be compared with T_a , T_b and/or base-cut-out T_b Bouma sequences. Rare cross-laminated quartz sand beds may be roughly equivalent to T_c Bouma sequences. As an alternative mechanism for segregation into sand-rich and sand-poorer layers, "flowing-grain layers" have been described (Sanders, 1965), in which coarser grains (or denser grains) are moved along the base of the flow as a traction carpet, resulting in internally structureless beds.

CONCLUSIONS

1. The lower contact of the "Fenstermaker Wash Formation," as defined by Hose and others (1982) is well within the lower member of the Denay Limestone. The name Fenstermaker Limestone (revised and restricted), is employed here for beds above ANA II 88 and below the Lower Mississippian Davis Spring Formation in the northern Antelope Range.
2. Resedimented beds of the Fenstermaker Limestone were deposited rapidly in Frasnian Montagne Noir Zone 13 and the Lower Famennian Middle *triangularis* Zone.
3. Intervals containing reworked conodonts within the Fenstermaker Limestone indicate erosion on the carbonate platform and are consistent with Upper Devonian lower and upper T-R cycle II d regressions as indicated by the Devonian eustatic curve of Johnson and Sandberg (1989) and western U. S. events 7 and 8 (Sandberg and others, 1989).
4. Sandy limestone of the Fenstermaker Limestone was probably deposited as sediment gravity flows on an outer-shelf-basin ramp in response to emergence and erosion on the inner or middle platform. Deposition by reciprocal sedimentation accounts for the observed upward-thickening sequence of interbedded shale and sandy limestone in the lower Fenstermaker in combination with incipient outer-shelf-basin filling.

5. Detrital quartz sand in all analyzed limestone samples attained its grain-size characteristics in a siliciclastic beach environment prior to final deposition in the carbonate lithotope.

6. Pitting and frosting of detrital quartz-sand grains in the Fenstermaker Limestone is diagenetic in origin, and not strictly a product of eolian transport.

7. Allochthonous (previously unidentified) southern Fish Creek Range limestone blocks A and C of Sans (1986) are assigned to the Fenstermaker Limestone and are considered to have been derived from the west.

8. Detrital quartz grains concentrated along stylolites, as in the Popovich Formation of the Tuscarora Mountains, can be used to quantify formational thickness losses.

9. Limestone coeval with the Fenstermaker Limestone is not present in the southern Cortez Mountains.

REFERENCES

- Alvarez, L. W., Alvarez, W., Asaro, F., and Michel, H. V., 1980, Extraterrestrial cause for the Cretaceous-Tertiary extinction: *Science*, v. 208, p. 1095-1108.
- Bathurst, R. G. C., 1975, Carbonate sediments and their diagenesis: *Developments in Sedimentology* 12, Elsevier, Amsterdam, 658 p.
- Belperio, A. P., and Searle, D. E., 1988, Terrigenous and carbonate sedimentation in the Great Barrier Reef province, *in* Doyle, L. J., and Roberts, H. H. (eds.), Carbonate-clastic transitions: *Developments in Sedimentology* 42, Elsevier, Amsterdam, chapt. 5, p. 144-174.
- Biller, E. J., 1976, Stratigraphy and petroleum possibilities of lower Upper Devonian (Frasnian and lower Famennian) strata, southwestern Utah: U. S. Geol. Survey Open File Report 76-0343, 105 p.
- Bissell, H.J., 1959, Silica in sediments of the upper Paleozoic of the Cordilleran area, *in* Ireland, H. A. (ed.), Silica in sediments: *Soc. Econ. Paleontol. Mineral. Spec. Pub.* 7, p. 150-185.
- Blatt, H., 1982, Sedimentary petrology: W. H. Freeman and Co., New York, 564 p.
- Bouma, A. H., 1962, Sedimentology of some flysch deposits: Elsevier, Amsterdam, 168 p.
- Bowen, A. J., 1969, The generation of longshore currents on a plane beach: *Jour. Mar. Res.*, v. 37, p. 206-215.
- Byers, C. W., 1977, Biofacies patterns in euxinic basins: a general model, *in* Cook, H. E., and Enos, P. (eds.), Deep-water carbonate environments: *Soc. Econ. Paleontol. Mineral. Spec. Pub.* 25, p. 5-17.
- Choquette, P. W., and James, N., 1987, Diagenesis #12. Limestones-3. The deep burial environment: *Geoscience Canada*, v. 14, n. 1, p. 3-35.
- _____, and Pray, L. C., 1970, Geologic nomenclature and classification of porosity in sedimentary carbonates: *Am. Assoc. Petrol. Geol. Bull.*, v. 54, p. 207-250.
- Colacicchi, R., and Baldanza, A., 1986, Carbonate turbidites in a Mesozoic pelagic basin: Scaglia Formation, Apennines-comparison with siliciclastic depositional models: *Sed. Geol.*, v. 48, p. 81-105.
- Coogan, A. H., 1970, Measurements of compaction in oolitic grainstone: *Jour. Sed. Pet.*, v. 40, p. 921-929.
- Cook, H. E., 1983, Ancient carbonate platform margins, slopes, and basins, *in* Cook, H. E., Hine, A. C., and Mullins, H. T. (eds.), Platform margin and deep water carbonates: *Soc. Econ. Paleontol. Mineral. Short Course No.* 12, p. 5-1—5-189.

- Cook, H. E., and Egbert, R. M., 1983, Diagenesis of deep-sea carbonates, in Larsen, G., and Chilingar, G. V. (eds.), *Diagenesis in sediments and sedimentary rocks*: Elsevier, Amsterdam, p. 213-288.
- _____, McDaniel, P. N., Mountjoy, E. W., and Pray, L. C., 1972, Allochthonous carbonate debris flows at Devonian bank ("reef") margins, Alberta, Canada: *Am. Assoc. Petrol. Geol. Bull.*, v. 20, p. 439-497.
- _____, and Taylor, M. E., 1977, Comparison of continental slope and shelf environments in the Upper Cambrian and lowest Ordovician of Nevada, in Cook, H. E., and Enos, P. (eds.), *Deep-water carbonate environments*: Soc. Econ. Paleontol. Mineral. Spec. Pub. 25, p. 51-81.
- Copper, P., 1986, Frasnian-Famennian mass extinction and cold-water oceans: *Geology*, v. 14, p. 835-839.
- Delair, J., and Leroux, C., 1978, Méthodes de quantification de la disparition de matière au niveau de stylolites tectoniques et mécanismes de la déformation cassante des calcaires: *Bull. Soc. Géol. France*, v. 7, p. 137-144.
- Dunham, R. J., 1962, Classification of carbonate rocks according to depositional texture, in Ham, W. E. (ed.), *Classification of carbonate rocks*: Amer. Assoc. Petrol. Geol. Mem. 1, p. 108-121.
- Epstein, A. G., Epstein, J. B., and Harris, L. D., 1977, Conodont color alteration-an index to organic metamorphism: U. S. Geol. Survey Prof. Paper 995, 27 p.
- Ettner, D. C., 1989, Stratigraphy and structure of the Devonian autochthonous rocks, north-central Carlin trend of the southern Tuscarora Mountains, northern Eureka County, Nevada: Boise State Univ., unpub. Ph.D. thesis, 177 p.
- Evans, J. G., 1980, Geology of the Rodeo Creek NE and Welches Canyon Quadrangles, Eureka County, Nevada: U. S. Geol. Survey Bull. 1473, 81 p.
- Flügel, E., 1982, *Microfacies analysis of limestones*: Springer-Verlag, Heidelberg, 633 p.
- Folk, R. L., 1962, Spectral subdivision of limestone types, in Ham, W. E. (ed.), *Classification of carbonate rocks*: Amer. Assoc. Petrol. Geol., Mem. 1, p. 62-84.
- _____, 1965, Some aspects of recrystallization in ancient limestones, in Pray, L. C., and Murray, R. C. (eds.), *Dolomitization and limestone diagenesis: A symposium*: Soc. Econ. Paleontol. Mineral., Spec. Pub. 13, p. 14-48.
- _____, 1968, Bimodal supermature sandstones: product of the desert floor: *Proc. 23rd Int. Geol. Cong.*, Sec. 8, p. 9-32.
- Friedman, G. M., 1961, Distinction between dune, beach and river sand from their textural characteristics: *Jour. Sed. Pet.*, v. 31, p. 514-529.

- Friedman, G. M., 1967, Dynamic processes and statistical parameters compared for size frequency distribution of beach and river sands: *Jour. Sed. Pet.*, v. 37, p. 327-354.
- _____, 1988, Case histories of coexisting reefs and terrigenous sediments: The Gulf of Elat (Red Sea), Java Sea, and Neogene basin of the Negev, Israel, in Doyle, L. J., and Roberts, H. H. (eds.), *Carbonate-clastic transitions: Developments in Sedimentology 42*, Elsevier, Amsterdam, chapt. 3, p. 77-97.
- Geldsetzer, H. H. J., Goodfellow, W. D., McLaren, D. J., and Orchard, M. J., 1985, The Frasnian-Famennian boundary near Jasper, Alberta: *Geol. Soc. America Abstracts with Programs*, v. 17, p. 589.
- Gilluly, J., and Masursky, H., 1965, Geology of the Cortez quadrangle, Nevada: *U. S. Geol. Survey Bull.* 1175, 117 p.
- Ginsburg, R. N., Marszalek, D. S., Schneidermann, N., 1971, Ultrastructure of carbonate cements in a Holocene algal reef of Bermuda: *Jour. Sed. Pet.*, v. 41, p. 472-482.
- Hardie, B. S., 1966, Carlin gold mine, Lynn district, Nevada: *Nevada Bur. Mines Report* 13, p. 73-83.
- Harris, L. D., 1958, Syngenetic chert in the Middle Ordovician Hardy Creek Limestone of southwest Virginia: *Jour. Sed. Pet.*, v. 28, p. 205-208.
- Hine, A. C., 1983, Modern shallow water carbonate platform margins, in Cook, H. E., Hine, A. C., and Mullins, H. T. (eds.), *Platform margin and deep water carbonates: Soc. Econ. Paleontol. Mineral. Short Course No. 12*, p. 3-1—3-100.
- Holmes, C. W., 1988, Carbonate to siliciclastic periplatform sediments: southwest Florida, in Doyle, L. J., and Roberts, H. H. (eds.), *Carbonate-clastic transitions: Developments in Sedimentology 42*, Elsevier, Amsterdam, chapt. 10, p. 271-287.
- Hopkins, J. C., 1977, Production of foreslope breccia by differential submarine cementation and downslope displacement of carbonate sands, Miette and Ancient Wall buildups, Devonian, Canada, in Cook, H. E., and Enos, P. (eds.), *Deep-water carbonate environments: Soc. Econ. Paleontol. Mineral. Spec. Pub. 25*, p. 51-81.
- Hose, R. K., 1978, Preliminary map of the Cockalorum Wash quadrangle, Nye and Eureka Counties, Nevada: *U. S. Geol. Survey Open File Report* 78-216.
- _____, 1983, Geologic map of the Cockalorum Wash quadrangle, Eureka and Nye Counties, Nevada: *U. S. Geol. Survey Map* 1-1410.
- _____, Armstrong, A. K., Harris, A. G., and Mamet, B. L., 1982, Devonian and Mississippian rocks of the northern Antelope Range, Eureka County, Nevada: *U. S. Geol. Survey Prof. Paper* 1182, 19 p.

- Illing, L. V., 1954, Bahaman calcareous sands: *Am. Assoc. Petrol. Geol. Bull.*, v. 38, p. 1-95.
- Johnson, D. B., 1972, Devonian stratigraphy of the southern Cortez Mountains, Nevada: University of Iowa, unpub. M.S. thesis, 55 p.
- Johnson, J. G., 1965, Lower Devonian stratigraphy and correlation, northern Simpson Park Range, Nevada: *Canadian Petrol. Geol. Bull.*, v. 13, p. 365-381.
- Johnson, J. G., 1966, Middle Devonian brachiopods from the Roberts Mountains, central Nevada: *Palaeontology*, v. 9, p. 152-181.
- _____, 1970, Taghanic onlap and the end of North American Devonian provinciality: *Geol. Soc. America Bull.*, v. 81, p. 2077-2106.
- _____, 1974, Extinction of perched faunas: *Geology*, v. 2, p. 479-482.
- _____, 1989, Base of the Upper Devonian in the conodont zonation: *Newsl. Stratigr.*, v. 21, p. 11-14.
- _____, Klapper, G., and Sandberg, C. A., 1985, Devonian fluctuations in Euramerica: *Geol. Soc. America Bull.*, v. 96, p. 567-587.
- _____, Klapper, G., and Sandberg, C. A., 1986, Late Devonian eustatic cycles around margin of Old Red Continent: *Annales de la Soc. géol. de Belgique*, v. 109, p. 141-147.
- _____, Klapper, G., and Trojan, W. R., 1980, Brachiopod and conodont successions in the Devonian of the northern Antelope Range, central Nevada: *Geol. et Palaeontol.*, v. 14, p. 77-107.
- _____, and Murphy, M. A., 1984, Time-rock model for Siluro-Devonian continental shelf, western United States: *Geol. Soc. America Bull.*, v. 95, p. 1349-1359.
- _____, and Pendergast, A., 1981, Timing and mode of emplacement of the Roberts Mountains allochthon, Antler orogeny: *Geol. Soc. America Bull.*, v. 92, p. 648-658.
- _____, and Sandberg, C. A., 1977, Lower and Middle Devonian continental shelf rocks of the western United States, in Murphy, M. A., Berry, W. B. N., and Sandberg, C. A. (eds.), *Western North America: Devonian*: Univ. of Calif., Riverside Campus Mus. Contribution 4, p. 121-143.
- _____, _____, 1989, Devonian eustatic events in the western United States and their biostratigraphic responses, in McMillan, N. J., Embry, A. F., and Glass, D. J. (eds.), *Devonian of the world*: *Canadian Soc. Petrol. Geol., Mem. 14*, Proc. of the Second Int. Symposium on the Devonian System, Calgary, Canada, v. 3: Paleontology, paleoecology, and biostratigraphy, p. 171-178 (imp. 1988).

- Johnson, J. G., Sandberg, C. A., and Poole, F. G. 1989, Early and Middle Devonian paleogeography of the western United States, in McMillan, N. J., Embry, A. F., and Glass, D. J. (eds.), *Devonian of the world: Canadian Soc. Petrol. Geol., Mem. 14, Proc. of the Second Int. Symposium on the Devonian System, Calgary, Canada, v. 1: Regional synthesis*, p. 161-182 (imp. 1988).
- _____, and Trojan, W. R., 1982, The *Tecnocyrtina* brachiopod fauna (?Upper Devonian) of central Nevada: *Geol. et Palaeontol.*, v. 16, p. 119-150.
- Klapper, G., 1988, Intent and reality in biostratigraphic zonation: a reply to Sandberg, Ziegler, and Bultynck (1988): *Newsl. Stratigr.*, v. 19, p. 179-183.
- _____, 1989, The Montagne Noir Frasnian (Upper Devonian) conodont succession, in McMillan, N. J., Embry, A. F., and Glass, D. J. (eds.), *Devonian of the world: Canadian Soc. Petrol. Geol., Mem. 14, Proc. of the Second Int. Symposium on the Devonian System, Calgary, Canada, v. 3: Regional synthesis*, p. 449-468 (imp. 1988).
- _____, and Lane, H. R., 1985, Upper Devonian (Frasnian) of the *Polygnathus* biofacies, N. W. T., Canada: *Jour. Paleol.*, v. 59, p. 904-951.
- Komar, P. D., 1976, *Beach processes and sedimentation*: Prentice-Hall, Inc., Englewood Cliffs, New Jersey, 429 p.
- Kulm, L. D., Roush, R. C., Harlett, J. C., Neudeck, R. H., Chambers, D. M., and Runge, E. J., 1975, Oregon continental shelf sedimentation: interrelationships of facies distribution and sedimentary processes: *Jour. Geol.*, v. 83, p. 145-175.
- Lee, S. L., 1989, Mississippian flysch-trough sediments, sources, and structure of the southern Fish Creek Range, Eureka County, Nevada: Oregon State Univ., unpub. M.S. thesis, 73 p.
- Lehner, R. E., Tagg, K. M., Bell, M. M., and Roberts, R. J., 1961, Preliminary geologic map of Eureka County, Nevada: U. S. Geol. Survey Misc. Field Studies Map MF-178, scale 1:200,000.
- Matti, J. C., and McKee, E. H., 1977, Silurian and Lower Devonian paleogeography of the outer continental shelf of the Cordilleran miogeocline, central Nevada, in Stewart, J. H., Stevens, C. H., and Fritsche, A. E. (eds.), *Paleozoic paleogeography of the western United States: Soc. Econ. Paleontol. Mineral., Pacific Section, Pacific Coast Paleogeography Symposium 1*, p. 181-215.
- _____, Murphy, M. A., and Finney, S. C., 1975, Silurian and Lower Devonian basin and basin-slope limestones, Copenhagen Canyon, Nevada: *Geol. Soc. America Spec. Paper 159*, 48 p.
- McIlreath, I. A., 1977, Accumulation of a Middle Cambrian, deep-water limestone debris apron adjacent to a vertical, submarine carbonate escarpment, Southern Rocky Mountains, Canada, in Cook, H. E., and Enos, P. (eds.), *Deep-water carbonate environments: Soc. Econ. Paleontol. Mineral. Spec. Pub. 25*, p. 113-124.

- McGhee, G. R., Jr., Gilmore, J. S., Orth, C. J., and Olsen, E., 1984, No geochemical evidence for an asteroidal impact at late Devonian mass extinction horizon: *Nature*, v. 308, p. 629-631.
- McLaren, D. J., 1982, Frasnian-Famennian extinctions: *Geol. Soc. America Spec. Paper* 190, p. 477-484.
- _____, 1985, Mass extinction and iridium anomaly in the Upper Devonian of Western Australia: A commentary: *Geology*, v. 13, p. 170-172.
- Meischner, K., 1964, Allodapische kalke, turbidite in riffnahen sedimentationsbecken, in Bouma, A., and Brouwer, A. (eds.), *Turbidites*: Elsevier, Amsterdam, p. 159-191.
- Merriam, C. W., 1963, Paleozoic rocks of Antelope Valley, Eureka and Nye Counties, Nevada: *U. S. Geol. Survey Prof. Paper* 423, 67 p.
- _____, 1967, New data on Devonian: *U. S. Geol. Survey Prof. Paper* 575-A, p. A117.
- _____, 1973, Middle Devonian rugose corals of the central Great Basin: *U. S. Geol. Survey Prof. Paper* 799, 53 p.
- Mount, J. F., 1984, Mixing of siliciclastic and carbonate sediments in shallow shelf environments: *Geology*, v. 12, p. 432-435.
- Mullins, H. T., and Cook, H. E., 1986, Carbonate apron models: alternatives to the submarine fan model for paleoenvironmental analysis and hydrocarbon exploration: *Sed. Geol.*, v. 48, p. 37-79.
- Mutti, E., and Lucchi, Ricci, 1972, Le torbiditedell'Appennino settentrionale: introduzione all'analisi di facies: *Memorie dell Soc. Geol. Italiana*, v. 11, p. 161-199.
- Murphy, M. A., 1977, Middle Devonian rocks of central Nevada, in Murphy, M. A., Berry, W. B. N., and Sandberg, C. A. (eds.), *Western North America: Devonian*, University of Calif., Riverside, Campus Mus. Contribution 4, p. 190-199.
- _____, McKee, E. H., Winterer, E. L., Matti, J. C., and Dunham, J. B., 1978, Preliminary geologic map of the Roberts Creek Mountain quadrangle, Nevada: *U. S. Geol. Survey Open File Report* 78-376, 2 sheets.
- The North American Commission on Stratigraphic Nomenclature, 1983, North American stratigraphic code: *Amer. Assoc. Petrol. Geol. Bull.*, v. 67, p. 841-875.
- Ogren, D. E., 1961, Stratigraphy of the Upper Mississippian rocks of Northern Arkansas: *Northwestern Univ.*, unpub. Ph.D. thesis, 159 p.

- Orth, C. J., Gilmore, J. S., Knight, J. D., Pillmore, C. L., Tschudy, R. H., and Fassett, J. E., 1981, An iridium abundance anomaly at the palynological Cretaceous-Tertiary boundary in northern New Mexico: *Science*, v. 214, p. 1341-1343.
- Passega, R., 1957, Texture as a characteristic of clastic deposition: *Amer. Assoc. Petrol. Geol. Bull.*, v. 41, p. 1952-1984.
- Playford, P. E., McLaren, D. J., Orth, C. J., Gilmore, J. S., and Goodfellow, W. D., 1984, Iridium anomaly in the Upper Devonian of the Canning Basin, Western Australia: *Science*, v. 226, p. 437-439.
- Plumley, W. J., Risley, G. A., Graves, R. W. Jr., and Kaley, M. E., 1962, Energy index for limestone interpretation and classification, *in* Ham, W. E. (ed.), *Classification of carbonate rocks*: *Amer. Assoc. Petrol. Geol. Mem.* 1, p. 85-107.
- Poole, F. G., Sandberg, C. A., and Green, G. N., 1983, Allochthonous Devonian eugeosynclinal rocks in southern Fish Creek Range of central Nevada: *Geol. Soc. America Abstracts with Programs*, v. 15, p. 304.
- Powers, M. C., 1953, A new roundness scale for sedimentary particles: *Jour. Sed. Pet.*, v. 23, p. 117-119.
- Read, J. F., 1982, Carbonate platforms of passive (extensional) continental margins: types, characteristics and evolution: *Tectonophysics*, v. 81, p. 195-212.
- , 1985, Carbonate platform facies models: *Amer. Assoc. Petrol. Geol. Bull.*, v. 69, p. 1-21.
- Rejebian, V. A., Harris, A. G., and Huebner, J. S., 1987, Conodont color and textural alteration: an index to regional metamorphism, contact metamorphism, and hydrothermal alteration: *Geol. Soc. America Bull.*, v. 99, p. 471-479.
- Roen, J. B., 1961, Geology of the Lynn Window, Tuscarora Mountains, Eureka County, Nevada: Univ. of Calif., Los Angeles, unpub. M.S. thesis, 99 p.
- Roberts, R. J., Montgomery, K. M., and Lehner, R. E., 1967, Geology and mineral resources of Eureka County, Nevada: *Nevada Bur. Mines Bull.* 64, 152 p.
- Rose, P. R., 1976, Mississippian carbonate shelf margins, western United States: *U. S. Geol. Survey Jour. Research*, v. 4, p. 449-466.
- Rupp, A., 1967, Origin, structure, and environmental significance of Recent and fossil calcispheres: *Geol. Soc. America Spec. Paper* 101, p. 186 (abstract).
- Sandberg, C. A., 1976, Conodont biofacies of Late Devonian *Polygnathus styriacus* Zone in western United States, *in* Barnes, C. R. (ed.), *Conodont paleoecology*: *Geol. Assoc. Canada Special Paper* 15, p. 171-186.

- Sandberg, C. A., Gutschnick, R. C., Johnson, J. G., Poole, F. G., and Sando, W. J., 1983, Middle Devonian to Late Mississippian geologic history of the overthrust belt region, western United States: *Rocky Mt. Assoc. Geol., Geologic studies of the Cordilleran thrust belt*, v. 2, p. 691-719.
- _____, and Poole, F. G., 1977, Conodont biostratigraphy and depositional complexes of Upper Devonian craton-platform and continental-shelf rocks in the western United States, in Murphy, M. A., Berry, W. B. N., and Sandberg, C. A. (eds.), *Western North America: Devonian*: University of Calif., Riverside, Campus Mus. Contribution 4, p. 144-182.
- _____, _____, and Johnson, J. G., 1989, Upper Devonian of Western United States: in McMillan, N. J., Embry, A. F., and Glass, D. J. (eds.), *Devonian of the world: Canadian Soc. Petrol. Geol., Mem. 14, Proc. of the Second Int. Symposium on the Devonian System, Calgary, Canada*, v. 1: Regional synthesis, p. 183-220 (imp. 1988).
- _____, and Ziegler, W., 1984, Narrowing of worldwide search for conodont-based Devonian-Carboniferous boundary stratotype: *Geol. Soc. America Abstracts with Programs*, v. 16, p. 192.
- _____, _____, and Bultynck, P., 1988a, Middle-Upper Devonian series boundary as an example of intent and reality in biostratigraphic zonation: *Newsl. Stratigr.*, v. 18, p. 117-121.
- _____, _____, and Dreesen, R., 1987, Abrupt conodont biofacies changes redate and delimit Frasnian (Late Devonian) extinction event in Euramerica: *Geol. Soc. America Abstracts with Programs*, v. 19, p. 177.
- _____, _____, and Butler, J. L., 1988b, Late Frasnian mass extinction: Conodont event stratigraphy, global changes, and possible causes: *Courier Forschungs-Institut Senckenberg*, v. 102, p. 263-307.
- Sans, R. S., 1986, Origin of the Devonian rock units in the southern Fish Creek Range, Nye County, Nevada: *Oregon State Univ.*, unpub. M. S. thesis, 69 p.
- Schlager, W., and James, N. P., Low-magnesian calcite limestones forming at the deep-sea floor, Tongue of the Ocean, Bahamas: *Sedimentology*, v. 25, p. 675-702.
- Shanmugam, G., and Moiola, R. J., 1982, Eustatic control of turbidites and winnowed turbidites: *Geology*, v. 10, p. 231-235.
- Sepkoski, J. J., Jr., 1982, Mass extinctions in the Phanerozoic oceans: A review: *Geol. Soc. America Spec. Paper 190*, p. 283-289.
- Smith, J. F., and Ketner, K. B., 1968, Devonian and Mississippian rocks and the date of the Roberts Mountains thrust in the Carlin-Pinon Range area: *U. S. Geol. Survey Bull. 1251-I*, p. 11-118.
- Sorauf, J. E., and Pedder, A. E. H., 1986, Late Devonian rugose corals and the Frasnian-Famennian crisis: *Canadian Jour. Earth Sci.*, v. 23, p. 1265-1287.

- Stauffer, P. H., 1967, Grain-flow deposits and their implications, Santa Ynez Mountains, California: *Jour. Sed. Pet.*, v. 37, p. 487-508.
- Stearn, C. W., 1987, Effect of the Frasnian extinction event on the stromatoporoids: *Geology*, v. 15, p. 677-679.
- Taylor, J. M. C., and Illing, L. V., 1969, Holocene intertidal calcium carbonate cementation, Qatar, Persian Gulf: *Sedimentology*, v. 12, p. 69-107.
- Trojan, W. R., 1978, Devonian stratigraphy and depositional environments of the northern Antelope Range, Eureka County, Nevada: Oregon State Univ., unpub. M.S. thesis, 134 p.
- Visher, G. S., 1969, Grain size distribution and depositional processes: *Jour. Sed. Pet.*, v. 39, p. 1074-1106.
- Wanless, H. R., Burton, E. A., and Dravis, J., 1981, Hydrodynamics of carbonate fecal pellets: *Jour. Sed. Pet.*, v. 51, p. 27-36.
- Wilson, J. L., 1967, Cyclic and reciprocal sedimentation in Virgilian strata of southern New Mexico: *Geol. Soc. America Bull.*, v. 78, p. 805-818.
- _____, 1969, Microfacies and sedimentary structures in "deeper water" lime mudstones, *in* Friedman, G. M. (ed.), *Depositional environments in carbonate rocks*: *Soc. Econ. Paleontol. Mineral. Spec. Pub.* 14, p. 4-19.
- _____, and Jordan, C., 1983, Middle shelf environment, *in* Scholle, P. A., Bebout, D. G., and Moore, C. H. (eds.), *Carbonate depositional environments*: *Am. Assoc. Petrol. Geol. Mem.* 33, p. 298-343.
- Ziegler, W., 1962, Taxonomie und phylogenie Oberdevonischer Conodonten und ihre stratigraphische Bedeutung: *Hessisches Landesamt Bodenforschung Abhandlungen* 38, 166 p.
- _____, 1971, Conodont stratigraphy of the European Devonian, *in* Sweet, W. C., and Bergstrom, S. M. (eds.), *Symposium on conodont biostratigraphy*: *Geol. Soc. America Memoir* 127, p. 227-284.

APPENDICES

APPENDIX A

FAUNAL COLLECTIONS

Devonian conodont collections were identified and assigned relative ages by Gilbert Klapper, University of Iowa, 1986-1989. ANA I collections were made by John Graham of Amoco, 1985. Brachiopods were identified by J. G. Johnson, Oregon State University, 1987, 1988. Radiolarians (ANA II 111) were identified by A. R. Ormiston, Amoco, 1988. Section locations are indicated on Figure 4.

Key: *A.*= *Ancyrognathus*, *An.*= *Ancyrodella*, *I.*= *Icriodus*, *M.*= *Mesotaxis*, *O.*= *Ozarkodina*, *P.*= *Polygnathus*, *Pa.*= *Palmatolepis*, *Pand.*= *Pandorinellina*, *Pel.*= *Pelekyognathus*, *S.*= *Schmidtognathus*

ANA I

Sample: ANA I 175

Formation: Fenstermaker Limestone

Conodonts:

An. nodosa
Pa. sp. indet.
P. sp. indet.

Sample: ANA I 189

Formation: Fenstermaker Limestone

Conodonts:

Pa. aff. *Pa. coronata*
Pa. sp. T
Pa. sp. indet.
An. sp. indet.
P. lodinensis
P. sp. indet.
I. sp.

Montagne Noir Zone 13, according to the projected range in graphic correlation of the first species listed.

Sample: ANA I 235

Formation: Fenstermaker Limestone

Conodonts:

Pa. rhenana
Pa. winchelli (= *Pa. subrecta*)
Pa. aff. *Pa. coronata*
Pa. sp. T?
An. ioides
An. nodosa --> *An. ioides*
An. sp. indet.
P. imparilis group
P. lodinensis

Sample: ANA I 245

Formation: Fenstermaker Limestone

Conodonts:

Pa. sp. T
Pa. n. sp. P, form 2
Pa. aff. Pa. coronata
An. sp. indet.
P. lodinensis

Sample: ANA I 255

Formation: Fenstermaker Limestone

Conodonts:

Pa. sp. T
Pa. n. sp. P, form 2
Pa. aff. Pa. coronata
An. nodosa --> An. ioides
P. lodinensis
I. alternatus juv.

Sample: ANA I 265

Formation: Fenstermaker Limestone

Conodonts:

Pa. rhenana
Pa. n. sp. P, form 2 ?
An. sp. indet.
P. brevis
P. imparilis
O. postera
M. sp.

Sample: ANA I 275

Formation: Fenstermaker Limestone

Conodonts:

Pa. aff. Pa. coronata
Pa. sp. indet.
P. lodinensis
P. sp. indet.
I. alternatus

Sample: ANA I 280 (Amoco)

Formation: Fenstermaker Limestone

Conodonts:

Pa. rhenana morph. B
Pa. aff. Pa. coronata
Pa. linguiformis
Pa. sp. T
Pa. rhenana
An. nodosa
An. ioides (fragment, stained, probably reworked)
A. n. sp. (broad)
P. brevis group
P. lodinensis
P. imparilis
P. unicornis
O. "confluens" homeomorph
I. sp.

upper part of Zone 13, equivalent to the uppermost *gigas* Zone of the standard zonation.

Sample: ANA I 280 (Johnson)

Formation: Fenstermaker Limestone

Conodonts:

Pa. rhenana morph. B
Pa. winchelli
Pa. rhenana
Pa. linguiformis
Pa. aff. Pa. coronata
Pa. sp.
An. nodosa
A. n. sp. (aff. "*bifurcatus*")
A. n. sp. (broad)
P. lodinensis
P. imparilis
P. angustidiscus
P. brevicarina
P. brevis group
I. alternatus
M. gradata
O. "confluens" homeomorph
Belodella sp.

As 280 (Amoco).

Brachiopods:

Schizophoria sp. 2
Gypidula sp. 6
 indet. flat-ribbed rhynchonellid sp. 2
 indet. coarse-ribbed, subcarinate atrypid sp. 6
Radiatrypa sp. 3
 indet. smooth brachiopod 1

Algae:

indet. amphiporid fragments

Corals:

indet. solitary tetracoral

Vertebrates:

fish fragments 5

Sample: ANA I 286

Formation: Fenstermaker Limestone

Conodonts:

Pa. winchelli
Pa. aff. Pa. coronata
Pa. linguiformis
 aff. *Pa.* n. sp. P, form 2?
Pa. n. sp. P, form 2
Pa. rhenana
Pa. semichatovae? (juv.)
Pa. domanicensis (reworked)
An. nodosa
An. nodosa --> *An. ioides*
A. n. sp. (aff. "*bifurcatus*")
A. sp. (cf. *amana*)
P. angustidiscus
P. brevicarina?
P. lodinensis
P. imparilis
I. sp.
Belodella sp.

upper part of Zone 13, equivalent to the uppermost *gigas* Zone.

Sample: ANA I 290

Formation: Fenstermaker Limestone

Conodonts:

Pa. winchelli
Pa. rhenana
Pa. rhenana morph. B
Pa. linguiformis
Pa. aff. Pa. coronata
Pa. n. sp. P form 2
Pa. sp. indet.
An. gigas form 3
An. nodosa --> *An. ioides*
An. curvata, late form
An. sp.
P. lodinensis
P. imparilis
P. brevis group
P. evidens ?
I. alternatus
I. subterminus
Pel. planus

upper part of Zone 13, equivalent to the uppermost *gigas* Zone.

TA IV / ANA II / ANA III

Sample: ANA II 0

Formation: Denay Ls.

Conodonts:

M. asymmetrica? (juv. indet.)
P. dubius
I. sp.

Sample: TA IV 8

Formation: Denay Ls.

Conodonts:

I. sp. aff. I. symmetricus
P. dengleri
Belodella sp.
P. sp.

Upper *disparilis* -Lowermost *asymmetrica* zones.

Sample: TA IV 12

Formation: Denay Ls.

Conodonts:

P. sp.
I. sp.

Sample: TA IV 20

Formation: Denay Ls.

Conodonts:

I. sp. aff. I. symmetricus

I. subterminus

Belodella sp.

O. brevis

P. sp.

P. pennatus

P. dubius

According to the list and superposition, the fauna could have the same range as that in TA IV 8.

Sample: ANA II 30

Formation: Denay Ls.

Conodonts:

indet. platform fragment

Sample: TA IV 40

Formation: Denay Ls.

Conodonts:

An. alata (late form)

An. rotundiloba (late form)

P. dengleri

P. alatus

P. pennatus

Pand. insita

I. symmetricus

Mesotaxis asymmetrica

M. ovalis

P. webbi

P. dubius

P. angustidiscus

I. sp.

A. ancyrognathoides ?

On the association of the first two listed species the range in terms of the Montagne Noire zonation is within Zone 3. The composite standard, however, shows the first ranging down into the upper part of Zone 2 and of course the second species has its lowest occurrence at the base of Zone 2.

Sample: ANA II 45

Formation: Denay Ls.

Conodonts:

An. sp. indet.

I. sp. indet.

Sample: TA IV 50

Formation: Denay Ls.

Conodonts:

An. alata ?
An. africana ? (indet. juv.)
P. dengleri
P. dubius
Mesotaxis ovalis
I. subterminus
Pand. insita

The highest occurrence of *P. dengleri* known in the composite standard so far is within Zone 3.

Sample: ANA II 50

Formation: Denay Ls.

Conodonts:

An. "lobata" ?
P. sp. indet.
I. sp. indet.

Sample: ANA II 53

Formation: Denay Ls.

Conodonts:

An. africana
M. asymmetrica ?
P. sp. indet.
I. sp. indet.

The known range of *An. africana* is from within Zone 3 to Zone 6.

Sample: ANA II 54

Formation: Denay Ls.

Conodonts:

An. alata (late form)
I. sp. indet.
P. sp. indet.

The highest known occurrence of the late form of *An. alata* is high within Zone 3.

Sample: ANA II 55

Formation: Denay Ls.

Conodonts:

An. sp. indet.
P. sp. indet.

Sample: TA IV 63

Formation: Denay Ls.

Conodonts:

Pa. punctata
A. ancyrognathoides
An. sp. indet.
M. ovalis
P. webbi
P. sp.
Pand. sp.
I. symmetricus

The association of the first two species is that of Montagne Noire Zone 6. *M. ovalis* is known to range as high as Zone 6.

Sample: ANA II 88

Formation: Fenstermaker Limestone

Conodonts:

Pa. winchelli
Pa. rhenana
Pa. foliacea ?
Pa. domanicensis ?
Pa. aff. Pa. rhenana
Pa. rhenana morph. B?
Pa. sp.
An. nodosa
An. nodosa --> *A. ioides*
An. curvata, late form
A. n. sp.
A. triangularis ? (juv.) (or *A. amana* ?)
P. brevis
P. brevis group
P. lodinensis
P. unicornis
P. sp. (P. longiposticus homeomorph)
P. spp.
I. symmetricus
I. alternatus

Montagne Noire Zones 12-13 (this is almost certainly a mixed fauna).

Sample: TA IV 95

Formation: Fenstermaker Limestone

Conodonts:

P. lodinensis
Pa. sp. indet.

P. lodinensis is known below this in ANA II 88.

Sample: ANA II 98

Formation: Fenstermaker Limestone

Conodonts:

Pa. aff. Pa. coronata
Pa. winchelli
Pa. rhenana
Pa. sp. T
Pa. n. sp. P, form 2
An. nodosa
An. nodosa --> An. ioides
An. sp.
A.? sp. indet.
P. lodinensis
P. pacificus
P. decorosus
P. angustidiscus
P. unicornis
P. brevis ?
P. sp.
I. symmetricus
I. alternatus
Belodella sp.

Zone 13, on evidence of the projected range in graphic correlation of the first species listed.

Sample: ANA II 103

Formation: Fenstermaker Limestone

Conodonts:

Pa. rhenana
Pa. n. sp. P, forms 1, 2
Pa. aff. Pa. coronata
Pa. sp. T
Pa. semichatovae *
Pa. aff. Pa. domanicensis *
Pa. ljaschenkoae *
An. curvata (* early & late forms)
An. nodosa
A. sp.
P. lodinensis
P. samueli (so far only known in equivalents of Zone 12;
 possibly reworked)
P. pacificus
P. n. sp. R
P. decorosus
I. symmetricus
I. alternatus
Pand. sp.
O. postera
Belodella sp.

Zone 13. This is a mixed fauna, with at least the forms marked with an asterisk reworked according to ranges known elsewhere.

Sample: ANA II 105

Formation: Fenstermaker Limestone

Conodonts:

Pa. aff. Pa. coronata
Pa. sp. T
Pa. hassi
Pa. sp.
An. nodosa
P. imparilis
P. lodinensis
P. pacificus
P. n. sp. R
I. sp.

Zone 13, on evidence of the first species listed.

Sample: ANA II 109

Formation: Fenstermaker Limestone

Conodonts:

Pa. rhenana fragment
Pa. n. sp. P, form 2
Pa. sp. T
An. nodosa
P. lodinensis
I. alternatus

Sample: ANA II 111

Formation: Fenstermaker Limestone

Conodonts:

Pa. winchelli
Pa. sp. T
An. nodosa
An. sp. indet.
P. lodinensis
P. decorosus
P. n. sp. R
I. sp.
Pand. sp.
Belodella sp.

Zone 13, by position. The ramiform elements in this collection are exceptionally well preserved for a Nevada Devonian fauna. There is evidently no reworking in this collection.

Radiolaria:

Ceratoikicum n. sp.
Entactinia additiva Foreman
Astroentactinia stellata Nazarov
Entactinia aff. *E. dissora* Nazarov
Entactinosphaera aff. *E. echinata* Hinde
Entactinosphaera cf. *E. grandis* Hinde
Spongentactinella ? sp.
Polyentactinia sp.

This assemblage is indicative of a Frasnian age. For example, *Ceratoikicum* n. sp. occurs elsewhere in the Canol Formation associated with early Frasnian conodonts. The species *stellata* and *dissora* are also indicative of Frasnian Age as indicated by their occurrences in the Soviet Union and Australia and the remaining species are all consistent with such an age assignment.

Sample: ANA II 120

Formation: Fenstermaker Limestone

Conodonts:

Pa. rhenana morph. B?

Pa. rhenana

Pa. aff. Pa. coronata

Pa. sp. T

Pa. winchelli ?

Pa. n. sp. P, form 2

An. nodosa

P. lodinensis

P. sp.

I. sp.

Zone 13.

Sample: ANA II 126

Formation: Fenstermaker Limestone

Conodonts:

Pa. sp. indet.

P. lodinensis

P. sp. indet.

(hopeless preservation)

Sample: ANA II 133

Formation: Fenstermaker Limestone

Conodonts:

Pa. rhenana (Pb element)

Pa. aff. Pa. coronata

An. nodosa

P. imparilis

P. lodinensis

Sample: ANA II 135

Formation: Fenstermaker Limestone

Conodonts:

Pa. rhenana (different Pb element)

An. nodosa

P. imparilis

P. lodinensis

Sample: ANA II 142 (= ANA III 0)

Formation: Fenstermaker Limestone

Conodonts:

Pa. rhenana

P. brevis

P. lodinensis

I. alternatus

Sample: ANA III 0 (= ANA II 142)
 Formation: Fenstermaker Limestone
 Footage above base ANA II: 142
Conodonts:

Pa. rhenana
Pa. n. sp. P, form 2
Pa. sp.
P. pacificus
P. sp.

Sample: ANA III 8
 Formation: Fenstermaker Limestone
 Footage above base ANA II: 150
Conodonts:

Pa. n. sp. P, form 2
Pa. sp. T ?
Pa. rhenana (& Pb element)
Pa. aff. Pa. coronata
An. nodosa
An. nodosa --> *An. ioides*
P. lodinensis

Zone 13, on the evidence of the *Pa. aff. Pa. coronata*.

Sample: ANA III 22
 Formation: Fenstermaker Limestone
 Footage above base ANA II: 164
Conodonts:

Pa. rhenana
Pa. n. sp. P, form 2
Pa. sp.
An. ioides (probably reworked)
P. lodinensis
P. cf. P. samueli

Sample: TA IV 165
 Formation: Fenstermaker Limestone
Conodonts:

An. ioides
Pa. sp. indet.
P. pacificus
P. sp. indet.
I. sp. indet.

Because collections lower in this section (e.g. ANA II 98 and 103) have been determined as Zone 13, *An. ioides* may be reworked here. This species is so far known in the composite standard low in Zone 12.

Sample: ANA III 33
 Formation: Fenstermaker Limestone
 Footage above base ANA II: 175
Conodonts:

Pa. sp. indet.
An. nodosa --> *An. ioides*
P. sp. indet.

Sample: ANA III 47
 Formation: Fenstermaker Limestone
 Footage above base ANA II: 189
Conodonts:

Pa. semichatovae (reworked, projected range by graphic correlation into the Montagne Noire zonation is in the lower part of Zone 11)
Pa. sp. (cf. *Pa.* n. sp. O)
Pa. aff. *Pa. coronata*
Pa. rhenana (Pb element)
Pa. sp.
An. nodosa
P. lodinensis
P. imparilis ?
P. pacificus
P. sp.
 cf. *Pel. planus*
 worn conodont

If the first species on the list is correctly identified, then it must be reworked.

Sample: ANA III 56
 Formation: Fenstermaker Limestone
 Footage above base ANA II: 198
Conodonts:

Pa. sp. indet.
P. imparilis ?

Sample: ANA III 66
 Formation: Fenstermaker Limestone
 Footage above base ANA II: 208
Conodonts:

Pa. semichatovae
Pa. sp.
A. triangularis
P. lodinensis
P. sp.

Same comment as for ANA III 47.

Sample: ANA III 76
 Formation: Fenstermaker Limestone
 Footage above base ANA II: 218
Conodonts:

Pa. sp. indet.
An. nodosa ?
P. lodinensis
P. evidens ?
P. sp.
P. sp. indet.
I. subterminus
 indet. cone

Sample: ANA III 96
 Formation: Fenstermaker Limestone
 Footage above base ANA II: 238
Conodonts:

Pa. n. sp. P, form 1
Pa. sp. indet.
An. sp. indet.
P. sp. indet.

Sample: ANA III 106
 Formation: Fenstermaker Limestone
 Footage above base ANA II: 248
Conodonts:

Pa. rhenana
Pa. linguiformis
Pa. winchelli ?
An. nodosa
An. nodosa --> *An. ioides*
P. imparilis
P. lodinensis
I. alternatus

upper part of Zone 13, equivalent to the uppermost *gigas* Zone of the standard zonation.

Sample: ANA III 107 (= WANA III 2)
 Formation: Fenstermaker Limestone
 Footage above base ANA II: 249
Conodonts:

Pa. rhenana
Pa. sp. indet.
P. lodinensis

Brachiopods:

Spinatrypina sp. 5
 indet. faintly ribbed atrypid sp. 2

Sample: ANA III 108 (= WANA III 3)

Formation: Fenstermaker Limestone

Footage above base ANA II: 250

Conodonts:

Pa. linguiformis

Pa. sp. T

Pa. rhenana

Pa. winchelli

Pa. sp. indet.

An. sp. indet.

P. imparilis

P. lodinensis

Pel. sp.

O. postera

upper part of Zone 13, equivalent to the uppermost *gigas* Zone of the standard zonation.

Sample: ANA III 109 (= WANA III 4)

Formation: Fenstermaker Limestone

Footage above base ANA II: 251

Conodonts:

Pa. sp. indet.

An. sp. indet.

P. imparilis

P. lodinensis

P. unicornis

P. sp. indet.

I. alternatus

Sample: ANA III 110 (= WANA III 5)

Formation: Fenstermaker Limestone

Footage above base ANA II: 252

Conodonts:

Pa. winchelli

Pa. sp. indet.

An. sp. indet.

P. lodinensis

I. alternatus

I. symmetricus

Sample: ANA III 111 (= WANA III 6)

Formation: Fenstermaker Limestone

Footage above base ANA II: 253

Conodonts:

Pa. sp. T

Pa. aff. Pa. coronata

Pa. sp. indet.

P. imparilis

P. lodinensis

Sample: ANA III 112 (= WANA III 7)

Formation: Fenstermaker Limestone

Footage above base ANA II: 254

Conodonts:

Pa. rhenana
Pa. rhenana morph. B
Pa. linguiformis
Pa. winchelli
Pa. n. sp. P, form 2
Pa. sp. T
Pa. aff. Pa. coronata
Pa. triangularis ? (1 specimen)
Pa. sp. indet.
An. nodosa
An. nodosa --> *ioides*
I. alternatus
P. imparilis
P. lodinensis
P. brevis group
P. sp.
O. dissimilis
Belodella sp.

upper part of Zone 13.

Algae:

indet. amphiporid 1

Corals:

indet. solitary tetracoral 2 fragments

Sample: ANA III 113 (= WANA III 8)

Formation: Fenstermaker Limestone

Footage above base ANA II: 255

Conodonts:

Pa. linguiformis
Pa. rhenana morph. B
Pa. aff. Pa. coronata
Pa. winchelli
Pa. sp. T
An. nodosa
A. sp.
P. lodinensis
P. imparilis
M. sp.
 indet. cones

Sample: ANA III 114 (= WANA III 9)

Formation: Fenstermaker Limestone

Footage above base ANA II: 256

Conodonts:

Pa. linguiformis

Pa. sp. T

Pa. sp. indet.

An. nodosa

I. alternatus

I. sp.

P. imparilis

P. lodinensis

Pel. sp.

M. sp.

Belodella sp.

Sample: ANA III 115 (= WANA III 10)

Formation: Fenstermaker Limestone

Footage above base ANA II: 257

Conodonts:

Pa. linguiformis

Pa. rhenana

Pa. sp. T

Pa. aff. Pa. coronata

Pa. winchelli

An. nodosa

P. lodinensis

I. sp.

M. sp.

Belodella sp.

Brachiopods:

indet. atrypid 1 fragment

Corals:

indet. coral fragment

Sample: ANA III 116 (= WANA III 11)

Formation: Fenstermaker Limestone

Footage above base ANA II: 258

Conodonts:

Pa. linguiformis

Pa. aff. Pa. coronata

Pa. sp. T

Pa. rhenana morph. B

An. sp.

P. imparilis

P. lodinensis

P. sp.

Belodella sp.

upper part of Zone 13.

Brachiopods:

indet. atripid 2 fragments

Corals:

indet. solitary tetracoral 1

Sample: ANA III 117 (= WANA III 12) (both collections)

Formation: Fenstermaker Limestone

Footage above base ANA II: 259

Conodonts:

P. lodinensis

Pa., *P.*, and *An. sp.* indet.

Belodella sp.

Sample: ANA III 117.5 (= WANA III 12.5)

Formation: Fenstermaker Limestone

Footage above base ANA II: 259.5

Conodonts:

Pa. linguiformis

Pa. rhenana

Pa. sp. T

Pa. aff. Pa. coronata

Pa. triangularis ? (1 specimen)

P. lodinensis

P. pacificus

P. imparilis

An. sp. indet.

Pel. planus

I. alternatus

upper part of Zone 13, equivalent to the uppermost *gigas* Zone of the standard zonation.

Sample: ANA III 118 (= WANA III 13)

Formation: Fenstermaker Limestone

Footage above base ANA II: 260

Conodonts:

Pa. rhenana
Pa. sp. T
Pa. sp. indet.
An. sp. indet.
A. sp. indet.
P. imparilis
P. lodinensis
P. brevis
M. sp.

Brachiopods:

indet. atrypid 3 fragments

Sample: ANA III 119 (= WANA III 14)

Formation: Fenstermaker Limestone

Footage above base ANA II: 261

Conodonts:

Pa. triangularis
Pa. delicatula ?
Pa. sp. indet.
I. alternatus
P. lodinensis (probably reworked)
P. sp. indet.
An. sp. indet.

triangularis Zone undifferentiated (this sample probably correlates with WNA I sample 9 [WNA I 389]).

Sample: ANA III 120 (= WANA III 15)

Formation: Fenstermaker Limestone

Footage above base ANA II: 262

Conodonts:

Pa. triangularis
Pa. delicatula delicatula
Pa. delicatula ?
Pa. sp. indet.
I. alternatus
P. brevilaminus
P. imparilis (probably reworked)
P. lodinensis (probably reworked)
M. sp.

Middle *triangularis* Zone.

Sample: ANA III 121 (= WANA III 16)

Formation: Fenstermaker Limestone

Footage above base ANA II: 263

Conodonts:

Pa. triangularis
Pa. delicatula clarki
Pa. winchelli (probably reworked)
An. sp. indet. (probably reworked)
I. alternatus
P. brevilaminus
P. imparilis

Middle *triangularis* Zone.

Sample: ANA III 122 (= WANA III 17)

Formation: Fenstermaker Limestone

Footage above base ANA II: 264

Conodonts:

Pa. triangularis
Pa. delicatula delicatula
Pa. delicatula clarki
Pa. minuta minuta ?
Pa. rhenana (probably reworked)
Pa. rhenana morph. B?
Pa. sp. indet.
I. alternatus
P. brevilaminus
P. imparilis
P. unicornis (probably reworked)
P. sp.
M. sp.

probably Middle *triangularis* Zone.

Brachiopods:

indet. ribbed brachiopod
Cyrtospirifer? sp. 5 fragments

Corals:

indet. solitary tetracoral 2 fragments

Sample: ANA III 126 (Amoco) (remeasured to 123 ft.)

Formation: Fenstermaker Limestone

Footage above base ANA II: 265

Conodonts:

Pa. triangularis ? (fragment)
Pa. triangularis ? (juv.)
Pa. delicatula clarki
Pa. rhenana (Pb element) (reworked)
P. brevicarina (reworked)
P. imparilis (reworked)
P. sp.
I. alternatus
I. iowaensis ?

Middle *triangularis* Zone

Sample: ANA III 126 (Johnson) (remeasured to 123 ft.)

Formation: Fenstermaker Limestone

Footage above base ANA II: 265

Conodonts:

Pa. triangularis
Pa. delicatula clarki
Pa. sp. (Famennian)
I. iowaensis ?

Middle *triangularis* Zone.

Brachiopods:

indet. coarse-ribbed brachiopod 1
 as in WNA I 10, probably a rhynchonellid

WNA I

Sample: WNA I 0 (base)

Formation: Denay Ls.

Conodonts:

P. and *I.* sp. indet.

Brachiopods:

Schizophoria sp. 4
Radiatrypa sp. 1
Spinatrypina sp. 2

Algae:

Amphipora sp. 1 bat

Corals:

indet. tabulate coral 7 fragments

Sample: WNA I 168
Formation: Denay Ls.

Conodonts:

Pa. n. sp. P, form indet.
P. samueli
P. imparilis?
P. lodinensis
P. sp.
An. nodosa
A. sp. indet.

Equivalent to Zone 12, on evidence of the projected range in graphic correlation of *P. samueli*.

Sample: WNA I 331 (= WNA I 1)
Formation: Fenstermaker Limestone

Conodonts:

Pa. rhenana?
Pa. sp. indet.
An. sp. indet.
P. lodinensis
P. brevis group

Sample: WNA I 334 (= WNA I 2)
Formation: Fenstermaker Limestone

Conodonts:

Pa. sp. indet.
P. sp. indet.

Sample: WNA I 339 (= WNA I 3)
Formation: Fenstermaker Limestone

Conodonts:

Pa. rhenana morph. B (informal designation, this is probably
a new species)
Pa. sp. indet.
An. nodosa
P. sp. indet.

Sample: WNA I 344 (= WNA I 4)
Formation: Fenstermaker Limestone

Conodonts:

Pa. rhenana morph. B
Pa. sp. indet.
P. lodinensis
P. unicornis?
P. sp. indet.

Sample: WNA I 346 (= WNA I 5)
 Formation: Fenstermaker Limestone
Conodonts:

Pa. winchelli
Pa. rhenana morph. B
Pa. sp. indet.
P. lodinensis
P. sp. indet.
M. sp.

Sample: WNA I 349 (= WNA I 6)
 Formation: Fenstermaker Limestone
Conodonts:

Pa. sp. T
Pa. aff. *Pa. coronata*
Pa. sp. indet.
P. imparilis
P. lodinensis
P. brevis group
P. sp. indet.

Zone 13, on evidence from graphic correlation of the range of *Pa.* aff. *Pa. coronata*.

Sample: WNA I 352 (= WNA I 7)
 Formation: Fenstermaker Limestone
Conodonts:

Pa. sp. indet.
P. imparilis
P. sp. indet.

Sample: WNA I 354 (= WNA I 8)
 Formation: Fenstermaker Limestone
Conodonts:

Pa. sp. T
Pa. linguiformis
Pa. rhenana
Pa. hassi?
Pa. sp. indet.
An. nodosa
P. sp.
P. imparilis
P. lodinensis
P. sp. indet.
M. sp.

upper part of Zone 13, equivalent to the uppermost *gigas* Zone of the standard zonation.

Sample: WNA I 389 (= WNA I 9)
Formation: Fenstermaker Limestone

Conodonts:

Pa. delicatula ?
Pa. sp. indet.
I. alternatus
P. brevilaminus
M. sp.

triangularis Zone undifferentiated.

Sample: WNA I 395 (= WNA I 10)
Formation: Fenstermaker Limestone

Conodonts:

Pa. triangularis
Pa. delicatula subsp. indet.
I. alternatus
P. brevilaminus
P. imparilis (probably reworked)

Middle *triangularis* Zone.

Brachiopods:

indet. coarse-ribbed brachiopod 1
Cyrtospirifer ? sp. 3

Sample: WNA I 400 (= WNA I 11)
Formation: Fenstermaker Limestone

Conodonts:

Pa. winchelli (probably reworked)
Pa. sp. indet.
An. sp. indet.
P. brevilaminus
P. lodinensis (probably reworked)
P. imparilis (probably reworked)
P. brevis group
Belodella sp.
indet. cones

Sample: WNA I 417 (= WNA I 12) (top)

Formation: Fenstermaker Limestone

Conodonts:

Pa. triangularis

Pa. sp. indet.

I. alternatus

P. brevilaminus

P. sp.

M. sp.

Belodella sp.

triangularis Zone undifferentiated.

WNA II

Sample: WNA II 1

Formation: Denay Ls.

Conodonts:

Pa. disparalvea

P. webbi

P. dengleri

P. dubius

P. sp.

S.? gracilis

S. sp.

upper *disparilis* Zone.

Brachiopods:

indet. brachiopod 1

indet. coarse-ribbed atrypid sp. 2

indet. ambocoelid spp. 4

Echinoderms:

common crinoids, discarded

Sample: WNA II 170

Formation: Fenstermaker Limestone

Conodonts:

Pa. aff. Pa. coronata
Pa. sp. T
Pa. rhenana
Pa. winchelli
Pa. n. sp. P, form 2
 (Pb element of *Pa. bogartensis*)
An nodosa
An. nodosa --> *An. ioides*
A. tsiensi
Ancyrodelloides? homeomorph
P. webbi
P. brevis
P. lodinensis
P. pacificus
P. decorosus
P. n. sp. R
P. imparilis
I. alternatus
Pel. planus
O. sp.
Belodella sp.

Montagne Noire Zone 13

Sample: WNA II 196

Formation: Fenstermaker Limestone

Conodonts:

Pa. n. sp. P, form indet.
Pa. sp. indet.
P. ettremae
P. lodinensis
P. sp. indet.
I. sp. indet.

Sample: WNA II 227

Formation: Fenstermaker Limestone

Conodonts:

An. nodosa
A. sp. indet.
Pa. n. sp. P, form 2
Pa. sp. indet.
P. unicornis
P. n. sp. R
P. sp. indet.

Brachiopods:

Gypidula sp. 1

Sample: WNA II 245
Formation: Fenstermaker Limestone
Conodonts:

Pa. sp. indet.
P. lodinensis
P. sp. indet.

Sample: WNA II 289
Formation: Fenstermaker Limestone
Conodonts:

An. nodosa
Pa. sp. indet.
P. sp.
I. sp. indet.

Brachiopods:

Spinatrypa sp. 1

Sample: WNA II 303
Formation: Fenstermaker Limestone
Conodonts:

Pa. n. sp. P, form 2
P. imparilis
P. sp. indet.

Brachiopods:

Radiatrypa sp. 1
Spinatrypa sp. 4

Algae:

Amphipora sp. 3 bats

Sample: WNA II 323
Formation: Fenstermaker Limestone
Conodonts:

P. lodinensis
An. sp. indet.

Sample: WNA II 341

Formation: Fenstermaker Limestone

Conodonts:

Pa. linguiformis
Pa. sp. T
Pa. rhenana
Pa. aff. Pa. coronata
P. imparilis
P. pacificus
P. lodinensis
A. n. sp. (broad; same as in ANA I 280)
A. sp. indet.
An. lobata?
Ancyrodelloides? homeomorph (possibly three forms
 represented, one of which is in the sample at 170)
Pand. insita
I. alternatus

upper part of Zone 13, equivalent to the uppermost gigas Zone of the standard zonation.

Sample: WNA II 363

Formation: Fenstermaker Limestone

Conodonts:

Pa. sp. indet.
P. n. sp.
P. imparilis
P. sp. indet.
A. sp. indet.

Sample: WNA II 386

Formation: Fenstermaker Limestone

Conodonts:

Pa. delicatula delicatula
Pa. triangularis?
Pa. rhenana?
P. lodinensis
P. brevilaminus
I. alternatus

Famennian, Middle *triangularis* Zone

Brachiopods:

indet. rynchonellid sp. 1
 indet. faintly ribbed atrypid sp. 2
 indet. spiriferid sp. 1
 indet. brachiopod fragments

Sample: WNA II 409

Formation: Fenstermaker Limestone

Conodonts:

Pa., *P.* and *I.* sp. indet.

WFC

Sample: WFC 1

Formation: Fenstermaker Limestone?

Conodonts:

Pa. aff. Pa. coronata

Pa. sp. T

P. lodinensis

P. brevis group

P. imparilis

P. sp. indet.

An. sp. indet.

Montagne Noire Frasnian Zone 13, on the restricted occurrence at Sweetland Creek of the first species listed.

Sample: WFC 3

Formation: Fenstermaker Limestone?

Conodonts:

Pa. sp. indet.

P. sp. indet.

An. sp. indet.

Frasnian, provided that the single specimen of *Ancyrodella* is not reworked.

WRC I

Sample: WRC I 122

Formation: Popovich Formation

Conodonts:

An. alata (late form)
An. africana
M. ovalis
I. sp. indet.
Mehlina sp. indet.
P. webbi
P. sp. indet.
 indet. ramiform elements

The overlap of the first three species in the Montagne Noir Frasnian zonation is from upper Zone 3 to lower Zone 4. The first two species also occur in a collection of David Ettner (88VN74).

Brachiopods:

Schizophoria sp. 2
 indet. ribbed atrypid sp. 2
Radiatrypa multcostellata 10
 indet. ribbed spiriferid
 indet. smooth-radiate spiriferid sp. 35
 indet. terebratulid sp. 1

Frasnian; probably early Frasnian based on *R. multcostellata*.

Sample: WRC I 212

Formation: Popovich Formation

Conodonts:

P. dubius
P. sp. indet.
I. symmetricus
Pa. sp. indet. (including Pb element)
Pand. sp. indet.
 indet. ramiform elements

The first species listed ranges from the late Middle Devonian to as high as Montagne Noir Frasnian Zone 7. The single Pa element of *Palmatolepis* is an extremely small indeterminate specimen but it belongs to the Frasnian subgenus "*Manticolepis*"; the fragmentary Pb element is undoubtedly of a Frasnian species.

CW I

Sample: CW I 2

Formation: Denay Limestone

Conodonts:

Pa. transitans
An. gigas form 1
An. africana
M. asymmetrica
M. ovalis
P. aff. P. dengleri
P. dubius
P. webbi
I. symmetricus
Pand. sp.

In terms of the Montagne Noir Frasnian zonation (Klapper, 1988, p. 7-8), the fauna of this collection correlates directly with Zone 4.

Sample: CW I 10

Formation: Denay Limestone

Conodonts:

An. gigas form 1
An. africana --> *An. gigas*
M. asymmetrica
P. dubius
I. symmetricus
Belodella sp.

Sample: CW I 15

Formation: Denay Limestone

Conodonts:

Pa. transitans
Pa. punctata
An. gigas form 1
An. africana
An. africana --> *An. gigas*
An. sp.
M. asymmetrica
M. ovalis
P. aff. P. dengleri
P. dubius
P. webbi
Playfordia sp.
Pand. insita
I. symmetricus
Belodella sp.

The fauna of this collection correlates with Montagne Noir Frasnian Zone 5 (Klapper, 1988, p. 8-9).

APPENDIX B

Statistical Parameters from Sieve Analysis of Quartz Sand Fractions

Sample	Md (phi)	Mz (phi)	SK1	S1 (phi)	Kg	Coarsest 1% (phi)	Bimo- dality	Modal Class (phi)	Verbal Terms		
									Sorting (s1)	Skewness (SK1)	Kurtosis (Kg)
FENSTERMAKER LIMESTONE											
ANA I 175	2.55	2.43	-0.28	0.52	0.93	0.95		2.5-3	Mod.	Neg.	Meso.
ANA I 265	2.15	2.19	0.077	0.49	0.82	0.95		1.5-2	Well	Near sym.	Platy.
ANA I 280	1.93	1.97	0.034	0.68	0.9	0.45	X	1.5-2	Mod.	Near sym.	Meso.
ANA II 103	2	2.09	0.28	0.44	0.82	1.35		1.5-2	Well	Pos.	Platy.
ANA II 142	2.25	2.25	0	0.48	0.82	1.23	X	1.5-2	Well	Sym.	Platy.
ANA III 0	1.95	2.04	0.16	0.56	0.91	0.85		1.5-2	Mod.	Pos.	Meso.
ANA III 8	2.15	2.175	0.021	0.51	0.85	0.9		1.5-2	Mod.	Near sym.	Platy.
ANA III 47	2.2	2.2	0.017	0.47	0.77	0.975		1.5-2	Well	Near sym.	Platy.
ANA III 76	2.1	2.17	0.15	0.52	0.81	1	X	1.5-2	Mod.	Pos.	Platy.
ANA III 96	2.15	2.18	0.037	0.59	0.81	0.9	X	1.5-2	Mod.	Near sym.	Platy.
ANA III 113	2.48	2.39	-0.34	0.49	1.27	0.775		2.5-3	Well	V. Neg.	Lepto.
WNA I 168	2.2	2.23	0.066	0.45	0.75	1.25	X	1.5-2	Well	Near sym.	Platy.
WNA I 223	2.25	2.23	-0.062	0.45	-2.3	1.1	X	2.5-3	Well	Near Sym.	V. Platy.
WNA I 349	2.55	2.42	-0.45	0.45	1.05	0.85		1.5-2	Well	V. Neg.	Meso.
WNA II 170	2.15	2.18	0.019	0.49	0.85	0.775	X	1.5-2	Well	Near sym.	Platy.
WNA II 196	2.38	2.28	-0.28	0.55	0.87	0.775	X	2.5-3	Mod.	Neg.	Platy.
WNA II 341	2.4	2.34	-0.19	0.47	0.85	1		2.5-3	Well	Neg.	Platy.
WNA II 409	2.33	2.22	-0.28	0.68	1.01	0.5		2.5-3	Mod.	Neg.	Meso.
WFC 1	1.98	2.08	0.19	0.52	0.85	0.75	X	1.5-2	Mod.	Pos.	Platy.
WFC 2	2.1	2.17	0.14	0.48	0.78	0.625	X	1.5-2	Well	Pos.	Platy.
WFC 3	2.56	2.51	-0.24	0.39	1.11	1.3		2.5-3	Well	Neg.	Meso.
AVERAGES:	2.23	2.23	-0.045	0.51	0.74	0.92					

APPENDIX B (Continued)

Statistical Parameters from Sieve Analysis of Quartz Sand Fractions

Sample	Md (phi)	Mz (phi)	SK1	S1 (phi)	Kg	Coarsest 1% (phi)	Bimo- dality	Modal Class (phi)	Verbal Terms		
									Sorting (s1)	Skewness (SK1)	Kurtosis (Kg)
MCCOLLEY CANYON FORMATION											
Coils Creek Member											
TA V O	3.5	3.42	-0.27	0.7	1.02	1.45		3.5-4	Mod.	Neg.	Meso.
OXYOKE CANYON FORMATION											
Dno	1.65	1.68	0.094	0.59	1	0.55		1.5-2	Mod.	Near sym.	Meso.
POPOVICH FORMATION											
WRC I 61	1.83	1.92	0.33	0.418	1.35	1.1		1.5-2	Well	V. Pos.	Lepto.
WRC I 212	2.15	2.18	0.024	0.676	0.82	0.75	X	2.5-3	Mod.	Near sym.	Platy.
GUILMETTE FORMATION											
WBH 1d	2.5	2.48	0.013	0.677	0.76	1.225	X	1.5-2	Mod.	Near Sym.	Platy.
WBH 1e	1.925	2.08	0.35	0.58	0.84	0.975	X	1.5-2	Mod.	V. Pos.	Platy.
WBH 1f	2.88	2.75	-0.17	0.69	1.09	1.4	X	2.5-3	Mod.	Neg.	Meso.
PILOT SHALE											
Lower Tongue of Lower Member											
WIC 1	1.65	1.74	0.22	0.665	1.29	0.5		1.5-2	Mod.	Pos.	Lepto.